

# MODELLING DIRECT BIOTIC INTERACTIONS

with a focus on filamentous fungi

Danis Kiziridis

Submitted to Swansea University in fulfilment of the requirements for the Degree of  
Doctor of Philosophy

*2018, Swansea University*



# Summary

This thesis models direct biotic interactions in general, and fungal competition for space in particular, under a generalising perspective. Direct intraspecific and interspecific interactions in food webs, consumption, pollination, herbivory, seed dispersal, predation, parasitism, interference competition, and other systems, have been investigated with proximate and evolutionary questions. Interest in particular questions or systems has led to specialised conceptual and mathematical descriptions of how interactions occur. Aim of this thesis was to theoretically generalise in four areas. First, I propose a mechanistic framework in which interactions in any ecological network can be described in standardised form, providing a common mechanistic basis, and facilitating the generation of hypotheses and models for social network dynamics (in territoriality, fighting, dominance, or cooperation), assembly or invasion (in trophic, antagonistic, or mutualistic communities), and coevolution. Second, a method based on the framework is developed for finding the minimum number of functional traits required for the mechanistic explanation of all interaction outcomes in an ecological network. This method reduces the risk of omitting important traits, to improve modelling, understanding, explaining, and predicting community structure, and structure-dependent community, ecosystem, and evolutionary processes. Third, I experimentally quantify six elements of spatial competition between wood decay fungi, to acquire a comprehensive view about forces driving fungal community dynamics on agar substrate. Fourth, I develop models (lattice, ordinary, partial differential equations) which accurately predict fungal community dynamics in the experiments only if all six quantified elements are incorporated, with implications for the predictability of natural community dynamics, and hence of ecosystem processes such as biogeochemical cycling, primary production, biocontrol, and bioremediation in which filamentous fungi are key players. This thesis demonstrates the possibility for further theoretical generalisation in direct biotic interactions, to better address proximate and evolutionary questions about interactions in different ecological systems.





# Declaration and Statements

## DECLARATION

This work has not been previously accepted in substance for any degree, and is not being concurrently submitted in candidature for any degree.

Signed ..... (candidate)

Date .....

## STATEMENT 1

This thesis is the result of my own investigations, except where otherwise stated. The list of references cited in the main text is appended.

Signed ..... (candidate)

Date .....

## STATEMENT 2

I hereby give consent for my thesis, if accepted, to be available for photocopying and for inter-library loan, and for the title and summary to be made available to outside organisations.

Signed ..... (candidate)

Date .....



# Acknowledgements

I would like to thank the following:

Chenggui Yuan and Mike Fowler, my formal supervisors, for their supervision, support, and will to pass over their experience to a difficult student.

Dan Eastwood and Lynne Boddy, my informal supervisors, for their support, help, and time for discussion and reflection.

Dimitra Georgopoulou for her support, feedback, and guidance in all parts of this thesis.

Jennifer Hiscox, Suzy Moody and Georgina Powell for the teaching and training they provided for the experimental part of this thesis.

Ian Tew, James Taylor, Hilary Williams and Sarah Walmsley for their training and help in the lab rooms.

Tomás Sintés for his comments on the initial stages of developing the lattice model.

David Gilljam for his comments on an earlier manuscript for the mechanistic framework and the minimum dimensionality.

My mother, father, brother, grandmother, aunt and uncle for their support.

Friends from the Departments of Biosciences and Mathematics for sharing sad or happy moments in our studies or work: Claudio de la O, Bibiana Montoya, Dania Albini, Yongqiang Suo, Davide de Battisti, Nia Fry, Razia Bano, Khalid Abdul, Hussein Asker, Ifan Johnston, Dan Jones, Muneefah Alenezi and Daniel Strömbom.

Anyone else who believes that has helped somehow.



# Contents

<b>Summary</b>	<b>iii</b>
<b>Declaration and Statements</b>	<b>v</b>
<b>Acknowledgements</b>	<b>vii</b>
<b>1 Introduction</b>	<b>1</b>
1.1 Functional traits in interaction networks . . . . .	2
1.1.1 Describing direct biotic interactions with functional traits . . . . .	2
1.1.2 Finding the minimum mechanistic dimensionality of networks . . . . .	5
1.2 Fungal community dynamics of spatial competition . . . . .	7
1.2.1 Quantifying six basic elements of spatial competition . . . . .	7
1.2.2 Modelling and predicting fungal community dynamics . . . . .	8
1.3 Summary . . . . .	10
<b>2 Framework for direct interactions</b>	<b>11</b>
2.1 The mechanistic framework . . . . .	11
2.1.1 Stage 1: Defining the study system . . . . .	11
2.1.2 Stage 2: Charting the modes of interaction . . . . .	14
2.1.3 Stage 3: Explaining the subtask outcomes . . . . .	15
2.2 Framework overview with an empirical system . . . . .	17
2.2.1 Stage 1: Defining the study system . . . . .	17
2.2.2 Stage 2: Charting the modes of interaction . . . . .	18
2.2.3 Stage 3: Explaining the subtask outcomes . . . . .	18
2.3 Summary . . . . .	20
<b>3 Minimum mechanistic dimensionality</b>	<b>23</b>
3.1 Methods . . . . .	23
3.1.1 The minimum mechanistic dimensionality of networks . . . . .	23
3.1.2 Comparing the minimum dimensionality of empirical networks under five perspectives . . . . .	29
3.2 Results . . . . .	32

3.2.1	Multimodal versus unimodal dimensionality . . . . .	32
3.2.2	Included versus excluded failure outcomes . . . . .	32
3.2.3	Mechanistic versus phenomenological dimensionality . . . . .	32
3.3	Summary . . . . .	34
<b>4</b>	<b>Experiments on fungal competition for space</b>	<b>35</b>
4.1	Materials and methods . . . . .	35
4.1.1	Study species and general setting . . . . .	35
4.1.2	Element 1: extension rate in relation to mycelial size, shape, position, age . . . . .	36
4.1.3	Element 2: extension rate in presence of other mycelia . . . . .	38
4.1.4	Element 3: replacement rate in relation to age of mycelial regions	39
4.1.5	Element 4: replacement rate in relation to mycelial cover . . . . .	39
4.1.6	Element 5: replacement rate in relation to multiple adjacent heterospecifics . . . . .	40
4.1.7	Element 6: additive or non-additive effects of competition . . . . .	40
4.1.8	Prediction of community dynamics . . . . .	40
4.2	Results . . . . .	43
4.2.1	Element 1: extension rate in relation to mycelial size, shape, position, age . . . . .	43
4.2.2	Element 2: extension rate in presence of other mycelia . . . . .	43
4.2.3	Element 3: replacement rate in relation to age of mycelial regions	43
4.2.4	Element 4: replacement rate in relation to mycelial cover . . . . .	43
4.2.5	Element 5: replacement rate in relation to multiple adjacent heterospecifics . . . . .	47
4.2.6	Element 6: additive or non-additive effects of competition . . . . .	47
4.3	Summary . . . . .	47
<b>5</b>	<b>Lattice model of fungal spatial competition</b>	<b>49</b>
5.1	Methods . . . . .	49
5.1.1	Lattice model general description . . . . .	49
5.1.2	Model general algorithm . . . . .	50
5.1.3	Model incorporation of spatial competition elements . . . . .	50
5.1.4	Model parameter estimation . . . . .	52
5.2	Results . . . . .	57
5.3	Summary . . . . .	62
<b>6</b>	<b>Differential equations for fungal competition</b>	<b>63</b>
6.1	Results . . . . .	63
6.1.1	1-species master equation . . . . .	63

<i>CONTENTS</i>	xi
6.1.2 1-species ODE model . . . . .	65
6.1.3 2-species master equation . . . . .	68
6.1.4 2- and 3-species ODE models . . . . .	69
6.1.5 1-species PDE model . . . . .	70
6.1.6 3-species PDE model . . . . .	71
6.2 Summary . . . . .	72
<b>7 Discussion</b>	<b>75</b>
7.1 Functional traits in interaction networks . . . . .	75
7.1.1 Describing direct biotic interactions with functional traits . . . . .	75
7.1.2 Finding the minimum mechanistic dimensionality of networks . . . . .	78
7.2 Fungal community dynamics of spatial competition . . . . .	80
7.2.1 Quantifying six basic elements of spatial competition . . . . .	80
7.2.2 Modelling and predicting fungal community dynamics . . . . .	82
7.3 Limitations and future directions . . . . .	85
<b>References</b>	<b>89</b>





# Chapter 1

## Introduction

Ecology (*sensu* Haeckel, 1866), the study of interactions between individuals and their environment, has long noted that individuals live in interaction rather than in isolation with other individuals of the same or different species, in ‘closely-knit communities or societies comparable to our own’ (Elton, 1927). Biotic interactions, between individuals of the same species (‘conspecifics’) or different species (‘heterospecifics’), are respectively called ‘intraspecific’ and ‘interspecific’. Different types of biotic interaction can occur within a community, for example, consumption, dominance, spatial replacement, parasitism, provisioning, protection, cleaning, dispersal, and pollination of other individuals (Morin, 2011; Davies *et al.*, 2012). Biotic interactions have been categorised on the basis of their positive, negative, or null outcome on population growth (Burkholder, 1952), or individual fitness (Hamilton, 1964). For example, mutualism is a positive net fitness outcome for both interacting individuals. Additionally, interactions have been categorised as direct or indirect (Abrams, 1987; Wootton, 1994). In direct interactions, which are the focus of this thesis, the effects of an interaction reach the interacting individuals directly, without any effects transferred via intermediary individuals or environmental variables.

Individuals are identified by specific qualities, parts, and actions, such as individual body mass, which are called ‘traits’ (Wagner, 2001). A wide range of questions about direct intraspecific and interspecific interactions are addressed with trait-based approaches. These questions can be categorised as proximate or evolutionary (Dewsbury, 1999). Examples of proximate (‘how’) questions address which key traits best explain interaction outcomes (Eklöf *et al.*, 2013; Vieira & Peixoto, 2013; Olito & Fox, 2015; Dehling *et al.*, 2016), and how are key traits involved in the interactions and outcomes (Ibanez *et al.*, 2012; Ryan & Cummings, 2013; Dy *et al.*, 2014). Examples of evolutionary (‘why’) questions focus on justifying key traits correlating with individual fitness (Sih *et al.*, 2012; Seppälä, 2015), on the relative impact of phylogenetic history (Becerra, 2003; Sanders *et al.*, 2014), and on the evolution of traits and population or community structure (Pinter-Wollman *et al.*, 2014; Strauss, 2014). Moreover, trait-based approaches can be regarded as mechanistic or phenomenological (Ings *et al.*, 2009). For

instance, explanation of food web structure can be attempted by assuming mechanistic rules of allometric foraging behaviour (Petchey *et al.*, 2008), or phenomenologically by assuming exploitation of resources with mainly smaller trait values in a range (Williams & Martinez, 2000). Mechanistic approaches employ ‘functional’ traits, which are measurable features of the interacting individuals, regarding their physiology, morphology, behaviour, and phenology (Arnold, 1983; McGill *et al.*, 2006; Violle *et al.*, 2007).

This thesis aimed to provide two main theoretical contributions, one for mechanistic approaches, the other for phenomenological. For mechanistic approaches, the aim was a generalising mechanistic description of direct biotic interactions independently of system type, which can incorporate alternative interaction modes, e.g. alternative feeding modes, since previous theoretical works focus on specific system types or questions (Poisot *et al.*, 2015; Bartomeus *et al.*, 2016). For phenomenological approaches, the aim was a generalising theoretical view on the basic elements of fungal competition for space, in an attempt to predict the dynamics of multi-species fungal communities, since the five relevant theoretical models in the literature lack such comprehensive view and link to empirical community dynamics (Halley *et al.*, 1994; Davidson *et al.*, 1996a; Bown *et al.*, 1999; Falconer *et al.*, 2008; Boswell, 2012). Details on the background knowledge, knowledge gaps, and motivation for each of the two main contributions are provided in Section 1.1 (for Chapters 2 and 3, about mechanistic approaches), and Section 1.2 (for Chapters 4, 5 and 6, about phenomenological approaches). The final Chapter 7 holds the discussion, conclusions and future directions of the thesis findings.

## 1.1 Functional traits in interaction networks

### 1.1.1 Describing direct biotic interactions with functional traits

Addressing study questions related to direct biotic interactions demands a theoretical—conceptual or mathematical—description of how interactions occur. For example, experimentally investigating key traits in phage–bacterium interactions requires a conceptual representation of the infection process (Dy *et al.*, 2014). The phylogenetic study of plant–herbivore coadaptation relies on understanding how plants and herbivores interact via defences and counterdefences (Becerra, 2003). Interaction mechanisms of trait complementarity and exploitation barriers underlie the theoretical study of plant–pollinator community structure (Santamaría & Rodríguez-Gironés, 2007).

Direct biotic interactions in different systems appear to occur sharing four common features: (1) interactions within a system can be of various types (Fig. 1.1a); (2) for each interaction type, there can be alternative interaction modes of achieving the same successful interaction outcome (Fig. 1.1b); (3) for a success via an interaction mode, multiple tasks may need to be accomplished (Fig. 1.1c); and (4) the outcome in each

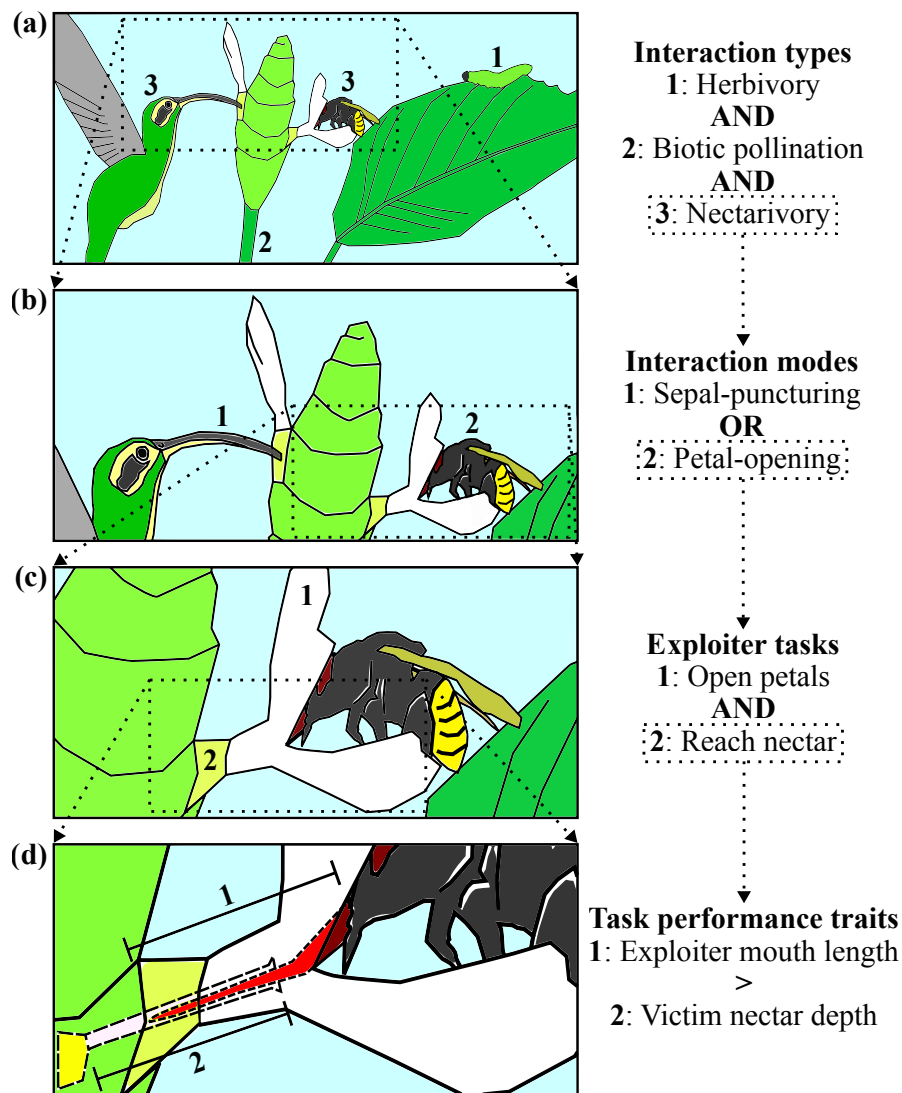


Figure 1.1: Summary of the four features of direct biotic interactions. In each feature's panel, the illustration of the hypothetical system on the left is accompanied on the right by the indexed examples of the illustration, and the logical operator associating these examples. Dotted boxes and arrows indicate focusing in to the next feature. The four features are: (a) different interaction types can appear in a system; (b) in a single interaction type, there can be alternative interaction modes leading to the successful interaction outcome; (c) for a success via an interaction mode, there can be multiple tasks which the exploiter must accomplish against the victim; and (d) for a task success in an interaction mode, the performance in a trait of the exploiter must be higher than the performance in a trait of the victim.

task depends on the comparison between a pair of traits of the interacting, exploiter–victim individuals (Fig. 1.1d). Interaction types range from mutualistic, to antagonistic, to intra- and interspecific helping, dominance, fighting, and territoriality interactions (Morin, 2011; Davies *et al.*, 2012). For one type of interaction, examples of alternative interaction modes are the different feeding modes employed for trophic consumption (Kiørboe, 2011), the alternative visual and olfactory floral signals for attracting plant

biotic pollination (Schiestl & Johnson, 2013), the independent pathways which phages follow for successful bacterial infection (Meyer *et al.*, 2012), and the different combative mechanisms when fungi interact antagonistically with one another (Boddy, 2000). An interaction mode usually includes multiple tasks. For example, a predator must succeed against a prey in all tasks of a typical predatory feeding mode: encounter, detection, identification, approach, subjugation, and consumption of prey (Endler, 1991); and a phage must succeed in all tasks of a bacterium exploitation mode, including attachment, DNA injection, replication, transcription, translation, assembly, and lysis (Dy *et al.*, 2014). For a specific task, the competing functional traits involved are measurable features of the exploiter–victim interacting individuals (Arnold, 1983; McGill *et al.*, 2006; Violle *et al.*, 2007): physiological (e.g. herbivore detoxification enzyme versus plant toxin concentration), morphological (e.g. animal proboscis length versus plant depth of nectar in floral tube), behavioural (e.g. cleaner fish cheating versus client punishment severity), and phenological (e.g. predator temporal presence versus prey absence).

Despite the accumulated empirical knowledge about how interactions occur, previous theoretical works lack an explicit incorporation of the feature of alternative interaction modes, and frequently other features in their mathematical descriptions. On one hand, theoretical works have focused on particular types of interaction in one mode, for example, on mutualistic (Santamaría & Rodríguez-Gironés, 2007; Vázquez *et al.*, 2009a; Campbell *et al.*, 2011; Guimarães Jr *et al.*, 2011; Nuismer *et al.*, 2013), antagonistic (Abrams, 2000; Nuismer *et al.*, 2005; Nuismer & Thompson, 2006; Gilman *et al.*, 2012), or trophic interactions (Cohen & Newman, 1985; Williams & Martinez, 2000; Cattin *et al.*, 2004; Stouffer *et al.*, 2006; Allesina *et al.*, 2008; Petchey *et al.*, 2008; Gravel *et al.*, 2013). On the other hand, theoretical works for different interaction types lack multiple tasks in the single interaction mode (Kopp & Gavrillets, 2006), lack a mechanistic perspective (Eklöf *et al.*, 2013; Bastazini *et al.*, 2017; Ovaskainen *et al.*, 2017), or an explicit reference to alternative interaction modes (Poisot *et al.*, 2015; Bartomeus *et al.*, 2016; Dalla Riva & Stouffer, 2016).

In Chapter 2, I aimed to develop a generalised description of how direct interactions occur. I present the framework in three stages, encompassing all four features in the description of interactions outlined by empirical studies (Fig. 1.1). Direct interactions in a system: (1) can be of different types called ‘focal tasks’ in the framework (first feature in the empirical description of interactions); (2) follow alternative ‘subtask’ strategies to focal task success, called ‘interaction modes’ in the framework (second and third features); and (3) are resolved by functional trait competition (fourth feature). Following the framework description, I summarise the framework by applying it to an empirical plant–pollinator system, showing the systematic charting of the interactions and traits, e.g. how alternative nectarivory modes of animals, and multiple plant exploitation

barriers against nectarivory, are described in a standardised way.

### 1.1.2 Finding the minimum mechanistic dimensionality of networks

The set of interaction outcomes in a group or community, i.e. the group or community structure, can be conceptually or mathematically represented with a network or graph (see Box 1.1 for definitions of network terms; for a review of network theory, see Newman, 2003).

Understanding community structure can improve our predictions of structure dependent population dynamics and stability (Berlow *et al.*, 2009; Valdovinos *et al.*, 2010), population evolution (Becerra, 2003; Sanders *et al.*, 2014), ecosystem processes and functioning (Woodward *et al.*, 2008; Rudolf & Rasmussen, 2013), and conservation and ecosystem management (Ribeiro Mello *et al.*, 2015; Pires *et al.*, 2017). Communities are structured by different forces (Vázquez *et al.*, 2009b; Poisot *et al.*, 2015; Bartomeus *et al.*, 2016), including: evolution; spatio-temporal distribution of species due to neutral,

#### Box 1.1: Definitions of terms in network (graph) theory

*Network (graph)*: A conceptual and mathematical representation of connections among objects (e.g. a food web representing who consumes whom).

*Edge (link)*: A connection among one or more objects of a network. Edges may have direction (e.g. directed from resources to consumers in a food web), can be of various types (e.g. predatory or parasitic interactions in a food web), and may have qualitative and quantitative attributes (e.g. consumer exploitation strategy and biomass consumed from each particular resource).

*Vertex (node)*: An object of a network. Vertices can be of various types (e.g. plant or herbivore), and may have qualitative and quantitative attributes (e.g. life stage and body mass of each individual or species).

*Part*: A set of vertices of the same type (e.g. the part of the plants, and the part of the herbivores).

*Multilayer network*: A network composed of multiple layers. Various aspects determine the network layers. Examples of aspects are the type of edges, the season that the data were collected, and the identity of the observer. Thus, we would create a layer for each combination of edge type, season, and observer. A layer can host a subset of the vertices, and edges can connect vertices in different layers.

*Unipartite graph*: A network with all vertices belonging to one part. Edges are allowed between any vertices (e.g. in a food web with potential consumption of an individual or species by any other individual or species).

*Bipartite graph*: A network with the vertices allocated in two parts. Each vertex can have edges only with vertices from the other part (e.g. in a plant–herbivore network, representing consumption of plants by herbivores).

*Weighted network*: A network with weighted edges, i.e. edges with quantitative attributes (e.g. a weighted food web can show not only who consumes whom, but also how much).

historical, dispersal, or habitat filtering processes; interaction neutrality; and traits of individuals. Regarding the contribution of individual traits, a first information we can ask for is the minimum number of traits that must be involved given the observed community structure, which I call ‘minimum dimensionality’ of a community. The minimum dimensionality of a system can concentrate our efforts investigating which traits are necessary and contribute more to community structure (Eklöf *et al.*, 2013).

A mechanistic method for estimating the minimum dimensionality must make assumptions about how interactions are expected to occur. Interactions in different systems appear to share four common features, as summarised graphically in Fig. 1.1. However, the two available methods to estimate minimum dimensionality lack a mechanistic perspective, or an explicit incorporation of the widespread feature of alternative interaction modes. Eklöf *et al.* (2013) developed the first method for the minimum dimensionality in different interaction types, rooted in theoretical works about food web intervality in niche space (Cohen, 1977; Williams & Martinez, 2000; Stouffer *et al.*, 2006; Allesina *et al.*, 2008; Rossberg *et al.*, 2010). The method attempts to order the species in each niche dimension, such that only the resources (exploiters) of each exploiter (resource) lie in the resulting niche. Minimum dimensionality is the minimum number of dimensions for a possible ordering, but dimensions originate phenomenologically, possibly accounting for multiple traits each. Additionally, the traits of exploiters (resources) have no place in the niche space because it is created by trait dimensions of the resources (exploiters), and some traits can be irrelevant in common niche space (e.g. plant traits for herbivores). Consequently, this method does not take into account the traits of both exploiters and resources simultaneously. The minimum dimensionality method of Dalla Riva & Stouffer (2016) avoids these issues by adopting a simple trait space representation for trophic interactions. Resource and exploiter traits are modelled explicitly, and network structure is explained mechanistically by resource–exploiter trait matching. However, Dalla Riva & Stouffer (2016) essentially model interactions via a single interaction mode, since the contributions from each resource–exploiter trait matching are incorporated in one sum with the dot product of the trait vectors, limiting alternative sums (interaction modes) to be incorporated. The same lack of incorporating alternative interaction modes appears and in Eklöf *et al.* (2013), because niche dimensions act in conjunction to determine the niche of the exploiter (resource).

In Chapter 3, I aimed to develop a new method for the minimum number of traits involved mechanistically in the direct biotic interactions of a system. This ‘minimum mechanistic dimensionality’ method is based on the mechanistic framework described in Chapter 2, encompassing all four features of interactions outlined by empirical studies, within a simple phenotype space representation. Applying the method, I ask if minimum mechanistic dimensionality is higher under the assumption of alternative interaction modes compared to a single mode, if it is higher with failure outcomes taken into

account instead of omitted, and if it is higher than the minimum dimensionality under the phenomenological, niche approach of Eklöf *et al.* (2013). I show that the minimum number of traits involved in 658 empirical systems can be underestimated by omitting the presence of alternative interaction modes, the trait-mediated failure outcomes, and the mechanistic involvement of traits competing in pairs.

## 1.2 Fungal community dynamics of spatial competition

### 1.2.1 Quantifying six basic elements of spatial competition

Mycelium, the vegetative growth form of filamentous fungi, comprises hyphae (fine filaments with chains of compartments) which elongate, branch, and fuse, creating an extending network (Plomley, 1959; Prosser & Trinci, 1979; Fricker *et al.*, 2017). Heterospecific, and somatically incompatible, non-fusing mycelia compete for resources in the substratum, essentially competing for space. Fungal competition for space is realised via three mechanisms according to ecological theory (Schoener, 1989; Boddy, 2000): preemption of unoccupied space; resource exploitation; and direct, harmful replacement after physical contact or chemical production. Different abiotic and biotic elements influence the outcomes of spatial competition (Boddy, 2000; Kennedy, 2010; Hiscox & Boddy, 2017): temperature, pH, water potential, gaseous regime, resource quality and concentration, type of substratum, invertebrate grazing, size of space occupied by a mycelium, multiple adjacent heterospecific mycelia, and species identity.

For given abiotic conditions, and in absence of non-fungal species, empirical findings can be grouped into six elements of spatial competition between fungal mycelia. First, mycelial boundary extent to unoccupied space is commonly linear in time (Brown, 1923; Fawcett, 1925; Ryan *et al.*, 1943; Plomley, 1959), with faster extending species preempting more space. Second, this ability to capture unoccupied space might be inhibited or enhanced by the presence of adjacent or distant conspecific or heterospecific mycelia (Griffith & Boddy, 1991; Heilmann-Clausen & Boddy, 2005; Evans *et al.*, 2008; Sonnenbichler *et al.*, 2009). Third, following the initial extension to an unoccupied site, a mycelium increases in hyphal density at that site (Plomley, 1959; Trinci, 1969), attaining its full density and hence potential to replace or to resist replacement locally as it matures (Stahl & Christensen, 1992). Fourth, the ability to replace or resist replacement is higher the greater the space occupied (Holmer & Stenlid, 1993; White *et al.*, 1998; Bown *et al.*, 1999; Sturrock *et al.*, 2002; Song *et al.*, 2015; Hiscox *et al.*, 2017), because local competitive ability is enhanced by translocation of resources from the whole mycelium (Jennings, 1987; Olsson, 1999; Lindahl *et al.*, 2001). Fifth, a mycelium commonly has to translocate and distribute its finite resources to multiple boundaries, to replace or resist replacement against multiple adjacent heterospecific mycelia, likely dividing its

competitive ability among the adjacent competitors (White *et al.*, 1998; Bown *et al.*, 1999; Sturrock *et al.*, 2002; Hiscox *et al.*, 2017). Sixth, competition between multiple species might differ from pairwise species interactions in isolation, due to higher-order interactions, i.e. existence of non-additive effects of competition (Hiscox *et al.*, 2017).

For Chapter 4, I quantified experimentally these six basic elements of spatial competition for three species of filamentous fungi in closed, dispersal-free laboratory communities, in presumably stable and homogeneous abiotic conditions. I found that three elements had the simplest form possible (constant extension rates; extension rates unaffected by other mycelia; and additive effects of competition), and the other three elements had a more involved form (faster replacement of younger regions of mycelia; faster replacement of smaller mycelia; and replacement as if mycelia are divided to multiple adjacent competitors proportionally to the length of boundary with each). These experimental findings could be incorporated to a relatively simple model for testing the predictability of 2- and 3-species fungal community dynamics (Chapters 5 and 6).

## 1.2.2 Modelling and predicting fungal community dynamics

The use of a theoretical model is beneficial for the study of community dynamics, even with the approximating assumptions underlying it. Only with a theoretical model can we solve or compute rapidly for the dynamics of a community. Additionally, building a theoretical model is an exercise of testing and keeping only the basic elements involved in the dynamics, such as the six experimentally quantified elements of spatial competition from Chapter 4.

In filamentous fungi, as a benefit from theoretical modelling, the enhanced understanding of the different basic elements of spatial competition can help us predict fungal community dynamics, and hence improve forecasts of community-dependent processes such as biogeochemical cycling, primary production, biocontrol, and bioremediation (Hiscox *et al.*, 2015; Moeller & Peay, 2016; Buchkowski *et al.*, 2017; Oliva *et al.*, 2017; Stella *et al.*, 2017). Nevertheless, despite the empirical literature on the six basic elements of spatial competition, no previous theoretical work has incorporated all of them in a single model. In my knowledge, only five theoretical models of interspecific interactions between filamentous fungi have appeared in the literature, a surprisingly small number for a whole kingdom of life (Halley *et al.*, 1994; Davidson *et al.*, 1996a; Bown *et al.*, 1999; Falconer *et al.*, 2008; Boswell, 2012).

In the first theoretical study of fungal interactions, the cellular automaton model assumes fixed replacement outcomes between species pairs, omitting any relation of replacement with mycelial age, size, and contact with multiple heterospecific mycelia (Halley *et al.*, 1994). Davidson *et al.* (1996a,b) modelled interacting mycelia as local concentrations of activator responsible for converting local concentrations of substrate



to biomass with a reaction–diffusion system of partial differential equations. Due to the nature of this activator–substrate model, there is no way for one mycelium to replace another, and for a mycelium to distribute its competitive ability between adjacent heterospecifics. Bown *et al.* (1999) attempt to predict 2-species community dynamics with a cellular automaton model. Their model omits the elements of whole mycelial cover because local changes in species occupancy are affected by only the local neighbourhood, and not by the entire cover of the adjacent mycelia, although one of the model parameters can be estimated such that it acts as surrogate for mycelial cover. Due to this lack of whole mycelium integration, the model omits the element of distribution of competitive ability to multiple adjacent heterospecifics as well. In the detailed, physiological model of Falconer *et al.* (2008), each mycelium is described by a system of partial differential equations, and replacement can occur if the replacing mycelium can inhibit the extension of the replaced mycelium, and the replaced mycelium possesses autophagic abilities to surrender the occupied space to the replacing mycelium. Although the replacing mycelium’s cover appears to be at play, due to the diffusion of mobilised biomass towards the replaced mycelium, a larger cover of the replaced mycelium will not decrease its replacement rate. Thus, this model does not incorporate the empirical element of replacement rates depending on the mycelial cover of both competitors. Similarly, in the partial differential equations model of Boswell (2012), replacement rate depends on the local biomass of the replacing mycelium, but not on the biomass of the replaced mycelium.

In Chapter 5, I aimed to develop a spatially explicit, lattice model incorporating all six basic elements of spatial competition between filamentous fungi. In particular, I aimed to test if all six elements are necessary for accurate model prediction of the dispersal-free laboratory community dynamics consisting of two and three species of wood decay fungi (Chapter 4). I found that incorporating all six elements in their experimentally quantified form was necessary for an accurate theoretical prediction of empirical community dynamics.

A main characteristic of the lattice model in Chapter 5 is its stochastic nature. Running once the lattice model simulates one stochastic realisation of the modelled phenomenon. Thus, multiple simulation runs are needed for inference about, for instance, the average behaviour of the modelled system. Ordinary differential equations (ODE) and partial differential equations (PDE) can model the average behaviour of a system deterministically, and they are liable to mathematical analysis which offers comprehensive insight about the dynamics and the underlying parameter values.

In Chapter 6, I develop simple ODE and PDE models, for predicting fungal community dynamics (validated against the empirical data from the experiments in Chapter 4). The basic processes of extension and replacement in the lattice model of Chapter 5 were incorporated in the derivation of master equations. I took mean-field approximations for

the master equations' first moment, to arrive to ODE for the mean relative abundance of species in well-mixed culture of dispersed mycelia. The non-spatial nature of the ODE model prevented the prediction of even 1-species dynamics on experimental Petri dish. The ODE models were then incorporated as reaction terms in reaction–diffusion PDE. These spatial, PDE models were able to predict 1-species empirical dynamics, but suffer from limitations in incorporating particular elements of fungal competition for space, and in modelling multi-species interactions in general.

### **1.3 Summary**

The aim of this thesis was to develop novel generalising mechanistic approaches to direct biotic interactions in general, and to phenomenologically-based community dynamics of fungal competition for space in particular. Chapter 2 describes a novel generalising mechanistic perspective on direct biotic interactions. With the generalising description of biotic interactions from Chapter 2, I develop a method for the calculation of the minimum number of functional traits that must be involved mechanistically in the interactions of any type of system (Chapter 3). Passing to the phenomenological contributions, I experimentally quantified six basic elements of fungal competition for space between three wood decay fungi, to acquire a generalising view about the forces driving fungal community dynamics (Chapter 4). In Chapter 5, I developed a lattice model of fungal interactions in space which could incorporate the experimentally quantified elements from Chapter 4, and could precisely predict the spatial competition dynamics of the 2- and 3- species experimental, fungal communities. Lastly, I developed models of fungal interactions with ordinary and partial differential equations, showing that the lack of modelling space in the ordinary differential equations, and the modelling characteristics of partial differential equations, can reduce the plausibility of the models, and their ability to predict empirical dynamics of fungal communities (Chapter 6). The final Chapter 7 holds a general discussion, conclusions and future directions of the thesis findings.

## Chapter 2

# How direct biotic interactions occur: a mechanistic framework

A generalising description of how direct interactions occur will be presented. This mechanistic framework is described in three stages. I then apply the framework to an empirical plant–animal network. This mechanistic framework will be the base for a method which evaluates the minimum number of functional traits involved in the interactions given the interaction outcomes of a network, in the following Chapter 3.

### 2.1 The mechanistic framework

Before presenting the framework, I raise three points. First, the framework is applicable to individuals, but also to other levels of biological organisation, e.g. populations, species, or other taxonomic or functional groups, assuming it is sensible from a trait-based viewpoint (Ings *et al.*, 2009). Therefore, I broadly refer to interacting ‘players’ throughout. Second, the framework concerns direct interactions. Indirect interactions are out of scope, requiring intermediary players, or environmental variables (Abrams, 1987; Wootton, 1994). Third, I limit this first account of the framework to only pairwise interactions. The pairwise interaction is the simplest case, with the minimum number of players for an interaction to occur. Thus, systems in this chapter range from a pair of interacting players, to networks of pairwise interactions (see Box 1.1 for definitions of network terms; for a review of network theory, see Newman, 2003).

#### 2.1.1 Stage 1: Defining the study system

##### *Step 1: Player tasks*

The unifying concept underpinning the framework posits that interactions ‘appear’ to be directed by tasks. Common examples of player focal tasks are consumption, dominance,

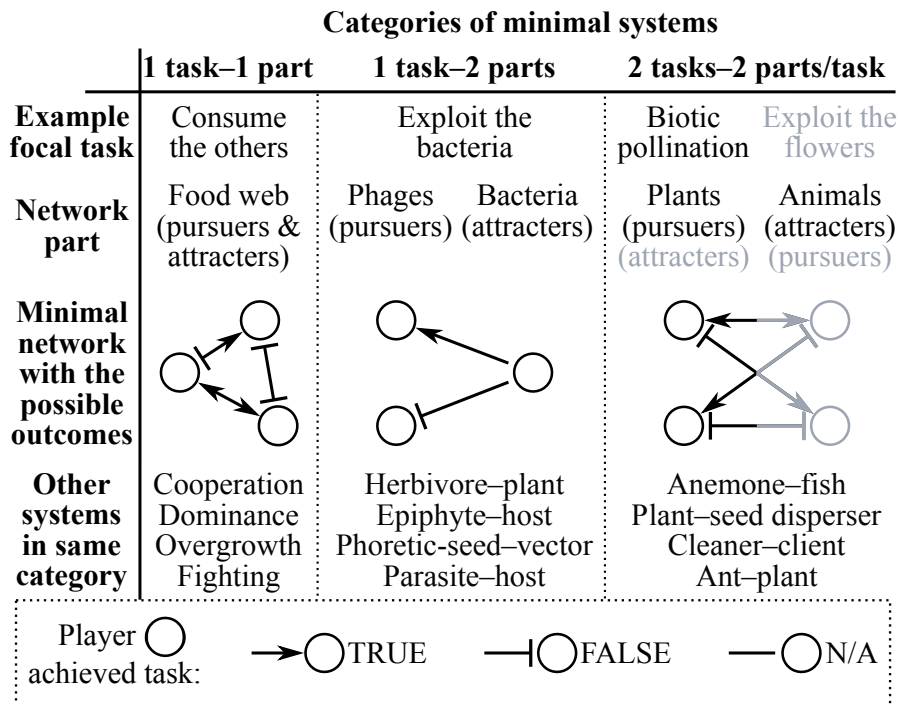


Figure 2.1: Framework stage 1: defining and categorising a study system. The framework determines player focal tasks, partitions players to task pursuers and attracters, and identifies the possible task pursuit outcomes (see Box 2.1 for definitions of framework terms). A system must have at least one underlying focal task, and task failures are also interaction outcomes. ‘Minimal’ systems have at most two focal tasks, with each player pursuing one task in maximum. In the third category of 2 tasks–2 parts/task, the two focal tasks are shaded differently, distinguishing the outcomes of each task in the minimal network.

replacement, capturing of territory, defeat, and parasitism of others; or attraction of their provisioning, protection, cleaning, dispersal, and pollination services. I expect at least one focal task to underlie a study system, and multiple tasks can be implemented in an integrated system, i.e. as a multilayer network (Ings *et al.*, 2009; Fontaine *et al.*, 2011; Kivelä *et al.*, 2014; Piloosof *et al.*, 2017). In a multilayer network, each layer relates to one focal task, i.e. one type of interaction (Fig. 1.1a). Commonly studied systems appear to be governed by one or two focal tasks (Fig. 2.1), for example, the food webs with the single task of consumption of the other players, and the phage–bacterium systems with the phages’ task to exploit the bacteria. Examples with two tasks are plant–animal systems with the plants’ task of receiving an animal service (e.g. pollination), and with the animals’ task of exploiting a plant resource (e.g. nectar or pollen). Hence, we represent such plant–animal systems with bilayer networks, with one layer for the plants’ task, and one layer for the animals’ task.

***Step 2: Task pursuers and attracters***

An interaction appears to occur due to a task pursued by one interacting player, the ‘pursuer’, attracted to the other player, the ‘attractor’. A player can be considered only pursuer, only attracter, or both pursuer and attracter of a focal task (Fig. 2.1). In the example of food webs, each player is both a potential consumer (pursuer) and a potential resource (attractor). We allocate all players to one group, called ‘part’, as both pursuers and attracters of consumption, representing food webs as unipartite graphs. In the example of phage–bacterium systems, the phages are only pursuers, and the bacteria are only attracters. In this case, we have two parts, representing phage–bacterium systems as bipartite graphs: the part of pursuers (the potential exploiters), and the part of attracters (the potentially exploited). As in bipartite graphs, we assume no interactions within the pursuers or the attracters of a part, since a task-directed interaction occurs only between a pursuer and an attracter. In general, there can be only two allocation possibilities in pairwise interactions: (1) unipartite, with players belonging to one part, considered both pursuers and attracters of a focal task; or (2) bipartite, with players allocated to two parts, the part of pursuers, and the part of attracters. In the example of the bilayer plant–animal system, both network layers are bipartite: in the first layer of the plants pursuing pollination, the plants are pursuers, and the animals are attracters; conversely, in the second layer, the animals are now pursuers of floral exploitation, whereas the plants are attracters.

***Step 3: Possible interaction outcomes***

Given the focal tasks, and the allocation to parts, we can identify the possible outcomes (Fig. 2.1). For example, there are three possible outcomes in a unipartite food web: one of the two interacting players consumes the other, neither consumes the other, or they are mutually consumed. Although the latter outcome of mutual consumption might be impossible in trophic interactions, it can be plausible in other unipartite systems (e.g. cooperation after mutual pursuit of help). In the example of a bipartite phage–bacterium system, there are two possible outcomes: a phage exploits a bacterium, or fails to do so. Lastly, in the example of the plant–animal system, we recognise four possible outcomes: the plant is pollinated, and the animal exploits the plant; neither the plant nor the animal succeed in exploiting the other; the plant is not pollinated, but it is exploited; or the plant is pollinated, and it is not exploited. Note that task failures are also considered interaction outcomes in the framework.

After defining the study system, we can categorise it based on the focal tasks, the allocation of players to parts, and the possible outcomes (see Fig. 2.1 for categories of minimal systems, i.e. of two tasks in maximum, with each player pursuing at most one task).

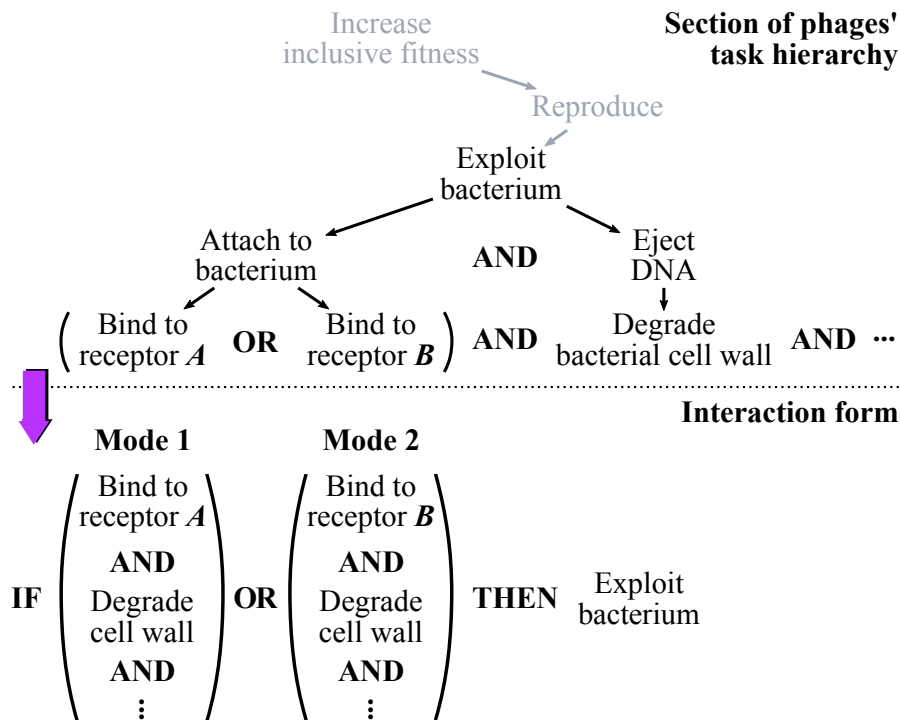


Figure 2.2: Framework stage 2: charting the modes of interaction. With a hypothetical phage–bacterium system, I illustrate the conversion of a section of a focal task hierarchy (to ‘exploit bacterium’) to the interaction form. In the task hierarchy, I list the subtasks upon which the achievement of a task depends, without limiting the list because of temporal dependencies, e.g. although a phage must attach to a bacterium before ejecting the DNA, I list these two prerequisites as subtasks of the task to exploit bacterium. Either all the listed subtasks must be achieved (branching subtasks associated with the logical operator ‘AND’), or at least one of them (operator ‘OR’). The lowest hierarchical level subtasks, with their logical association, are reorganised to the interaction form, a standardised way to describe the interactions regarding a focal task in a system. The interaction form posits that there can be alternative modes for focal task accomplishment (mode 1 and 2 in the phages’ example), whereas all mode subtasks must be achieved for a success via a mode. Logic assures that any logical structure (i.e. any logically associated, lowest hierarchical level subtasks) can be reorganised to the standardised structure of the so-called ‘disjunctive normal form’ (i.e. the interaction form).

## 2.1.2 Stage 2: Charting the modes of interaction

### *Step 1: Task hierarchy*

To achieve a focal task, the pursuers must succeed in subtasks. Achieving these subtasks depends on the success of further subtasks lower in the hierarchy, and so forth, leading to a branching hierarchy of tasks (Fig. 2.2). For example, two of the prerequisites for a phage to exploit a bacterium are the attachment to the bacterial surface, and the ejection of the viral DNA (Dy *et al.*, 2014). Although a phage must attach to a bacterium before ejecting the DNA, the task hierarchy lists these two subtasks, dismissing any temporal dependencies. Lower in the hierarchy of the attachment subtask, two different receptors

could be used for attachment, i.e. two alternative routes to achieve the attachment subtask. In general, a task might require success in all, or in at least one of its subtasks. In other words, subtask statements are associated with the logical operations of AND (conjunction), and OR (disjunction). Note that tasks regarding direct interactions can be understood as embedded in a general hierarchy of tasks, with the increase of inclusive fitness as the ultimate task at the top hierarchical level (Fig. 2.2). Hence, each individual appears as pursuing the maximisation of its inclusive fitness (Hamilton, 1964; West & Gardner, 2013), by strategically investing in the various subtasks of the whole task hierarchy.

### ***Step 2: Interaction form***

I reorganise the logically associated subtasks from the lowest level of the focal task hierarchy to the standardised structure of the ‘interaction form’ (Fig. 2.2). The interaction form is organised into clauses. I name a clause ‘mode’, a distinct strategy towards focal task achievement. The interaction form enables alternative, independent modes for focal task success (Fig. 1.1b). Success via even one mode is sufficient for the success of the focal task, due to the disjunctive OR connecting the modes (Fig. 2.2).

Each mode contains subtasks that must be achieved for a success in the focal task (Fig. 1.1c). If a pursuer fails in even one subtask of a mode, the focal task is not achieved via that mode, illustrated by the conjunctive AND connecting the subtasks. In general, the clauses of the interaction form give priority to the conjunctive operations inside each mode, first checking for success via each mode, and then across modes.

Essentially, the interaction form is the ‘disjunctive normal form’ in logic. Any structure of logical statements can be equivalently expressed in disjunctive normal form (Cohn, 2003). Similarly, any logical association of the subtasks in the lowest level of the task hierarchy can be equivalently charted in a standardised and comparable way by the interaction form.

## **2.1.3 Stage 3: Explaining the subtask outcomes**

### ***Step 1: Power–toughness subtask performance traits***

Conceptually, any outcome arises from a task. Mechanistically, an outcome is determined by the performance of the interacting players (Fig. 1.1d). In the card game *Magic: The Gathering*<sup>®</sup>, a creature has two traits (‘power’ and ‘toughness’) indicating respectively the power to inflict damage, and the toughness against enemy attacks (Garfield, 2017). Correspondingly in the framework, I identify a pursuer trait working towards subtask success, and an attracter trait preventing subtask success (Fig. 2.3). Whereas creatures in the card game interact with a single power–toughness pair of traits, real players

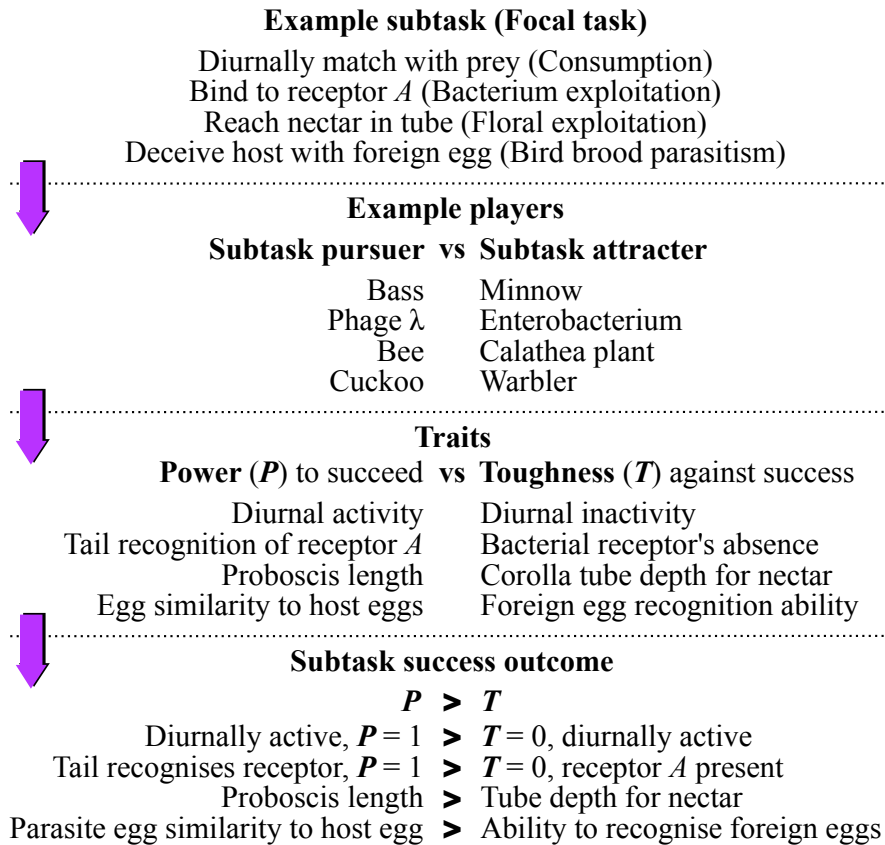


Figure 2.3: Framework stage 3: explaining the subtask outcomes. Four examples are given, passing from the subtask (of a focal task), to the respective players, subtask performance traits, and subtask success outcome in each example. For a subtask in the interaction form, a task pursuer trait competes with a task attracter trait. I call the pursuer trait ‘power’, and the attracter trait ‘toughness’, from the power–toughness creature traits of the card game *Magic: The Gathering*<sup>®</sup> (Garfield, 2017). To determine the subtask outcome, I compare the power and the toughness trait values with an inequality (taken from the creature combat rules of *Magic: The Gathering*<sup>®</sup>).

can possess multiple pairs for the potentially multiple subtasks in the interaction form. I consider that pursuer and attracter are challenged in one trait ‘dimension’ of their phenotype space for each subtask performance competition.

### ***Step 2: Inequality rule of performance competition***

The pursuer’s subtask success follows from the pursuer’s power superiority over the attracter’s toughness (Fig. 2.3). Simply, if the power of the pursuer is greater than the toughness of the attracter, the pursuer succeeds in the subtask, which is the creature combat rule in *Magic: The Gathering*<sup>®</sup> (Garfield, 2017). The inequality rule can demand more than the marginal superiority of the pursuer’s power. For example, to explain weighted subtask successes, the inequality rule can require power superiority proportional to the subtask success weight, instead of only marginal superiority for explaining qualitatively the successes.



**Box 1.2: Definitions of terms in the framework**

*Focal task*: A task that appears to direct one type of interaction. Multiple focal tasks can be studied with a multilayer network, where each focal task underlies a type of interaction (edge) in a layer.

*Players*: The interacting objects in a system. The players are the vertices in a network representation of a system.

*Pursuers*: Players regarded as pursuing a focal task (e.g. predators pursuing consumption of prey).

*Attractors*: Players regarded as attracting pursuers (e.g. prey attracting their consumption by predators).

*Part*: A group of only pursuers, only attractors, or both pursuers and attractors. Such a group is a network part in a network representation.

*Possible outcomes*: A task success or failure of a pursuer. In multiple focal tasks, the overall possible outcomes are the combination of successes and failures in all focal tasks.

*Task hierarchy*: Task achievement can depend on the achievement of other tasks, creating a hierarchy of tasks.

*Subtask*: A task lower than a focal task in the task hierarchy.

*Interaction form*: A standardised and generalised description of how direct interactions occur for a focal task: alternative strategies to focal task success.

*Mode*: A strategy based on subtasks via which a focal task can be reached.

*Power*: The pursuer trait acting towards success in a subtask of a mode.

*Toughness*: The attracter trait acting against pursuer success in a subtask of a mode.

*Dimension*: The pursuer or attracter phenotype space trait dimension which is challenged in a power–toughness performance competition for a mode subtask.

*Inequality rule*: If the pursuer power is sufficiently larger than the attracter toughness, the pursuer wins in the subtask performance competition of a mode.

## 2.2 Framework overview with an empirical system

I illustrate the use of the framework by applying it to an empirical plant–animal system from a lowland wet forest near Puerto Viejo, Heredia, Costa Rica (Kennedy, 1978). The first occurrence of a framework term is given in italics (see Box 2.1 for definitions). The *players* are representative individuals of species reported for that site (Fig. 2.4): three Euglossine bees (*Eulaema speciosa*, *E. seabrai*, and *E. meriana*), a hummingbird (*Phaethornis longirostris*), and a closed-flowered plant (*Calathea marantifolia*).

### 2.2.1 Stage 1: Defining the study system

A system is defined in three steps: determining the player *focal tasks*, allocating the players to *parts*, and identifying the types of *possible outcomes*. I determine two focal tasks (Fig. 2.4): the animals' task of consuming nectar, and the plant's task of receiving animal pollination services. In the animals' focal task, the animals are assigned to the part of *pursuers*, and the plant to the part of *attractors*; in the plant's focal task, the plant

is now the pursuer, and the animals are the attracters. Thus, we have one bipartite graph layer for each focal task. There are four types of possible outcomes in this category of minimal systems (category of 2 tasks–2 parts/task, in Fig. 2.1).

### 2.2.2 Stage 2: Charting the modes of interaction

The first step is to decompose a focal task to *subtasks* in a *task hierarchy*. The second step reorganises the task hierarchy's lowest level subtasks to the standardised *interaction form*. Note that the interaction forms will contain only a few subtasks for the sake of illustration.

For the animals' focal task of consuming nectar, there are two alternative strategies to success: by opening the petals OR through the calyx. This is translated to two disjunctively associated subtasks branching from the focal task in the task hierarchy. The first subtask of consuming nectar by opening the petals requires success in five subtasks: matching spatially AND cutting the flower tip AND separating the petals AND fitting the mouth part in the corolla tube AND reaching nectar down in the holding chamber. Thus, the first subtask of consuming nectar by opening the petals further branches to the five conjunctively associated subtasks. The second subtask of accessing nectar directly through the calyx requires: spatial match AND puncturing of the sepals. Passing to the animals' interaction form, the initial disjunctive branching in the task hierarchy translates to two alternative *modes* to focal task success (Fig. 2.4): the first mode includes the five subtasks that all must be achieved for the opening and exploitation of a flower; and the second mode has two subtasks, puncturing the sepals included.

The plant's focal task mode of biotic pollination implements a specialised mechanism with a trigger that must be pressed inside the flower, releasing the style to hit the animal for pollination. In the task hierarchy, the focal task requires: spatial matching AND hitting an animal with the triggered style. Thus, the plant's interaction form comprises a four-dimensional mode (Fig. 2.4).

### 2.2.3 Stage 3: Explaining the subtask outcomes

In the first step of identifying traits for the subtask pursuits (Fig. 2.4), an animal nectarivory pursuer has to overcome plant toughness traits which are exploitation barriers (Santamaría & Rodríguez-Gironés, 2015). For the plant's focal task, the power of a functional trigger mechanism contributes to the precise transfer of pollen with the style (Santamaría & Rodríguez-Gironés, 2015). The animals might avoid the mechanism by not pressing the trigger, or by not being present on the movement path of the triggered style.

In the second step, I attempt to infer any *inequalities in subtask performance competition* based on the descriptions of Kennedy (1978). All bees achieve the nectarivory focal

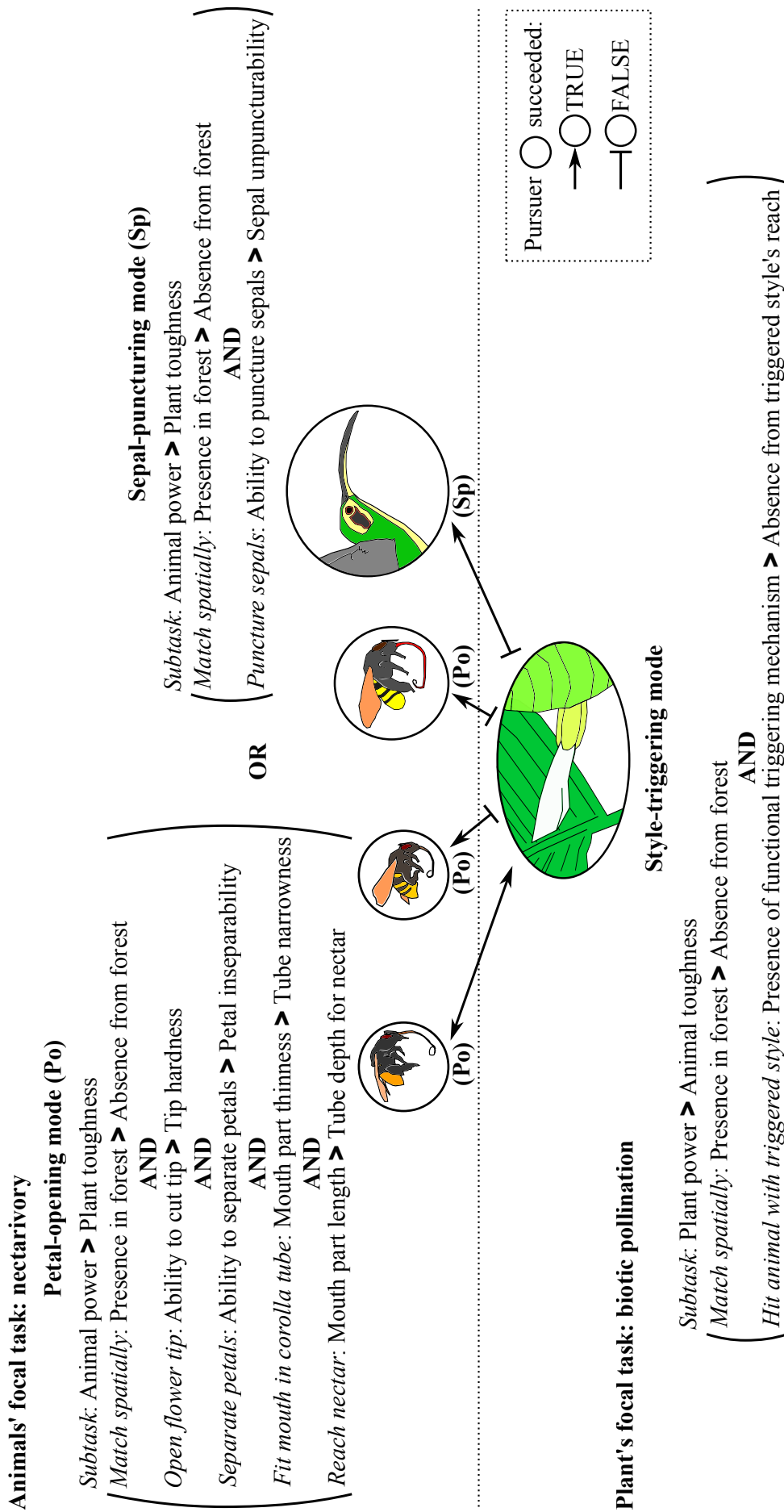


Figure 2.4: Illustrative application of the framework for an empirical system (lowland wet forest near Puerto Viejo, Heredia, Costa Rica, in Kennedy, 1978). From left to right, the animals reported are the three Euglossine bees *Eulaema speciosa*, *E. seabrai*, and *E. meriana*, and the hummingbird is *Phaethornis longirostris*. The plant species is the closed-flowered *Calathea marantifolia* (a closed, white flower is shown in the species token). The modes via which animal pursuers succeed are given in parentheses next to the arrowed outcomes. Species token size indicates the relative size of the representative individual.

task via the first mode of opening flowers, the hummingbird via the second mode of puncturing flowers, and the plant is pollinated only by the *E. speciosa* bee (Fig. 2.4). Bees appear unable to puncture the relatively tough calyx, failing via the second nectarivory mode. The hummingbird does not appear to use the first nectarivory mode, perhaps due to expected failure in at least one subtask (e.g. mouth part cannot fit in the thin corolla tube). For the plant, given the presence of a functional pollination mechanism (the plant power equals one), the animals' toughness depends on the way they handle flowers. The pollinating bee *E. speciosa* forces its head into the flower (the bee's toughness equals zero, inferior to the plant's power), activating the trigger, and the style hits the bee's head. *E. seabrai* has similar proboscis length, but this bee forces the proboscis in by keeping the head outside of the flower (this bee's toughness equals one, equivalent to the plant's power), and out of the style's reach. The larger *E. meriana*, with the lengthier proboscis, does not trigger the mechanism because there is no need to force its head closer to the tube opening to reach nectar (bee's toughness equals one). Lastly, the hummingbird does not pollinate because it robs nectar through the calyx (bird's toughness equals one).

## 2.3 Summary

Trait-based approaches in direct intraspecific and interspecific interactions address proximate and evolutionary questions across biological systems. However, interest in particular questions or systems has led to specialised conceptual and mathematical descriptions of how interactions occur. I propose a generalised description in which interactions can be: defined by 'focal tasks' (i.e. the 'interaction types' in the literature; for example, animal dominance, food web consumption, parasitism, pollination, seed dispersal); analysed and charted systematically in 'subtasks' (i.e. tasks hierarchically associated with logic statements); and explained by subtask 'performance inequalities' (i.e. comparing traits of interacting individuals quantitatively). One framework consequence is that trait-mediated outcomes of interaction are not only the focal task successes which are called 'interactions' in the literature, but also the failures which have been called 'forbidden interactions' or 'forbidden links'. Another consequence is the possibility to model alternative interaction modes, e.g. alternative feeding modes, a feature lacking from previous conceptual and mathematical descriptions. Lastly, the framework can model different types of traits, and I show that matching traits can be reformulated as difference traits. To illustrate, I apply the framework to an empirical plant–animal system. The empirical system is defined by two focal tasks: biotic pollination pursued by the plant species, and nectarivory pursued by the animal species. For the plant species pursuing pollination, a single pollination mode with one subtask is reported, and the plant trait represents a mechanism for the precise transfer of pollen. For the animal species pursuing nectarivory, two alternative nectarivory modes are described, one with

a single and another with four subtasks, with plant traits acting as nectar exploitation barriers. The framework's standardised formulation enables the systematic charting of interactions, allowing comparisons with systems of the same, pollination interaction type, or different interaction type. In general, the framework can provide a common mechanistic basis for proximate and evolutionary questions, facilitating the generation of new hypotheses and trait-based models of social network dynamics, antagonistic or mutualistic community assembly or invasion, and coevolution.



## Chapter 3

# Finding the minimum number of functional traits involved in ecological networks of interactions

Based on the mechanistic framework of Chapter 2, I develop a new method for the minimum number of traits involved mechanistically in the direct biotic interactions of a system. I apply the method to 658 empirical networks, showing that the minimum number of traits involved in the interactions can be underestimated by omitting the presence of alternative interaction modes, the trait-mediated failure outcomes, and the mechanistic involvement of traits competing in pairs.

### 3.1 Methods

#### 3.1.1 The minimum mechanistic dimensionality of networks

In the plant–animal illustration of the mechanistic framework in Chapter 2 (Fig. 2.4), the four animal pursuers of nectarivory succeeded via two alternative modes, one ten-dimensional (bees), the other four-dimensional (hummingbird). Minimally, we could observe these four animal successes in nectarivory via a two-dimensional mode: all animals present at the forest could ‘easily’ consume nectar from a plant with open, wide and short flowers (Fig. 2.4). In other words, if this system was mechanistically minimal, the same outcomes would have occurred only because of spatial matching. Thus, the idea behind this approach is to find a minimal interaction form which is sufficient for the mechanistic explanation of all the observed interaction outcomes of a system. By comparing a theoretically minimal interaction form with the empirically observed one, we can gain insight into the extra strategies, measures, or defences of the players. In the example illustrated in Fig. 2.4, the plant attracter imposed at least five exploitation

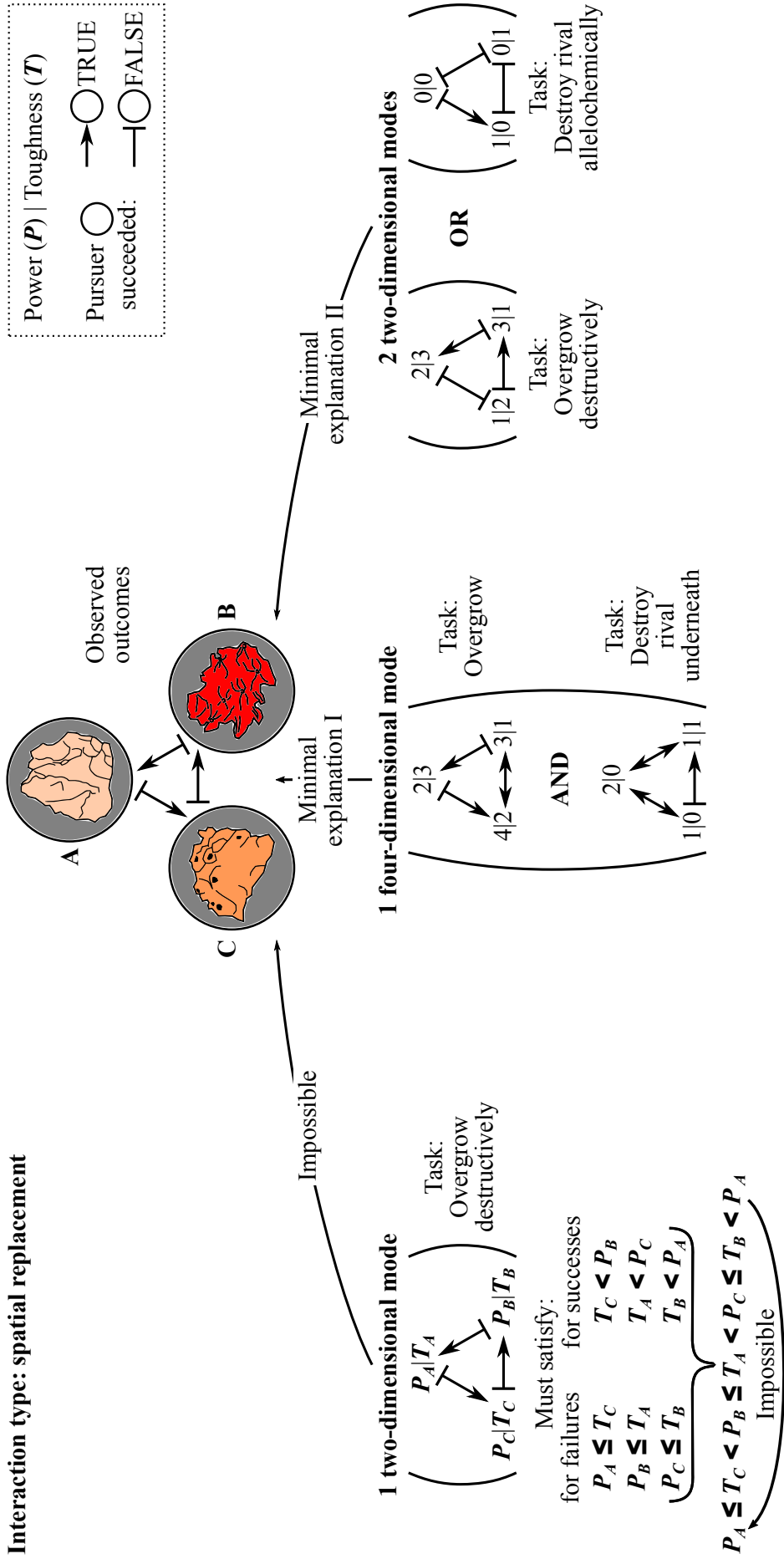


Figure 3.1: The mechanistic explanation of the intransitive interaction outcomes in a rock–paper–scissors empirical system. The empirical system is reported in Jackson & Buss (1975). I show three attempts to explain minimally the observed outcomes, with the first attempt being mechanistically impossible. The mechanistic framework suggests two feasible minimal explanations, the second of which is similar to that suggested by Jackson & Buss (1975). Hypothetical tasks, and trait power|toughness scores are indicated in arbitrary units of performance.



barriers (Santamaría & Rodríguez-Gironés, 2015), challenging the animal nectarivory pursuers in five dimensions instead of the theoretically required one dimension.

### ***Rock–paper–scissors needs at least four dimensions***

The success of the nectarivory pursuers at the empirical plant–animal system in Kennedy (1978) could minimally arise by interactions in a pair of pursuer–attractor trait dimensions. However, two dimensions are not sufficient to explain mechanistically the outcomes of an intransitive network of outcomes between three species, such as the cyclic spatial replacement of marine invertebrates studied by Jackson & Buss (1975): ectoproct species *Stylopoma spongites* (player A) replaces sponge species *Tenaciella* sp. (player B), which in turn replaces sponge species *Toxemna* sp. (player C), which in turn replaces the ectoproct species player A. According to the mechanistic framework (Chapter 2), I consider all three species both pursuers and attracters of spatial replacement (Fig. 3.1).

It is impossible to explain the observed outcomes in this unipartite graph with interactions via a two-dimensional interaction mode. The single pair of power–toughness traits is involved in a system of six inequalities, to satisfy three successes and three failures. For the successful replacements, the power of a winning pursuer must be greater than the toughness of a defeated attracter. For the failures, the power of a losing pursuer must be less than or equal to the toughness of an undefeated attracter. This system of six linear inequalities creates a cyclic sequence of ever-increasing power–toughness scores (impossible attempt in Fig. 3.1).

The mechanistic framework provides two alternative minimal mechanistic explanations for the emergence of a rock–paper–scissors system. First, we can find solutions if we add a second pair of power–toughness traits in the same mode (Fig. 3.1). We explain the failure of players A and B as failure in the first dimension (e.g. overgrowth), and the failure of C as failure in the second dimension (e.g. destruction of rival, even if C can overgrow B). Second, we can find solutions if we add a second pair of power–toughness traits in a new two-dimensional mode (Fig. 3.1). In that case, we explain the success of A and B as success via the first mode (e.g. destructive overgrowth), and the success of C as success via the second mode (e.g. allelochemical elimination). Minimal explanation II is described by Jackson & Buss (1975) for this cryptic reef system: ectoproct player A replaces via overgrowth sponge player B, sponge player B replaces via overgrowth sponge player C, but ectoproct player A does not replace sponge player C via overgrowth as well; instead, ectoproct player A is replaced by sponge player C via toxic effects.

*Linear inequalities method for calculating minimum mechanistic dimensionality*

As I illustrated with the rock–paper–scissors example (Fig. 3.1), systems might require more than one pair of traits for the mechanistic explanation of their outcomes. One method to find the minimum number of trait pairs is by attempting to solve a system of linear inequalities. If the system of linear inequalities is impossible, a simple strategy is to increase the number of trait pairs  $d$  by one, and retry. The minimum  $d \geq 1$  for a feasible system of inequalities is the minimum mechanistic dimensionality (in number of paired traits, i.e.  $2d$ ). In the example of Fig. 3.1, there were two minimal explanations: an additional trait pair belonging to the same mode (minimal explanation I); or belonging to a new two-dimensional mode (minimal explanation II). I will focus on these two extreme explanations, although there could be intermediate minimal interaction forms for more than two trait pairs.

Under minimal explanation I (Fig. 3.1), the  $d$  trait pairs must be involved in the same mode. On one hand, an observed success of pursuer A against attractor B must be the result of success in all tasks (e.g. a successful parasite has overcome all the host defences). Specifically, the power of pursuer A in any trait pair  $i$ ,  $P_{A,i} \geq 0$ , must be greater than the toughness of attractor B in that trait pair,  $T_{B,i} \geq 0$ :  $P_{A,i} > T_{B,i}$ . Since success might require more than the marginal superiority of the pursuer’s power (e.g. for explaining weighted successes with power superiority proportional to the success weight), we can add a superiority threshold,  $t_{A,B,i} > 0$ , making the task success requirement  $P_{A,i} \geq T_{B,i} + t_{A,B,i}$ . On the other hand, an observed failure of pursuer A against attractor B must be the result of failure in at least one task (e.g. a parasite fails against at least one host defence). We can use a binary variable as an indicator of failure in trait pair  $i$ ,  $f_{A,B,i}$  (Williams, 2013). If  $f_{A,B,i} = 1$ , then pursuer A fails against attractor B in trait pair  $i$ ; otherwise,  $f_{A,B,i} = 0$ , a success. The demand for a failure in at least one trait pair  $i$  can be formulated with the linear inequality  $\sum_{i=1}^d f_{A,B,i} \geq 1$ . Finally, I include bounds for the power–toughness differences (Williams, 2013): the sufficiently negative lower bound of the pursuer’s power inferiority in case of task failure,  $m$ ; and the sufficiently positive upper bound of the pursuer’s power superiority in case of task success,  $M$ . Thus, for an observed failure, the following pair of inequalities must be satisfied in any trait pair  $i$ :

$$P_{A,i} + Mf_{A,B,i} \leq T_{B,i} + M, \quad 3.1$$

$$P_{A,i} - mf_{A,B,i} \geq T_{B,i} + t_{A,B,i}. \quad 3.2$$

The extra inequality  $\sum_{i=1}^d f_{A,B,i} \geq 1$  forces at least one of the indicator variables to equal one, i.e. failure in at least one task. In the case of a task failure in trait pair  $i$ ,  $f_{A,B,i} = 1$ , Inequality 3.1 is the task failure requirement, and Inequality 3.2 is the lower bound for the pursuer’s power inferiority. In case of a task success,  $f_{A,B,i} = 0$ , Inequality 3.1

gives the upper bound for the pursuer's power superiority, and Inequality 3.2 becomes a success requirement.

For example, 12 linear inequalities constitute the complete system of linear inequalities under minimal explanation I with a single trait pair for the observed outcomes in the rock–paper–scissors example (Fig. 3.1):

$$P_{A,1} \geq T_{B,1} + t_{A,B,1} \quad 3.3$$

$$P_{B,1} \geq T_{C,1} + t_{B,C,1} \quad 3.4$$

$$P_{C,1} \geq T_{A,1} + t_{C,A,1} \quad 3.5$$

$$P_{B,1} + Mf_{B,A,1} \leq T_{A,1} + M \quad 3.6$$

$$P_{B,1} - mf_{B,A,1} \geq T_{A,1} + t_{B,A,1} \quad 3.7$$

$$f_{B,A,1} \geq 1 \quad 3.8$$

$$P_{C,1} + Mf_{C,B,1} \leq T_{B,1} + M \quad 3.9$$

$$P_{C,1} - mf_{C,B,1} \geq T_{B,1} + t_{C,B,1} \quad 3.10$$

$$f_{C,B,1} \geq 1 \quad 3.11$$

$$P_{A,1} + Mf_{A,C,1} \leq T_{C,1} + M \quad 3.12$$

$$P_{A,1} - mf_{A,C,1} \geq T_{C,1} + t_{A,C,1} \quad 3.13$$

$$f_{A,C,1} \geq 1 \quad 3.14$$

One trait pair,  $d = 1$ , is assumed to be involved in the interactions, i.e. the assumed interaction form is a single two-dimensional mode. Three of the six observed outcomes were observed successes (to be explained by Inequalities 3.3–3.5): for invertebrate player A replacing B, for B replacing C, and for C replacing A. The other three observed outcomes were failures: of player B to replace A, (to be explained by Inequalities 3.6–3.8), of C to replace B (Inequalities 3.9–3.11), and of B to replace A (Inequalities 3.12–3.14). Since  $d = 1$ , the sum of failure indicator variables has only one term in the inequality  $\sum_{i=1}^d f_{X,Y,i} \geq 1$ , for any unsuccessful pursuer X against an attracter Y (Inequalities 3.8, 3.11 and 3.14). The single indicator variable is forced to equal one, and an observed failure must be explained as failure in the single task.

Under minimal explanation II (Fig. 3.1), each one of the  $d$  trait pairs must be involved in a different two-dimensional mode. On one hand, an observed failure of any pursuer A against any attracter B must be the result of failure in all  $d$  modes,  $P_{A,i} \leq T_{B,i}$  in any mode  $i$  (e.g. a parasite cannot invade via any of the alternative host entrances like the mouth or nose). On the other hand, an observed success of pursuer A against attracter B must come from success via at least one mode (e.g. a parasite successfully invaded via at least one host entrance). We now use a binary variable to indicate success via mode  $i$ ,  $s_{A,B,i}$ . Given the same bounds as in minimal explanation I, the following pair of

inequalities must be satisfied in any mode  $i$ :

$$P_{A,i} + m s_{A,B,i} \geq T_{B,i} + t_{A,B,i} + m, \quad 3.15$$

$$P_{A,i} - M s_{A,B,i} \leq T_{B,i}. \quad 3.16$$

With the extra inequality  $\sum_{i=1}^d s_{A,B,i} \geq 1$ , we force at least one of the indicator variables to equal one, i.e. success via at least one mode.

As an example of complete linear inequalities system under minimal explanation II, 12 linear inequalities are involved for a single trait pair in the observed outcomes of the rock–paper–scissors example (Fig. 3.1):

$$P_{A,1} + m s_{A,B,1} \geq T_{B,1} + t_{A,B,1} + m \quad 3.17$$

$$P_{A,1} - M s_{A,B,1} \leq T_{B,1} \quad 3.18$$

$$s_{A,B,1} \geq 1 \quad 3.19$$

$$P_{B,1} + m s_{B,C,1} \geq T_{C,1} + t_{B,C,1} + m \quad 3.20$$

$$P_{B,1} - M s_{B,C,1} \leq T_{C,1} \quad 3.21$$

$$s_{B,C,1} \geq 1 \quad 3.22$$

$$P_{C,1} + m s_{C,A,1} \geq T_{A,1} + t_{C,A,1} + m \quad 3.23$$

$$P_{C,1} - M s_{C,A,1} \leq T_{A,1} \quad 3.24$$

$$s_{C,A,1} \geq 1 \quad 3.25$$

$$P_{B,1} \leq T_{A,1} \quad 3.26$$

$$P_{C,1} \leq T_{B,1} \quad 3.27$$

$$P_{A,1} \leq T_{C,1} \quad 3.28$$

Again, the assumed interaction form is a single two-dimensional mode with one pair of competing traits,  $d = 1$ . The single indicator of success via the single mode is forced to equal one (with Inequalities 3.19, 3.22 and 3.25), and an observed success must be explained as success via the single two-dimensional mode. Invertebrate player A was replacing B (explained by Inequalities 3.17–3.19), B was replacing C (Inequalities 3.20–3.22), and C was replacing A (Inequalities 3.23–3.25). The other three observed outcomes were failures (explained by Inequalities 3.26–3.28).

Such systems of linear inequalities, with continuous traits and integer indicator variables, e.g. systems of linear Inequalities 3.3–3.14 or 3.17–3.28, can be formulated and solved as mixed integer programming problems (Williams, 2013).

### 3.1.2 Comparing the minimum dimensionality of empirical networks under five perspectives

I asked three questions about minimum mechanistic dimensionality: (1) Is it higher under the assumption of alternative two-dimensional modes, compared to the assumption of a single multidimensional mode? (2) Is it higher with observed failures taken into account instead of excluded? (3) Is it higher than the phenomenological dimensionality measure developed by Eklöf *et al.* (2013)? To answer these questions, I computed five minimum dimensionalities in each of 658 empirical systems. Assuming adequate sampling effort (e.g. no observed failures due to rarity), the first four of the five cases of minimum dimensionality presented below were based on my mechanistic framework, and the fifth was the dimensionality developed by Eklöf *et al.* (2013):

1. minimum mechanistic dimensionality under the assumption of a single, (potentially) multidimensional mode (minimal explanation I);
2. minimum mechanistic dimensionality under the assumption of (potentially) multiple, two-dimensional modes (minimal explanation II);
3. multimodal minimum mechanistic dimensionality of case 2, but excluding any linear inequalities required by observed failures, for example, excluding Inequalities 3.18, 3.21, 3.24 and 3.26–3.28 from the example system;
4. multimodal minimum mechanistic dimensionality with observed failures excluded of case 3, but with players interacting via a common trait per dimension, instead of a power against a toughness trait; and
5. minimum dimensionality of Eklöf *et al.* (2013), computed with the C code provided by the authors in their article's Supporting Information.

The systems of linear inequalities for the four minimum mechanistic dimensionalities were formulated and solved with the Gurobi Optimizer (Gurobi Optimization and Inc., 2017) as mixed integer programming problems (Williams, 2013). I computed the fifth dimensionality with code provided in the Supporting Information of Eklöf *et al.* (2013).

The compiled dataset of 658 empirical systems, covers six different types of ecological networks: animal dominance, food webs with basal species excluded, basal–consumer, plant–pollinator, host–parasite, and seed dispersal networks. I focused on one interaction type in each empirical system: (a) animal dominance in unipartite graphs (size range 6–31 individuals); (b) consumption of non-basal species in unipartite graphs (size range 6–57 species, basal species excluded from the original food webs); (c) consumption of basal species from consumers exclusively feeding on them in bipartite graphs (size range 11–91 species; from the same original food webs of (b)); (d) plant biotic

pollination in bipartite graphs (size range 8–114 species); (e) ectoparasitism of small mammals in bipartite graphs (size range 8–92 species); and (f) plant seed dispersal in bipartite graphs (size range 6–86 species). For empirical network sources and references, see Table S1 in the Supplementary Material of Kiziridis *et al.* (2017).

Interactions in animal dominance networks were between individuals. In these unipartite systems, all individuals were regarded as pursuers and attracters of dominance of the other social group members. Even a single dominance event of animal A against animal B was assumed an observed success of A against B, because of an expected benefit even after a single dominance success (e.g. animal A claimed a resting spot from animal B, even for short-term). In other words, I analysed data qualitatively, not considering the quantitative strength of interactions in this initial account of the method.

Interactions in non-basal consumption networks were between species (or other taxonomic or functional groups). For non-basal consumption, I removed the basal species (species without any resource) from the original food webs. I additionally excluded from the current considerations self-loop outcomes (successful self-consumption, and failure to self-consume). In the resulting unipartite systems, all species were pursuers and attracters of non-basal consumption of the other species. The same original food webs were studied for basal consumption as well.

Interactions in basal consumption networks were between species (or other groups). For basal consumption, I kept only the basal species (species without any resource), and the species exclusively feeding on basal species in the original food webs. In the resulting bipartite systems, the consumers of basal species were the pursuers, and the basal species were the attracters. Some of the basal species could not be considered representative individuals of species (e.g. fish eggs), or even biological organisms (e.g. detritus), but I supposed they possess traits acting against their consumption, to compete with individual traits of consumption-pursuing species. The same original food webs were studied for non-basal consumption as well.

Interactions in pollination networks were between species (or other groups). The input data files, retrieved from the source website (Ortega *et al.*, 2017), omit from the original networks any animals that do not pollinate any plant, and any plants that are not pollinated by any animal. In the resulting bipartite systems, the plants were the pursuers of pollination, and the animals were the attracters.

Interactions in ectoparasitism networks were between species (or other groups). In these bipartite systems, the potential parasites were the pursuers of ectoparasitism, and the mammals were the attracters.

Interactions in seed dispersal networks were between species (or other groups). The input data files, retrieved from the source website (Ortega *et al.*, 2017), omit from the original networks any animals that do not fruit-consume or seed-disperse any plant, and any plants that do not receive the respective services from any animal. In the resulting

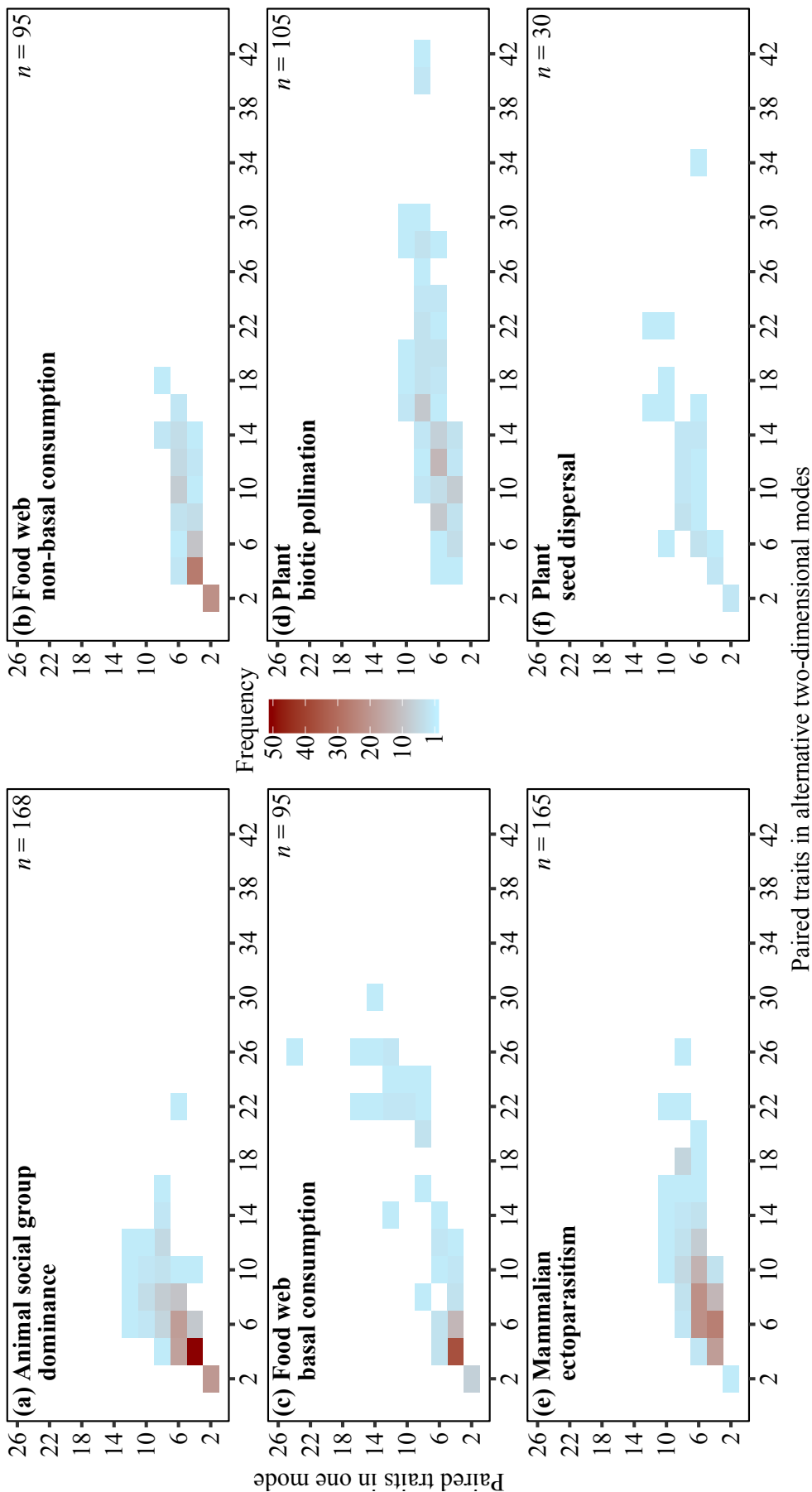


Figure 3.2: Minimum mechanistic dimensionality of 658 empirical systems. Cell shading shows the frequency of systems having the specific pair of values in my two minimum dimensionalities, i.e. number of paired traits in: alternative two-dimensional modes (x-axis; minimal explanation II); a single mode (y-axis; minimal explanation I). Parameter values in the linear inequalities method:  $m = -200$ ;  $M = 200$ ;  $t_{A,B,i} = 1$ , for all pairs of pursuer A with attractor B, in any trait pair  $i$ .

bipartite systems, the plants were the pursuers of seed dispersal, and the animals were the attracters.

## 3.2 Results

### 3.2.1 Multimodal versus unimodal minimum mechanistic dimensionality

The minimum mechanistic dimensionality was generally higher under the alternative, multiple modes explanation than under the single mode explanation (Fig. 3.2). The dimensionality assuming alternative modes (horizontal axes in Fig. 3.2) increased faster than the dimensionality assuming a single interaction mode (vertical axes in Fig. 3.2), especially in the systems of non-basal consumption, biotic pollination, ectoparasitism, and seed dispersal (Fig. 3.2b, d–f). 54% of the empirical systems had higher dimensionality if alternative modes were assumed, with only 7% of the systems having higher unimodal dimensionality (Fig. 3.3a).

### 3.2.2 Minimum mechanistic dimensionality with failure outcomes taken into account versus excluded

Minimum mechanistic dimensionality was higher in 92% of the empirical systems when failure outcomes were included, instead of excluded (Fig. 3.3b). For this question, I compared the minimum multimodal dimensionality with the same dimensionality but with any failure inequalities excluded from the linear inequalities system. The minimum dimensionality with failures excluded always equals one because all pursuers can have power greater than toughness in one dimension, explaining any structure of only observed successes unimodally. I further required that pursuers and attracters compete over one trait per dimension, instead of the default power–toughness pair. In that way, the unipartite systems of animal dominance and non-basal consumption could require more than one dimension with failures excluded, but again the minimum dimensionality of bipartite systems is always equal to one. Even with modelling trait competition with one common trait per dimension, 84% of the unipartite systems had higher minimum dimensionality with failures included rather than excluded.

### 3.2.3 Comparing mechanistic and phenomenological minimum dimensionality measures

In 90% of the empirical systems, the minimum mechanistic dimensionality was higher than the phenomenological dimensionality of Eklöf *et al.* (2013). I used the minimum



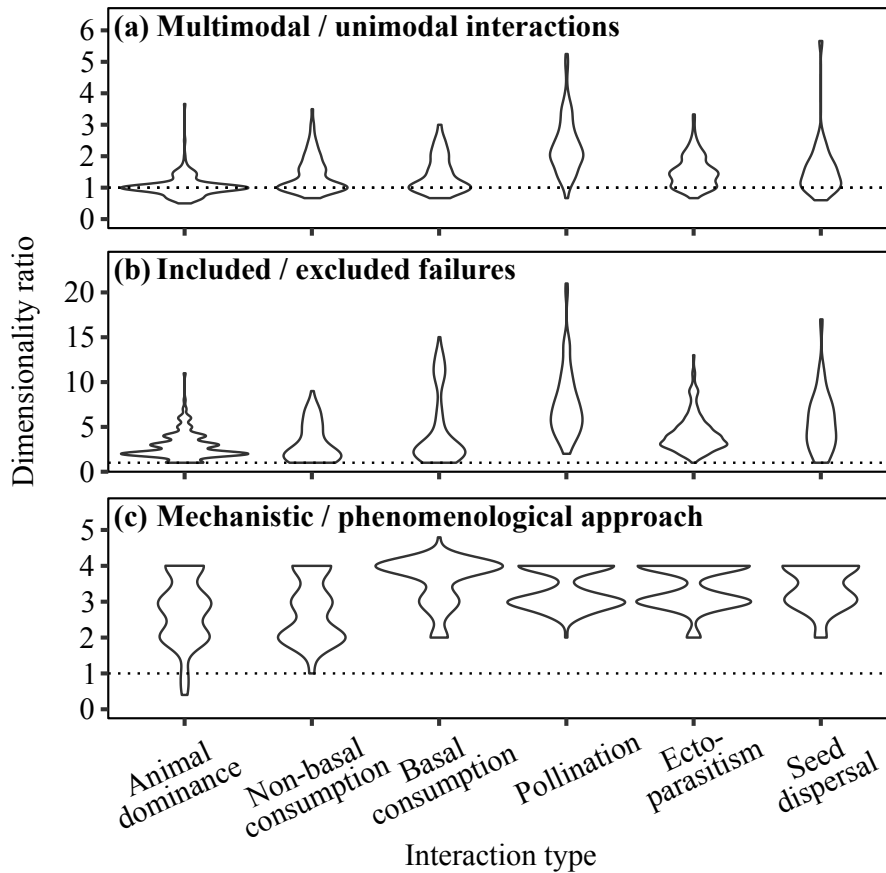


Figure 3.3: Three minimum dimensionality comparisons in the 658 empirical systems of the dataset (Fig. 3.2). For each empirical network, I calculated the ratio of: (a) the minimum mechanistic dimensionality under minimal explanation II (alternative two-dimensional modes), to the minimum mechanistic dimensionality under minimal explanation I (a single mode); (b) the minimum mechanistic dimensionality under minimal explanation II, to the same dimensionality with the failures excluded from the system of linear inequalities; and (c) the minimum mechanistic dimensionality under minimal explanation I, to the comparable minimum phenomenological dimensionality of Eklöf *et al.* (2013). Violin plots show the normalised distributions of the dimensionality ratio for the systems of each interaction type. The intercept horizontal lines equal a ratio of one.

dimensionality under the assumption of a single mode (minimal explanation I), which is comparable to the niche approach of Eklöf *et al.* (2013). Only six animal dominance networks had higher minimum dimensionality under the phenomenological approach (Fig. 3.3c). The minimum number of traits for the explanation of all outcomes according to the mechanistic framework was 3–4 times larger (median) than with the phenomenological dimensionality in any type of interaction.

### 3.3 Summary

Finding the minimum number of traits that must be involved in direct intraspecific and interspecific interactions, i.e. the ‘minimum dimensionality’, can concentrate our efforts to traits contributing more to community structure. Existing theoretical methods for minimum dimensionality are phenomenological, or lack the ubiquitous feature of alternative interaction modes (e.g. alternative feeding modes). Based on the mechanistic framework described in Chapter 2, I aimed to develop a method for the ‘minimum mechanistic dimensionality’ of an ecological network, able to assume alternative interaction modes. A system of linear inequalities is constructed, explaining the set of observed interaction outcomes, assuming how the competing traits are involved in alternative interaction modes. Minimum mechanistic dimensionality is the minimum number of traits for a solvable linear inequalities system. I illustrate how the assumption of alternative interaction modes alters the minimal mechanistic explanation of rock–paper–scissors intransitive systems. Additionally, by applying the method to 658 published empirical ecological networks, I show that minimum dimensionality can be underestimated by the omission of concepts emerging from the framework (generalisation to alternative interaction modes, trait-mediated ‘forbidden links’ or ‘forbidden interactions’, mechanistic perspective). Hence, the method can inform network models about the necessary number of traits mechanistically involved in the interactions, for the generation of realistic ecological networks at the interaction outcome level. In general, it can reduce the risk of omitting important traits, for better understanding, explaining, and predicting community structure, and structure-dependent community, ecosystem, and evolutionary processes.

## Chapter 4

# Experimental quantification of six elements of fungal competition for space

I present the experimental quantification of the six basic elements of spatial competition for three species of filamentous fungi in closed, dispersal-free laboratory communities, in stable and homogeneous abiotic conditions. The experimental findings will be incorporated to relatively simple models for testing the predictability of 2- and 3-species fungal community dynamics (Chapters 5 and 6).

### 4.1 Materials and methods

#### 4.1.1 Study species and general setting

I employed three strains of wood-decay basidiomycete fungi from Cardiff University culture collection: *Vuileminia comedens* (abbreviated 'Vc' hereafter; strain VcWVJH1), *Trametes versicolor* ('Tv'; strain TvCCJH1), and *Hypholoma fasciculare* ('Hf'; strain HfDD3). In preliminary interspecific interactions between different species, these three species had the clearest boundaries between adjacent mycelia during replacement and deadlock (i.e. absence of replacement). Additionally, visual inspection was adequate for determining mycelial boundaries, shown by re-isolation of different mycelial regions, for example, of the bottom of mycelia overgrown by Hf cords, and of regions close to assumed boundaries between adjacent mycelia.

The general setting was the same for all experiments: approximately 0.5 cm thick, flat culture medium of 2% (w/v) malt agar—20 g malt extract from Oxoid™ (Basingstoke, UK), and 15 g agar from Sigma-Aldrich® (Irvine, UK), in 1 litre of distilled water—at 15° C in the dark. I chose a richer substratum for more dense mycelial development lead-

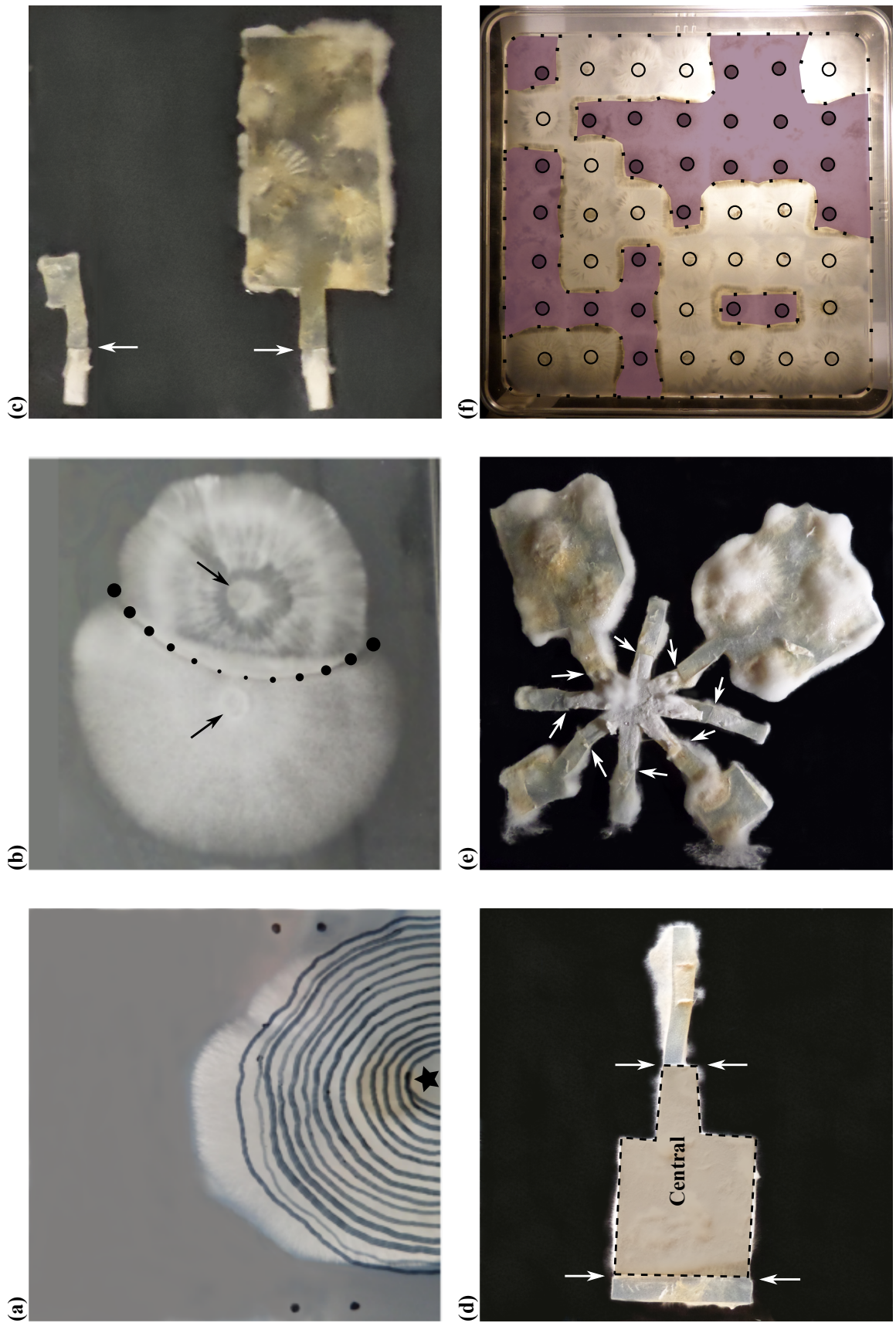
ing to ‘more territorial’ mycelia (Stahl & Christensen, 1992), and to minimise resource depletion affecting extension and replacement, given the duration of the experiments (the longest setting lasted 80 days).

The three species showed low standard deviation of extension and replacement rates in the preliminary samples. Thus, a sample size of  $n = 3$  or  $n = 4$  was adequate for small standard error. I performed all statistical analyses in R (R Core Team, 2017).

#### 4.1.2 Element 1: extension rate in relation to mycelial size, shape, position, age

Each species was inoculated at the centre of  $22.4 \times 22.4$  cm dishes, and the mycelial boundary as seen from the bottom of the dish was drawn in regular time intervals (e.g. Fig. 4.1a). I measured the extent of the boundary in time (taking the mean extent from four right-angled directions of unconstrained extension). Similarly, I measured extent in time for mycelia: (1) at dish corners, to determine the effect of position (mean extent from two right-angled directions of unconstrained extension); (2) at substratum strips, to determine the effect of mycelial shape (one direction of extent on 0.8 cm wide strip); and (3) from pieces of aged culture that I attached next to unoccupied substratum, to determine the effect of age (one direction of extent on 0.5 cm wide, unoccupied substratum). When mycelial extension was linear in time, mean extension rate was obtained from the slope of the least-squares line fitted to the extent–time relationship, assuming no extent at time zero (zero intercept). I hypothesised that mean extension rate of each species is independent of mycelial size, shape, position, and age ( $n = 3$  mycelia per setting; tested with Kruskal–Wallis one-way analysis of variance).

Figure 4.1: The empirical system used for the main experiments. White arrows point to initial boundaries between mycelia. (a) Unconstrained mycelial extension on a Petri dish, overlaid by a transparency depicting the bottom view mycelial boundary in regular time intervals, starting from the inoculation site (star). (b) Unconstrained mycelial extension and replacement on agar. The mycelium on the right (*Hypholoma fasciculare*) is replacing the mycelium on the left (*Vuileminia comedens*). Arrows indicate the inoculation sites. The dotted curve denotes the assumed boundary between the mycelia, with larger dots at the replaced mycelium’s younger regions. (c) Pairing mature mycelia in different cover ratios, but with fixed length of boundary between the competitors (0.5 cm). (d) A pair of mycelia of one species flanking a central mycelium of another species in two different boundary lengths (4 and 0.5 cm). (e) A central mycelium of one species, cut to provide eight boundaries of fixed length (0.5 cm), against eight heterospecific mycelia of different cover. (f) Competition on a  $22.4 \times 22.4$  cm agar dish, after randomly assigning the species to 49 inoculation sites (circles), regularly configured on a square grid of 3 cm horizontal and vertical distance between inoculation site centres. In this 2-species example, mycelia have covered the dish, and replacement is observed (dotted curves denote boundaries of mycelia, and the mycelia of the replaced species are shaded).



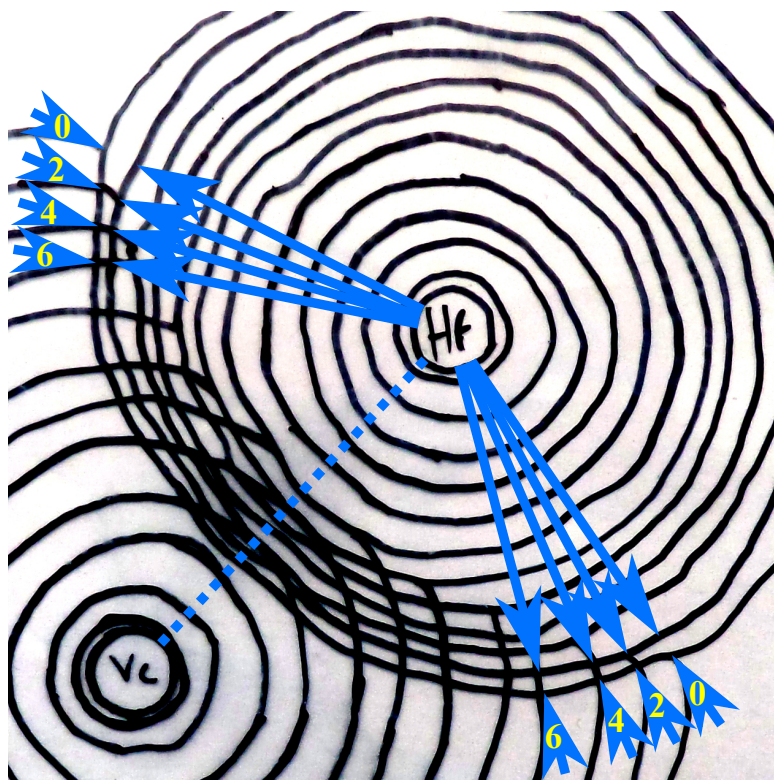


Figure 4.2: Method for quantifying the relation between replacement rate and age of replaced mycelium's regions. In this example, bottom view mycelium boundaries were marked every two days, with the two mycelia extending unconstrained from their inoculation sites, and the Hf mycelium on the right replacing the Vc mycelium on the left. The dotted line connecting the two inoculation sites splits the boundary into two sides. The short arrows indicate the age of the pointed Vc boundary with a number (in days), with the last time of boundary marking set to  $t = 0$  d. During the last two days, Hf has replaced Vc regions of different age, with the replacement extent measured between each pair of short and long arrow for different region ages of Vc. Thus, the replacement rate ( $\text{cm d}^{-1}$ ) in these local regions was the measured replacement extent (in cm) divided by two (in d). For each age of replaced mycelium's regions, I plotted the mean replacement rate from the two sides of the boundary between the two mycelia.

### 4.1.3 Element 2: extension rate in presence of other mycelia

I inoculated a mycelium of one species with a mycelium of the same or of another species in different positions and distances on the dish ( $n = 3$  or  $n = 4$ ). I measured three extension rates of each mycelium (method as for Element 1): (1) towards the other mycelium; (2) away before making contact with the other mycelium; and (3) away after making contact. These three extension rates were compared with each other using Friedman rank-sum test, and with the fungus growing alone on dishes using Wilcoxon rank-sum test.



#### 4.1.4 Element 3: replacement rate in relation to age of mycelial regions

I aimed to quantify any relation between replacement rate and age of mycelial region replaced. I assumed that a very young and sparse mycelial region would impose no resistance to a replacing mycelium, getting replaced as fast as unoccupied space. This replacement rate was expected to decrease on older regions of the replaced mycelium (Fig. 4.1b).

A mycelium can be replaced in regions of different age (e.g. as in Fig. 4.2). Focusing on the last time of boundary marking, I measured how much a replacing mycelium had replaced in the last two days, to find the local replacement rate ( $n = 4$  mycelium pairs per paired species combination). The age of the replaced mycelium's regions was implied by the age of the mycelium's boundaries, as marked on the transparency (detailed example in Fig. 4.2). By measuring local replacement rates at a snapshot of time, I could control for the effects of mycelial cover and length of boundary with heterospecifics, which both can change during replacement.

#### 4.1.5 Element 4: replacement rate in relation to mycelial cover

I hereafter focus on mycelial 'cover', which is the area covered by a mycelium's bottom view boundary. I aimed to quantify any relation between replacement rate and cover ratio of paired mature mycelia of different species. I measured replacement rates in paired mature mycelia of different cover ratios (Fig. 4.1c), cut from aged cultures in shapes that limited the boundary to fixed width (0.5 cm). The cut pieces were paired in contact to each other on empty dishes without medium. The smallest pieces cut from mature mycelia covered  $1 \text{ cm}^2$  ( $0.5 \times 2 \text{ cm}$  bottom view dimensions), because smaller pieces dehydrated rapidly. I measured the replacement extent two days since mycelium of the replacing species was noted on its opponent, and replacement rate (in  $\text{cm d}^{-1}$ ) was the extent (in cm) divided by two (in d) ( $n = 3$  per cover ratio per species pair).

To test that only the cover ratio matters, and not the absolute mycelial cover, pairings were set up with the following three Hf/Vc and Tv/Vc basic cover ratios (absolute cover in  $\text{cm}^2/\text{cm}^2$ ): 1/1, 2/2 and 4/4; 4/1, 8/2 and 16/4; 16/1, 32/2 and 64/4. I did not set up pairings for Hf/Tv because they deadlocked at extreme cover ratios in preliminary investigations. Kruskal–Wallis one-way analysis of variance was used to test differences between the three different absolute cover ratios of each basic ratio ( $n = 3$  per absolute cover ratio).

### 4.1.6 Element 5: replacement rate against multiple adjacent heterospecifics

First, I hypothesised that replacement rate is independent of the length of boundary between a pair of mature mycelia of specific cover ratio. I paired mycelia as in Element 4 but on 4 cm wide boundaries with the following mycelium cover ratios (absolute cover in  $\text{cm}^2/\text{cm}^2$ ): 2/4, 2/2, and 4/2 for Hf/Vc; and 2/2, 4/2, and 8/2 for Tv/Vc. I tested if replacement rates for each cover ratio were as in the 0.5 cm boundary for Element 4 (Wilcoxon rank-sum test;  $n = 3$ ).

Additionally, I set a central mycelium of one species,  $18 \text{ cm}^2$  cover, against two competitor mycelia of another species, both  $2 \text{ cm}^2$  cover, but one with 0.5 cm wide boundary (narrow competitor), and the other with 4 cm (wide competitor) (as in Fig. 4.1d). I hypothesised that the observed replacement rates were as if the central mycelium: (1) retained its full cover-related competitive ability against both competitors (expected replacement rates as in paired mature mycelia of 18/2 central/wide, and 18/2 central/narrow competitor cover ratio from Element 4); (2) is divided equally to each competitor (replacement rates as from 9/2 central/wide, and 9/2 central/narrow cover ratios); or (3) is divided proportionally to the length of boundary with each competitor (replacement rates as from 16/2 central/wide, and 2/2 central/narrow cover ratios; the 16/2 division of the central mycelium cover is equal to the 4/0.5 cm wide/narrow ratio of the two boundary lengths). I compared expected with observed replacement rates at both boundaries with the Wilcoxon rank-sum test ( $n = 3$  for each species in the position of the central mycelium against each other species).

### 4.1.7 Element 6: additive or non-additive effects of competition

I set a central mycelium of one species ( $8 \text{ cm}^2$  cover) against mycelia of both other species (two mycelia of  $1 \text{ cm}^2$  and two of  $16 \text{ cm}^2$  from each species, with 0.5 cm wide boundary; star-like setting as in Fig. 4.1e). In case of additive effects of competition, the observed replacement rates in these 3-species settings would be similar with replacement rates expected from paired mature mycelia for Element 4, after considering how the central mycelium is divided to the eight competitors according to the results for Element 5 (Wilcoxon rank-sum test;  $n = 3$ ). For each replicate, the observed replacement rate was the mean from the two boundaries with the same-cover and same-species competitors.

### 4.1.8 Prediction of community dynamics

In Chapters 5 and 6, I aimed to test the ability of theoretical models to predict the mycelial spatial configurations, and total mycelial cover, for each species in empirical communities in time. Thus, I prepared initial configurations of 2- and 3-species empirical



communities by randomly assigning a species at each of 49 inoculation sites, covering a  $22.4 \times 22.4$  cm polystyrene square bioassay Petri dish (Corning<sup>®</sup>, Buckinghamshire, UK). At each inoculation site, I transferred a cylindrical plug of 0.8 cm diameter, cut with a cork borer from a culture of the randomly selected species (Fig. 4.1f). The plug was set with the aerial mycelium touching the new substratum. All plugs were removed after two days, to prevent any plug effects on the dynamics. I prepared four test cases: a 3-species community, and three 2-species communities (all paired combinations of three species). The experiments were run until no further dynamics were observed, either because of deadlock, or because of species covering the whole plate.

To compare with a theoretical model's predictions (Chapters 5 and 6), the mycelial boundary drawings of the empirical communities were processed with ImageJ (Rasband, 2016), to discretise dish space to  $45 \times 45$  occupancy sites on a square lattice. Occupant of a square lattice site was considered the species, unoccupied space included, covering most site area. I accomplished this aim in four stages. First, a photograph of the transparency was taken (e.g. Fig. 4.3a). Second, the following sequence of ImageJ commands was run on the photograph, with an ImageJ Macro (Rasband, 2016):

1. `setOption("BlackBackground", false);`
2. `run("Make Binary");`
3. `run("Skeletonize");`
4. `run("RGB Color");`

Commands 1 and 2 created a binary version of the original photograph, so that I could 'skeletonize' the image with command 3. Command 3 was thinning the marked curves representing mycelial boundaries to one pixel width. With command 4, the image was turned to RGB type (Fig. 4.3b). Third, mycelial boundaries were filled with colours representing different species, allowed due to the RGB type (Fig. 4.3c). Fourth, I created and ran an ImageJ plugin on the coloured image from the previous stage, for a coarse-grained, reduced version of the image (Fig. 4.3d).

My ImageJ plugin creates a new image which is the result of rescaling the original image to fewer pixels. For example, if the original image is  $500 \times 500$  pixels (e.g. Fig. 4.3c), and the aim is to reduce its size to a new  $50 \times 50$  pixels lattice model image (Fig. 4.3d), the binning factor for both  $x$  and  $y$  dimensions is 10. That is, the pixels of the original image have to be binned in groups of  $10 \times 10$  pixels, becoming one pixel in the new image. The pixel of the new image takes the colour, i.e. species occupancy, that the majority of the  $10 \times 10$  pixels in the original image has. If two or more colours are equally prevalent, then I select one of those colours at random. Thus, re-running the plugin might lead to slightly different results due to this random choice. The code is an extension of the Binner plugin (Stuurman, 2006). The Binner plugin can reduce the size of the original image by taking the average, minimum, maximum, or median of the grouped pixels' colour, whereas my plugin takes the colour of the majority.

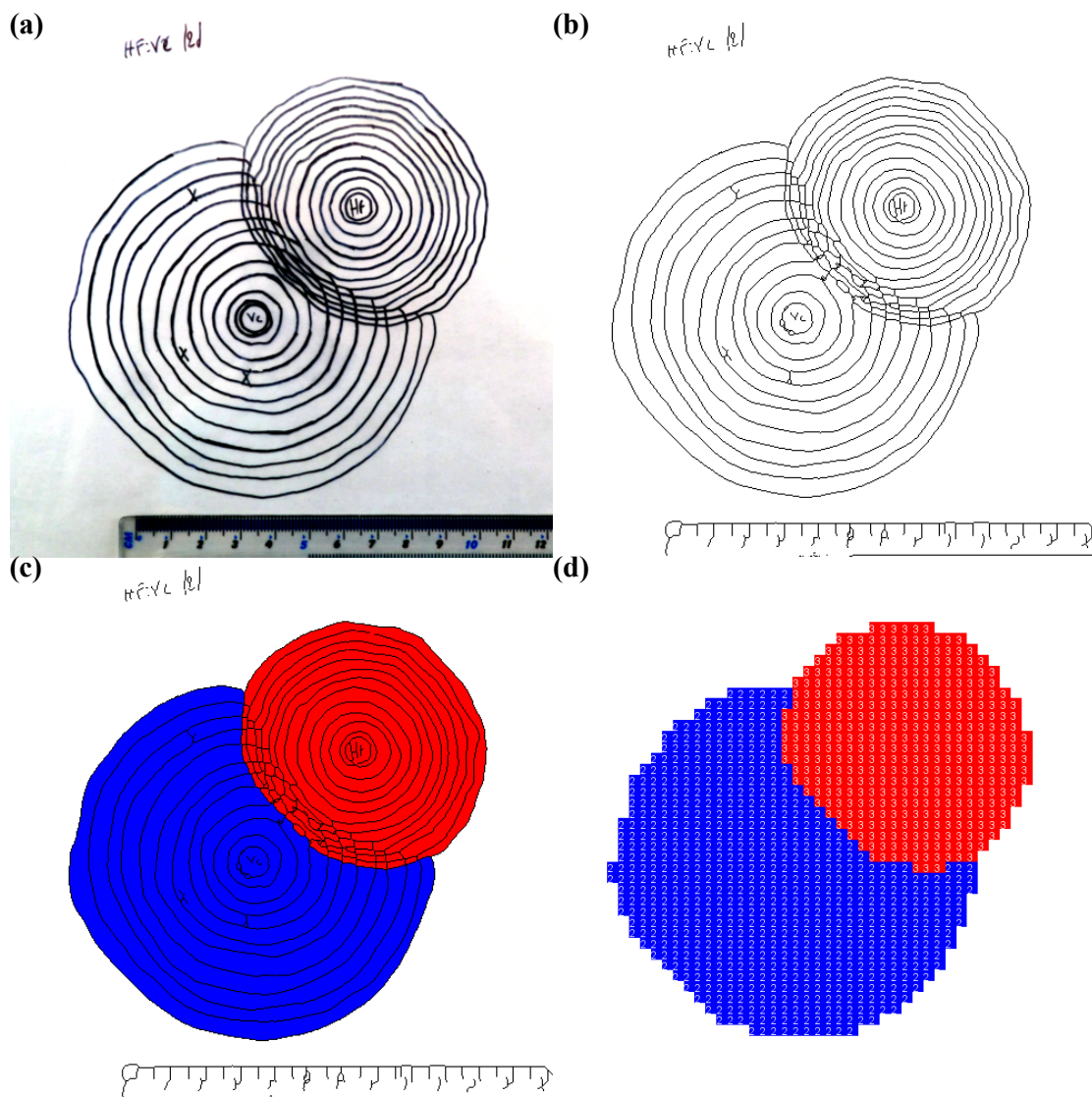


Figure 4.3: The four stages of coarse-graining empirical Petri dish space for the theoretical models (Chapters 5 and 6). (a)  $500 \times 500$  pixels photograph of a transparency with marked boundaries of two mycelia that have extended freely from their inoculation sites, and with Hf on the right replacing Vc on the left. Boundaries were marked every two days. (b) The photograph of (a) ‘skeletonised’ with an ImageJ Macro, making it an RGB black–white image, with the boundaries having one pixel width. (c) The image of (b), after filling with different colour each species, at the last time of measurement. (d) The coarse-grained, reduced version of (c) with  $50 \times 50$  pixels dimensions. The  $x$  and  $y$  binning factors were equal to 10, so that  $10 \times 10$  pixels of (c) became one pixel in the reduced image. The new pixel has the colour that the majority of its binned pixels has in (c).

Additionally, my plugin calculates each mycelium’s size (in number of lattice sites), and each mycelium’s length of boundary with heterospecifics (in number of adjacent lattice sites of another species) in the new, reduced image. Mycelia are identified with a ‘Hybrid cluster identification’ method (Martín-Herrero, 2004).

## 4.2 Results

### 4.2.1 Element 1: extension rate in relation to mycelial size, shape, position, age

The boundary extent of empirical mycelia inoculated alone on Petri dishes was apparently linear in time (Fig. 4.4a–d), even in large mycelia, relative to the dish dimensions (e.g. Fig. 4.4a). Thus, I could calculate mean extension rates from the slopes of the extent–time linear relationships under the four different settings of mycelia at dish centres, at dish corners, on substratum strips, and from aged mycelia of the three species. I found no differences in mean extension rates between the four settings ( $p = 0.31$  for Hf,  $p = 0.86$  for Tv, and  $p = 0.28$  for Vc; Kruskal–Wallis test). The mean boundary extension rate ( $\pm$  margin of error) of Hf was  $0.14 \pm 0.01 \text{ cm d}^{-1}$ , of Tv was  $0.36 \pm 0.06 \text{ cm d}^{-1}$ , and of Vc was  $0.22 \pm 0.02 \text{ cm d}^{-1}$ .

### 4.2.2 Element 2: extension rate in presence of other mycelia

Colony extension rates were unaffected by the presence of distant or adjacent conspecific or heterospecific mycelia (Fig. 4.4e;  $p > 0.05$  for all combinations in all species; Wilcoxon test). No significant differences were found in mycelial extension rates towards, away pre-contact, and away post-contact ( $p > 0.05$  for all combinations of mycelia in pairs, species self-pairings included; Friedman test).

### 4.2.3 Element 3: replacement rate in relation to age of mycelial regions

Young hyphae at the periphery of Vc mycelia were replaced as fast as unoccupied space by Hf and Tv (see replacement rates of Vc at zero days old mycelial regions in Fig. 4.5a,c, respectively). Replacement rates decreased across the boundary of the Hf–Vc and Tv–Vc pairs, from the Vc mycelial margins until the 4–8 days old Vc mycelial regions. Thus, I assumed that zero days old Vc mycelium was replaced at the mean extension rates of Hf and Tv, and replacement rates decreased linearly until 6 days old Vc mycelial regions. Older Vc regions were replaced at the mean replacement rate obtained by the paired mature mycelia setting of the next Element 4.

### 4.2.4 Element 4: replacement rate in relation to mycelial cover

There was deadlock at 1/256 Hf/Vc (1/1 Tv/Vc) mature mycelium cover ratio, and Hf (Tv) started to replace Vc at 1/128 Hf/Vc (2/1 Tv/Vc) cover ratio (Fig. 4.5b,d). The replacement rate increased linearly with the logarithm of cover ratio, and became as

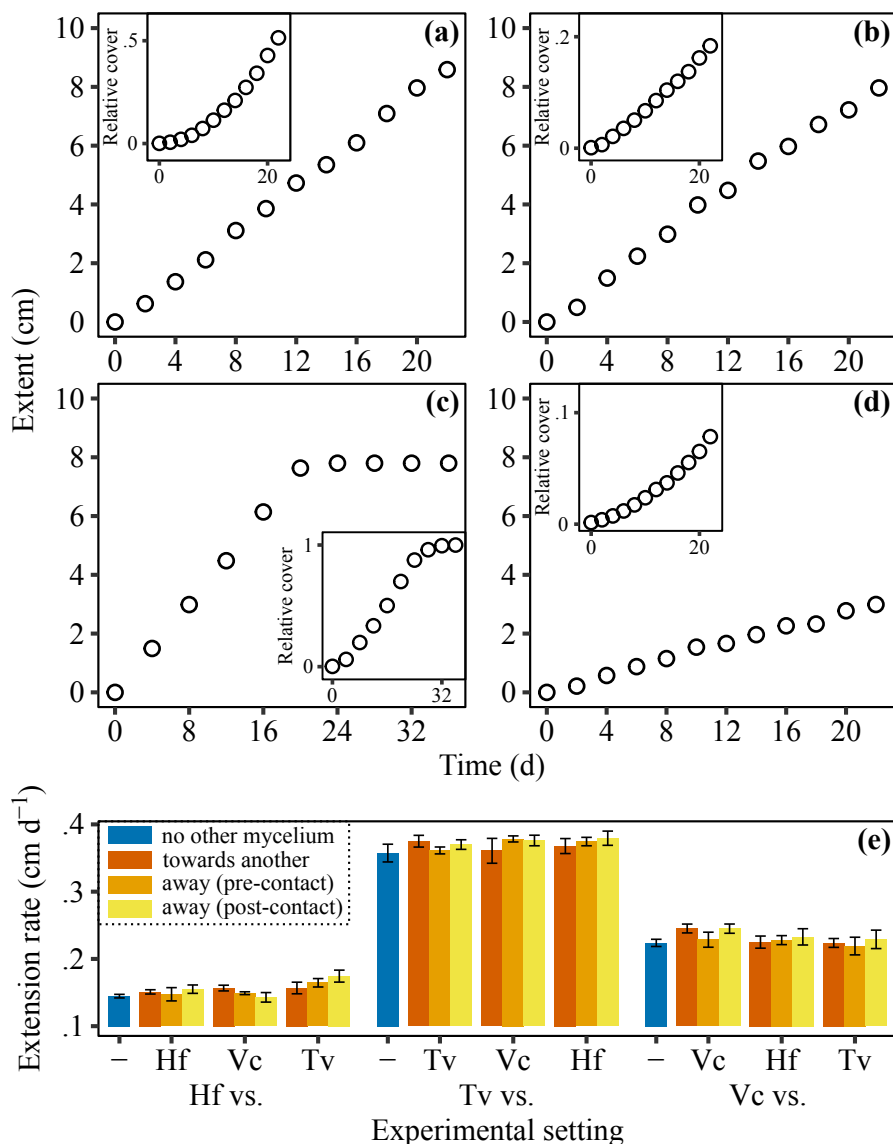


Figure 4.4: Empirical extent (relative cover in insets), and extension in relation to presence of other mycelia (for Elements 1 and 2, respectively). (a) Example of a Tv mycelium developing from an inoculated site, extending and covering the dish unconstrained (i.e. before reaching the dish boundaries). (b) Example of a Tv mycelium developing from a dish corner. (c) Example of three Tv mycelia closely inoculated at the dish centre, fusing to form one mycelium that extended and covered the dish. (d) Example of an Hf mycelium developing from the dish centre, extending and covering the dish at a slower rate than Tv. (e) Mean extension rate ( $\pm$  standard error) of mycelium towards and away from another mycelium before and after making contact ( $n = 3$  or  $n = 4$  for each setting; extension rate with no other mycelium on the dish is given for reference). In panels (a–d), extent is the mean from 2–4 directions of unconstrained empirical and model mycelial extension, except in (c) where the mycelium reached the dish boundaries after around 20 days.

fast as the mean cover extension rate of Hf in unoccupied space at around 64/1 Hf/Vc cover ratio (replacing Tv did not attain a maximum replacement rate equal to its extension rate against Vc in the maximum 256/1 Tv/Vc cover ratio setting). Thus, for the theoretical

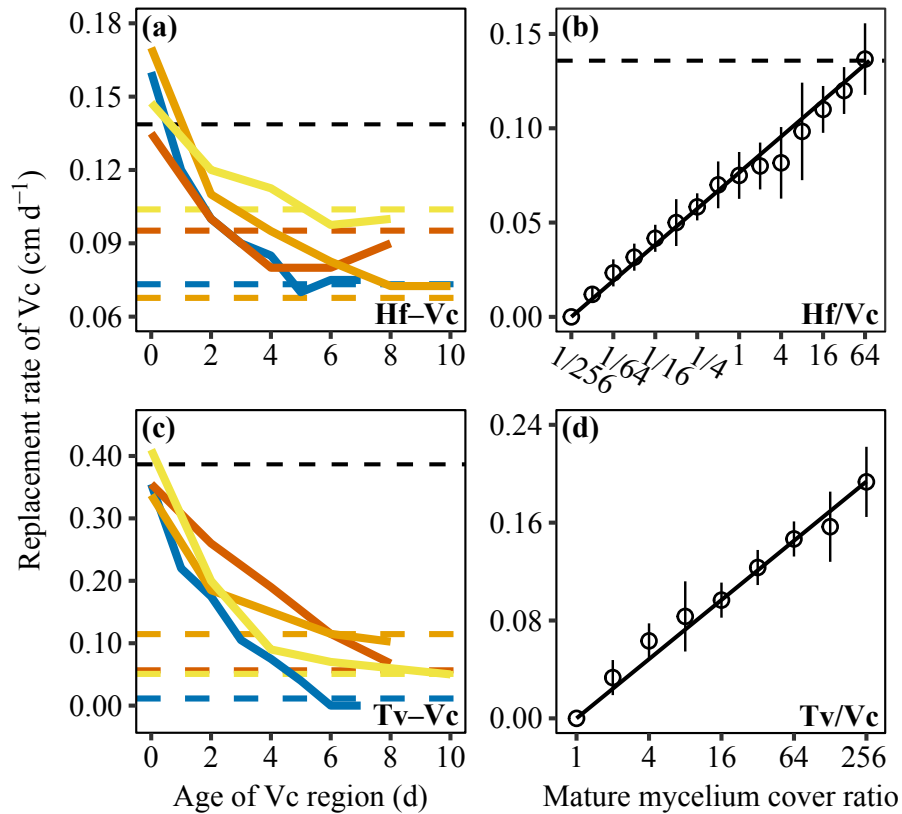


Figure 4.5: Empirical replacement in relation to age of mycelial region, and mycelial cover (for Elements 3 and 4, respectively). Black dashed line indicates the mean extension rate of the replacing species to unoccupied space. (a) Replacement rate across the boundary between four pairs of Hf–Vc mycelia (Fig. 4.1b). (b) Mean replacement rate of Vc by Hf given their Hf/Vc mature mycelium cover ratio (Fig. 4.1c). (c) Replacement rate across the boundary between four pairs of Tv–Vc mycelia (Fig. 4.1b). (d) Mean replacement rate of Vc by Tv given their Tv/Vc mature mycelium cover ratio (Fig. 4.1c). In panels (a, c), each line concerns a different Hf–Tv or Tv–Vc pair, and a same-colour dashed line indicates the replacement rate expected from mature mycelia of the pair’s cover ratio, according to panels (b, d). In panels (b, d), error bars are 95% confidence intervals for the mean replacement rate ( $n = 3$ ), and solid lines denote the linear relationships between mean replacement rate and logarithm of cover ratio incorporated to the theoretical models in Chapters 5 and 6 ( $0.0092 \log_2(\text{Hf/Vc}) + 0.074$ , and  $0.024 \log_2(\text{Tv/Vc})$ ).

models in Chapters 5 and 6, I assumed deadlock for 1/256 (1/1) and smaller Hf/Vc (Tv/Vc) cover ratio, a linear increase of the mean replacement rate with the logarithm of cover ratio for larger than 1/256 (1/1) cover ratio, with an upper bound equal to the mean extension rate of Hf (Tv).

Replacement rates of Vc by Hf and Tv were unaffected by the absolute cover in the cover ratios ( $p > 0.05$  in the three absolute cover ratios of each basic cover ratio; Kruskal–Wallis test).

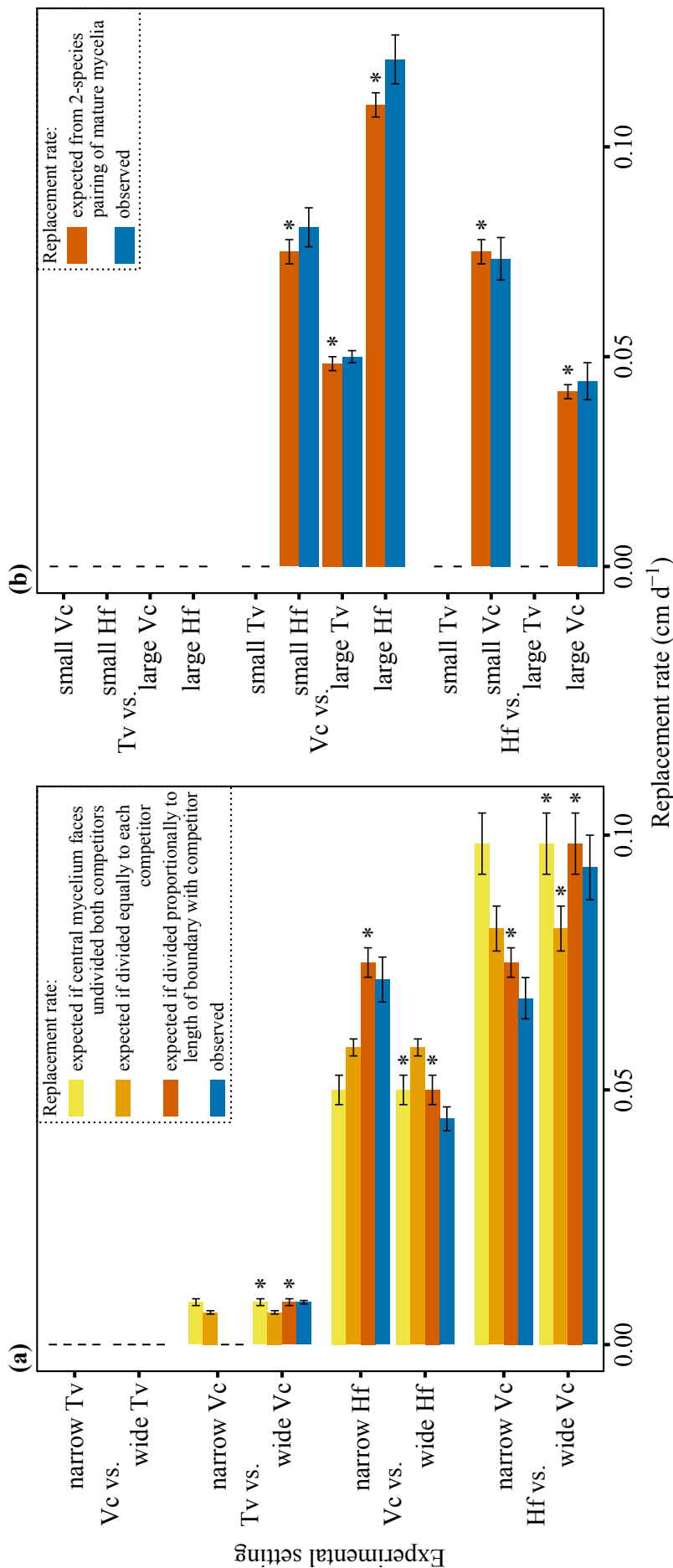


Figure 4.6: Empirical replacement against multiple adjacent competitors, and against multiple species (for Elements 5 and 6, respectively). In both panels, non-zero replacement rates refer to Hf and Tv replacing Vc. (a) Replacement rates observed in one central mycelium against two competitors of another species with different boundary lengths (Fig. 4.1d), compared to replacement rates expected from 2-species pairings (Fig 4.5b,d). (b) Replacement rates observed in 3-species settings of a central mycelium against the other two species with two different mycelial covers (similar to Fig. 4.1e), compared to replacement rates expected from 2-species pairings (Fig 4.5b,d). Bars denote mean replacement rate ( $\pm$  the standard error;  $n = 3$ ). An asterisk indicates no significant difference between expected and observed replacement rates (Wilcoxon rank-sum test).

#### **4.2.5 Element 5: replacement rate against multiple adjacent heterospecifics**

Boundary length did not appear to have an effect on replacement rates between paired mature mycelia of same cover ratio ( $p > 0.05$  for the three cover ratios in Hf/Vc or Tv/Vc; Wilcoxon test).

Nevertheless, observed replacement rates in the two-against-one setting showed that the central mycelium divided its competitive ability proportionally to the length of boundary with each of the smaller but equally-sized competitors (Fig. 4.6a). In accordance to the 4/0.5 cm wide/narrow boundary length ratio, the flanking competitor from the wide boundary realised an 8 times larger central mycelium than the flanking competitor from the narrow boundary ( $p > 0.05$  for the difference between observed replacement rates and expected from the  $4/0.5 = 16/2$  division of the  $18 \text{ cm}^2$  central mycelium; Wilcoxon test; Fig. 4.6a): the central mycelium of Hf replaced Vc from the wide boundary faster than from the narrow boundary; the central mycelium of Vc was replaced faster from the narrow boundary with Hf; and the central mycelium of Tv could replace Vc from the wide boundary, but deadlocked with Vc from the narrow.

#### **4.2.6 Element 6: additive or non-additive effects of competition**

There was no evidence of non-additive effects of competition (Fig. 4.6b). In the 3-species settings, assuming from the results of Element 5 that the central mycelium was divided equally to the eight competitors (because each competitor had the same boundary length), the observed replacement rates were not different from those expected from the 2-species settings of paired mature mycelia for Element 4 in Fig. 4.5b,d ( $p > 0.05$  Wilcoxon test).

### **4.3 Summary**

Abiotic and biotic factors influence the outcomes of interaction between filamentous fungi, and drive fungal community dynamics. In constant abiotic regime, basic elements of fungal spatial competition at play include the: (1) different rates of mycelial extension to unoccupied space; (2) inhibition or stimulation of extension by other mycelia; (3) mycelial replacement in relation to mycelial age; (4) replacement in relation to mycelial size; (5) distribution of competitive ability against multiple adjacent heterospecifics; and (6) competitive additivity of multi-species interactions. No previous work has investigated all six elements for a given set of species. Thus, I aimed to experimentally quantify the six elements for three wood decay fungal species competing for agar space. The following element forms were found: (1) each species having different but constant extension rate; (2) extension rates unaffected by distant or adjacent mycelia; (3) faster

replacement of younger mycelial regions; (4) faster replacement of relatively smaller mycelia; (5) distribution of competitive ability to multiple adjacent heterospecifics proportionally to the length of boundary with each; and (6) additive effects of competition. The spatial competition elements had relatively simple form in this laboratory community, with constant and unaffected extension rates, linear relation of replacement rate with age of replaced mycelial region, linear relation of replacement rate with the logarithm of mycelial cover ratio, uniform distribution of mycelial competitive ability across the boundary with heterospecifics, and absence of species-specific interaction outcomes and replacement rates. Thus, a relatively simple model could incorporate these elements, to test the predictability of this community's dynamics (Chapter 5).



# Chapter 5

## Lattice model predicts fungal community dynamics driven by competition for space

I develop a spatially explicit, lattice model incorporating all six basic elements of spatial competition between filamentous fungi from Chapter 4. In particular, I test if all six elements are necessary for accurate model prediction of the dispersal-free laboratory community dynamics consisting of two and three species of wood decay fungi (Chapter 4).

### 5.1 Methods

As in Chapter 4, code names of species are used throughout: ‘Hf’ for *Hypholoma fasciculare*, ‘Tv’ for *Trametes versicolor*, and ‘Vc’ for *Vuilemenia comedens*.

#### 5.1.1 Lattice model general description

To test the model’s predictive ability, I have set 3- and 2-species empirical communities on  $22.4 \times 22.4$  cm empirical Petri dishes, as described in Section 4.1.8. The lattice model represented the  $22.4 \times 22.4$  cm empirical Petri dish with a square, closed-boundary lattice of  $45 \times 45$  square sites. A lattice site could be occupied by one species at a time. Only the eight lattice sites surrounding a site were considered adjacent to it, which is called a ‘Moore neighbourhood’. A cluster of lattice sites connected via Moore neighbourhood, and occupied by the same species, represented a mycelium.

Given a state of the lattice at time  $t = 0$ , two types of event could minimally change the current state, by changing the occupancy of one lattice site at time  $t + \Delta t$ : an unoccupied site could become occupied by a mycelium extending from a neighbouring site; or a site occupied by one mycelium could be replaced by another mycelium invading

from a neighbouring site. A current lattice state could change to different new states due to the possible different extension or replacement events. Knowing the current lattice state, and all possible events with their rates of occurrence, allows predictions about the next lattice state with the algorithm described in Section 5.1.2.

### 5.1.2 Model general algorithm

I numerically simulated the temporal change in the lattice state with a rejection-free Kinetic Monte Carlo algorithm, also called dynamic Monte Carlo, n-fold way, residence time, or Gillespie algorithm (Bortz *et al.*, 1975; Gillespie, 1976). Given an initial lattice state at  $t = 0$  (i.e. taken from the mycelial occupancy discretisation in an empirical dish described in Section 4.1.8), the algorithm could simulate one stochastic realisation of the dynamics in continuous time, generating the next lattice state, and its time of appearance, at each repetition of the following main steps:

1. Calculate the rate of each possible extension and replacement event, according to the experimentally characterised elements of spatial competition (Section 5.1.3), and the model parameters estimated from the experiments (Section 5.1.4).
2. Calculate the sum,  $R$ , of the rates from step 1. The next event will be realised after an inter-event time  $\Delta t$ , randomly drawn from an exponential distribution with parameter  $\lambda = R$  (fewer and slower events lead to longer inter-event times on average). Increment current time  $t$  by  $\Delta t$ .
3. Select randomly one of the events from step 1, with probability weighted by its rate (a faster event is more probable to occur next). Realise the event.

Steps 1–3 were repeated until  $t$  exceeded a specified time limit, or until no event was possible ( $R = 0$ ).

### 5.1.3 Model incorporation of spatial competition elements

The six elements of spatial competition, characterised by the experiments (Chapter 4), had the following general form in the lattice model: (1) constant extension rates, independent of mycelial size, shape, position, or age (Fig. 5.1a); (2) extension rates unaffected by distant or adjacent conspecifics or heterospecifics (Fig. 5.1b); (3) faster replacement of younger mycelial regions (Fig. 5.1c); (4) faster replacement of smaller mycelia (Fig. 5.1d); (5) replacement as if mycelia are divided to multiple heterospecifics proportionally to the length of boundary with each (Fig. 5.1e); (6) additive effects of competition (Fig. 5.1f).

For Elements 1 and 2, I employed a parameter for the constant local extension rate of a species from occupied lattice sites to neighbouring unoccupied sites per day ( $\text{d}^{-1}$ ). The constant rate of extent of empirical mycelium boundary estimated from the experiments was (Chapter 4):  $0.14 \text{ cm d}^{-1}$  for Hf,  $0.36 \text{ cm d}^{-1}$  for Tv, and  $0.22 \text{ cm d}^{-1}$  for Vc. In

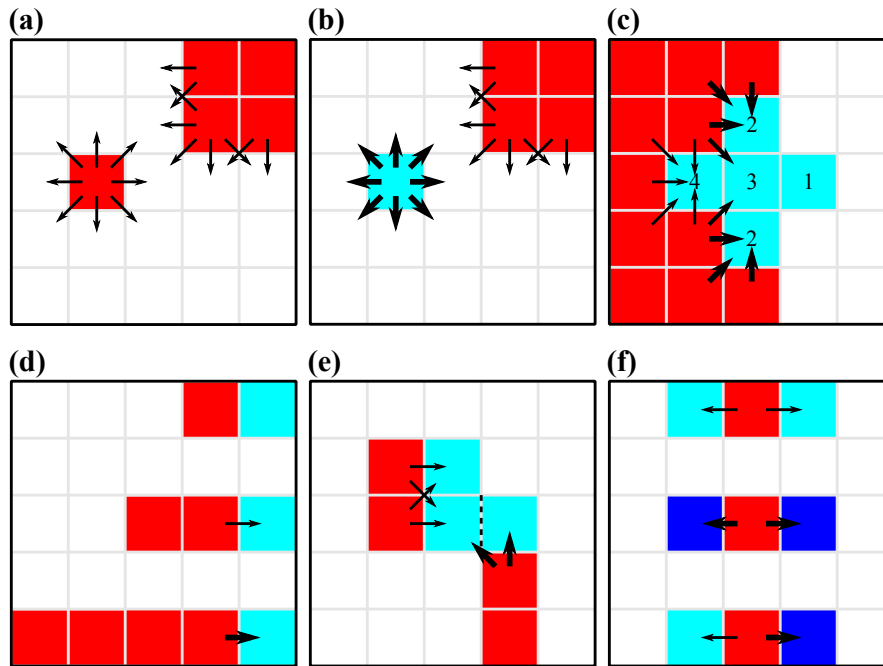


Figure 5.1: The incorporation to the theoretical lattice model of the six basic elements of spatial competition shown in Chapter 4. A white lattice site is unoccupied space; a Moore neighbourhood cluster of same-colour sites is a mycelium of a species; and a wider arrow symbolises faster extension, or replacement of a heterospecific mycelium. (a) Mycelia of a species extend to neighbouring unoccupied space with a constant mean rate (independent of mycelial size, shape, position, or age). (b) Extension to unoccupied space is not influenced by the presence of other conspecific or heterospecific mycelia. (c) Younger mycelial regions are replaced faster (hypothetical age of mycelial sites is given in numbers). (d) Relatively larger mycelial cover increases a mycelium's competitive ability to replace or resist replacement. (e) A central mycelium divides its competitive ability to multiple competitors proportionally to the length of the boundary with each (the dashed line divides the central mycelium to the cover that the competitors essentially interact with, i.e. the competitor on the twice larger boundary realises a twice larger central mycelium than the other competitor). (f) Replacement rates from 2-species settings are conserved in 3-species settings, i.e. additive effects of competition.

Section 5.1.4, I explain how to estimate the parameter of local extension rate in the model ( $d^{-1}$ ) from the rate of extent of empirical mycelium boundary in the experiments ( $\text{cm d}^{-1}$ ).

For Elements 4–6 which concern replacement events, I employed a parameter for the rate of local replacement of a species occupying a lattice site by another species occupying a neighbouring lattice site ( $d^{-1}$ ). According to the experiments (Chapter 4), replacement rate can be greater than zero only for Hf and Tv replacing Vc. By Element 3, zero days old Vc lattice sites were replaced at the extension rates of Hf and Tv, and boundary replacement rates decreased linearly until 6 days old Vc-occupied lattice sites; older Vc lattice sites were replaced at the boundary replacement rate obtained by the following relations of mycelial cover ratios of Element 4:  $0.0092 \log_2(C_{\text{Hf},i}/C_{\text{Vc},k}) + 0.074$ ,

and  $0.024 \log_2(C_{Tv,i}/C_{Vc,k})$ , where  $C_{X,i}/C_{Y,k}$  is the cover ratio of two adjacent mycelia  $i$  and  $k$  of species X and Y, respectively. These relations predict the rate of boundary replacement ( $\text{cm d}^{-1}$ ), not the local replacement rate between lattice sites ( $\text{d}^{-1}$ ), and I explain how to obtain the value for the local replacement rate parameter from the rate of boundary replacement in Section 5.1.4. The uniform distribution of competitive ability across the boundary with heterospecifics of Element 5 is incorporated by dividing the cover of each mycelium  $i$  by the mycelium's total length of boundary with heterospecifics,  $L_{X,i}$ , in the relations for Element 4:  $0.0092 \log_2((C_{Hf,i}/L_{Hf,i})/(C_{Vc,k}/L_{Vc,k})) + 0.074$ , and  $0.024 \log_2((C_{Tv,i}/L_{Tv,i})/(C_{Vc,k}/L_{Vc,k}))$ . The total length of the boundary with heterospecifics is a mycelium's number of neighbouring lattice sites occupied by any other species. Lastly, Element 6 required that local replacement rates were unaltered during interactions between adjacent mycelia of more than two species.

Since the lattice model is a spatial one, I had to implement an additional parameter for the smoothness of mycelial boundary, to be able to reproduce the relatively smooth boundaries observed on agar. The idea was that a mycelium with larger parameter value would extend more frequently from older mycelial sites, leading to a smoother boundary.

## 5.1.4 Model parameter estimation

### *Mycelial boundary shape parameter*

I first considered how empirical boundary extension or replacement is well reproduced on the discretised, coarse-grained representation of the lattice, in regard to diagonal extension due to the square geometry of the lattice. Because of the discretisation of empirical mycelia extending, the contribution to extension or replacement of an occupied site at the mycelial periphery appears two times faster towards lattice site neighbours to the horizontal and vertical directions, than to the diagonal directions (Fig. 5.2). Thus, the model local extension or replacement to the diagonal neighbours was assumed half of the actual rate.

Second, regarding the model parameter for adjusting the roughness of the mycelium boundaries, previous works have used a 'noise reduction parameter' denoting the number of times an event must be selected before actually realised (Tang, 1985; Kertesz & Vicsek, 1986; Nittmann & Stanley, 1986). Larger value of the noise reduction parameter leads to less noisy boundaries in models of growth. A disadvantage of this approach is that the simulation time is increased considerably. I developed another approach in which noise can be reduced, yet by choosing directly an event to realise. A mycelium-centric age of lattice sites was incorporated in the model. Since a mycelium increases its area by extension to unoccupied space, or replacement of other mycelia, I can characterise the mycelium sites by an integer age,  $a$ , denoting the number of extension and replacement events that have occurred in this mycelium since the occupancy of this site. I assumed

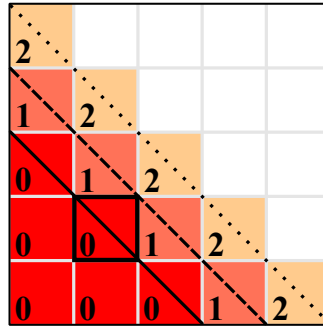


Figure 5.2: The lattice model local rate of extension and replacement of diagonally located neighbouring sites is halved. In this illustration, the empirical mycelium's actual boundary at  $t = 0$  is the solid line, discretised on the lattice by the sites numbered with zero. The focal site with the black border can contribute to extension horizontally (to the neighbouring site to its East), vertically (to the neighbouring site to its North), and diagonally (to the neighbouring site to its North-East). At  $t = 1$ , the empirical boundary has extended to the dashed line, adding to the model mycelium the lattice sites numbered with one. The focal site can contribute only horizontally and vertically to this addition. At  $t = 2$ , the empirical mycelium boundary extends further to the dotted line, and the focal site can now contribute diagonally. Thus, the contribution to model local extension and replacement diagonally can be taken as half of the actual rate.

that a mycelium 'selects' from which site of a free or heterospecific-adjacent boundary it will extend or replace based on the standardised age of the sites at that boundary (their actual age divided by the maximum site age at that boundary). I applied a power function to the standardised age of the boundary sites, to assign weights to the mycelium's selection for extension or replacement. The selection weight,  $w \in [0, 1]$ , was a function of standardised age,  $a \in [0, 1]$ , raised to the power of the mycelium shape parameter,  $s$ .

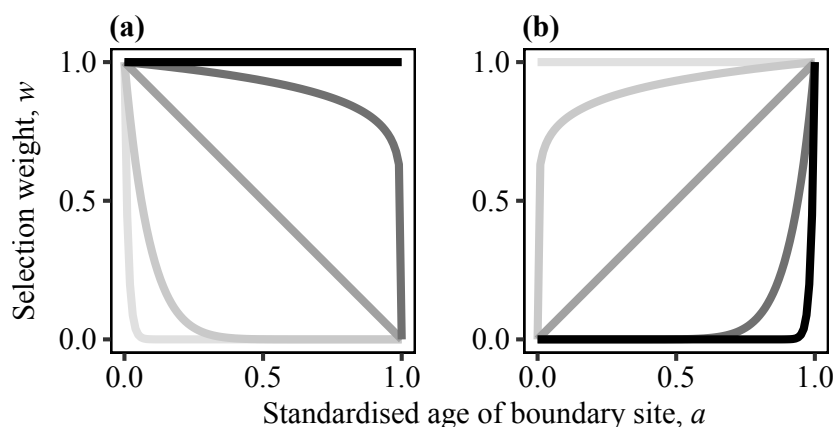


Figure 5.3: Weight,  $w$ , for the selection of a mycelium boundary site to extend or replace as a power function of its standardised age,  $a$ . (a) For model mycelium shape parameter  $s \leq 0$ , the power function was  $w(a) = (1 - a)^{-s}$ . Darker curve denotes larger shape parameter  $s = \{-80, -11, -1, -0.1, 0\}$ . (b) For shape parameter  $s \geq 0$ , the power function was  $w(a) = a^s$ . Darker curve denotes larger shape parameter  $s = \{0, 0.1, 1, 11, 80\}$ .

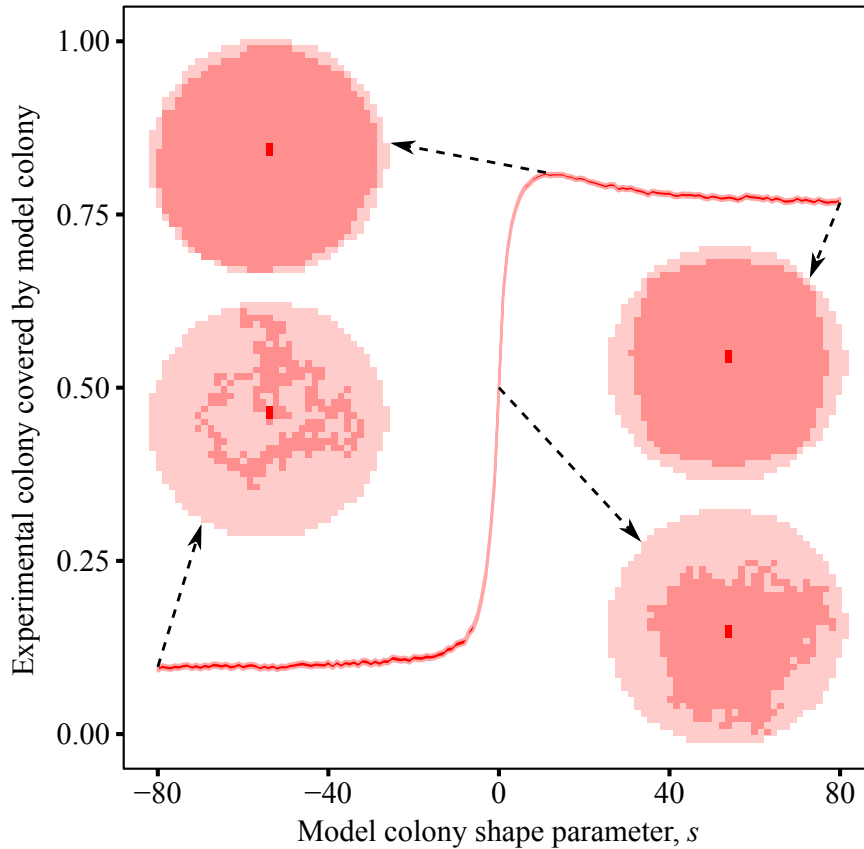


Figure 5.4: Estimation of mycelium shape parameter,  $s$ . The parameter was implemented as shown in Fig. 5.3. I scanned  $s$  parameter space, to identify values that maximise a measure of empirical–model mycelium shape similarity. I aimed to reproduce the shape of an empirical mycelium (lightest-shaded mycelium in all insets). This empirical mycelium extended from an inoculation site depicted by the darkest-shaded lattice sites in all insets. The occupied lattice sites of the empirical mycelium, and the inoculation site, were the input for the lattice model which simulated the extension of the mycelium, with the simulation terminating when the first model mycelium site had to extend beyond the empirical mycelium boundary (example mycelium with intermediate shading in all insets, for  $s = \{-80, 0, 11, 80\}$ ). The similarity measure was the mean ratio of the model to empirical mycelial cover. I show the 95% confidence region for the mean ratio from 1000 model simulations for each value of shape parameter,  $s$ .

For  $s \leq 0$ , the weight as a power function of age was  $w(a) = (1 - a)^{-s}$  (Fig. 5.3a); for  $s \geq 0$ ,  $w(a) = a^s$  (Fig. 5.3b).

For all species, in extension or replacement, I used the same parameter value that maximised model–empirical mycelium shape similarity. I estimated the value of the mycelium shape parameter that reproduces realistic shapes of mycelia (Fig. 5.4), given the power function relation of selection weights with the mycelium site age (Fig. 5.3). The empirical mycelial shape to be reproduced was a snapshot of a Tv mycelium which had extended from an inoculation site (Fig. 5.4). Extending from the same inoculation site as the empirical mycelium, the lattice model mycelium was allowed to extend until the first site had to extend beyond the empirical mycelium’s boundary. The ratio of the

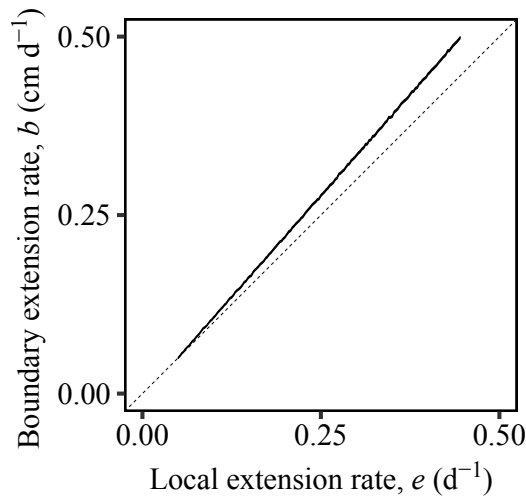


Figure 5.5: Relation between lattice model local extension rate and lattice model rate of boundary extension. The boundary extension rate is the mean from eight directions, and I show the 95% confidence region of the mean from 1000 simulations for each local extension rate value. By assuming a linear relation between the two extension rates, I could estimate backwards the local extension rate of a species in the model,  $e$ , from the measured boundary extension rate of empirical mycelia during extension to unoccupied space or replacement,  $b$ :  $e(b) = 0.88b + 0.0056$ . The dashed line for reference is the  $b(e) = e$  relation.

model to empirical mycelial cover was the measure of shape similarity. I found that the area of the experimental mycelium covered by the model mycelium was maximised for shape parameter  $s = 11$  (Fig. 5.4; and see Fig. 5.3b for the shape of the power function when  $s = 11$ ). I observed that the three species had similar, smooth boundaries during extension and replacement on empirical dishes, and hence I assumed  $s = 11$  for all species and model settings throughout.

#### ***Extension and replacement rate parameters***

Given realistic mycelial boundary shape with a proper value of the mycelium shape parameter (Fig. 5.4), I first investigated the relation between lattice model local extension rate and rate of boundary extension in model unconstrained mycelia. For each value in a range of local extension rate, I ran 1000 simulations of a mycelium extending unconstrained from an inoculation site. I measured the boundary extension rate of these mycelia (taking the mean from eight directions). I found an apparently linear relationship between the local extension or replacement rate,  $e$ , and the boundary extension or replacement rate,  $b$  (Fig. 5.5). Thus, I could use this relation to estimate backwards the model local extension or replacement rate parameter from measured rate of empirical mycelium boundaries in extension to unoccupied space, or in replacement of adjacent mycelia. The backwards linear relation used to estimate local extension and replacement rates for the lattice model was  $e(b) = 0.88b + 0.0056$ .

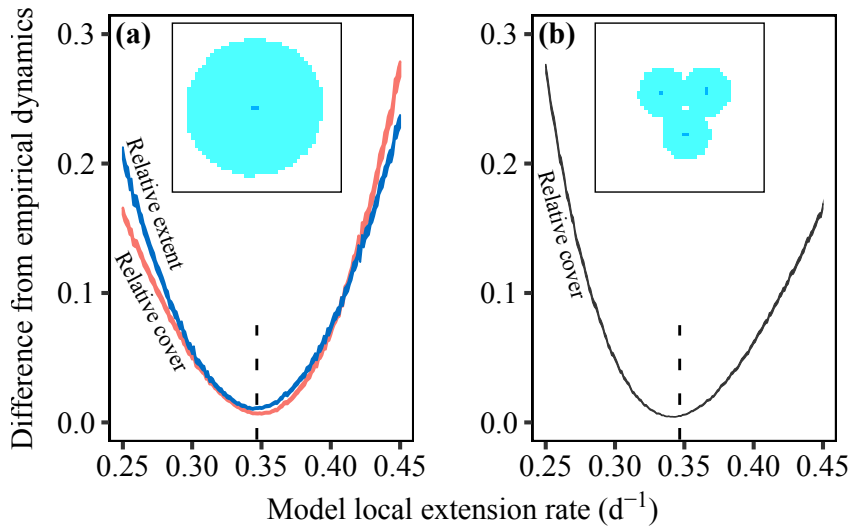


Figure 5.6: Parameter estimation of model local extension rate by minimising the sum of squared differences between empirical and model dynamics of relative cover and extent. I show two examples for the model local extension rate of Tv. (a) An empirical mycelium was extending from an inoculation site (inset shows a snapshot of an extended mycelium), and I measured the relative cover and mean relative extent from eight directions. The model was initialised with the same inoculation site, and the same two measures were taken at the same time points. I calculated the sum of squared differences across the time points, and finally took the mean from 1000 model simulations (95% confidence region for the mean is shown), for different values of the model local extension rate parameter. (b) Same as in (a), but with three empirical Tv mycelia extending from three inoculation sites (inset shows a snapshot of the mycelia fused), and measuring only the relative cover in time. Dashed vertical line segments point to the parameter value estimated by the backwards linear method (Fig. 5.5).

I tested if the backwards approach returns similar estimated parameter values as a sum of squared differences parameter estimation method (Hartig *et al.*, 2011). I tested the approach in two experimental settings. In one setting, an empirical Tv mycelium was extending from an inoculation site on a Petri dish; and in the other setting, three empirical Tv mycelia were extending from three inoculation sites, fusing to one mycelium, which covered the whole dish. I measured the dish relative mycelial cover in time for both settings, and the mean relative boundary extent from eight directions in time for the single mycelium's first setting. Both measurements were done in the discretised, coarse-grained representation of the empirical dish. I then run the model, scanning the parameter space of Tv model local extension rate, and calculated the sum of squared differences between the empirical and the theoretical measure in the simulation at each empirical and model time point  $t$  of measurement,  $m_{e,t}$  and  $m_{s,t}$ , respectively:  $\sum_t (m_{e,t} - m_{s,t})^2$ . Finally, I kept the mean sum from 1000 simulations for each scanned value of the model local extension rate. The range of model local rate of extension parameter values which minimised the sum of squared differences for both experimental settings, and for both measures of relative cover and extent, included the Tv model local extension rate parameter value



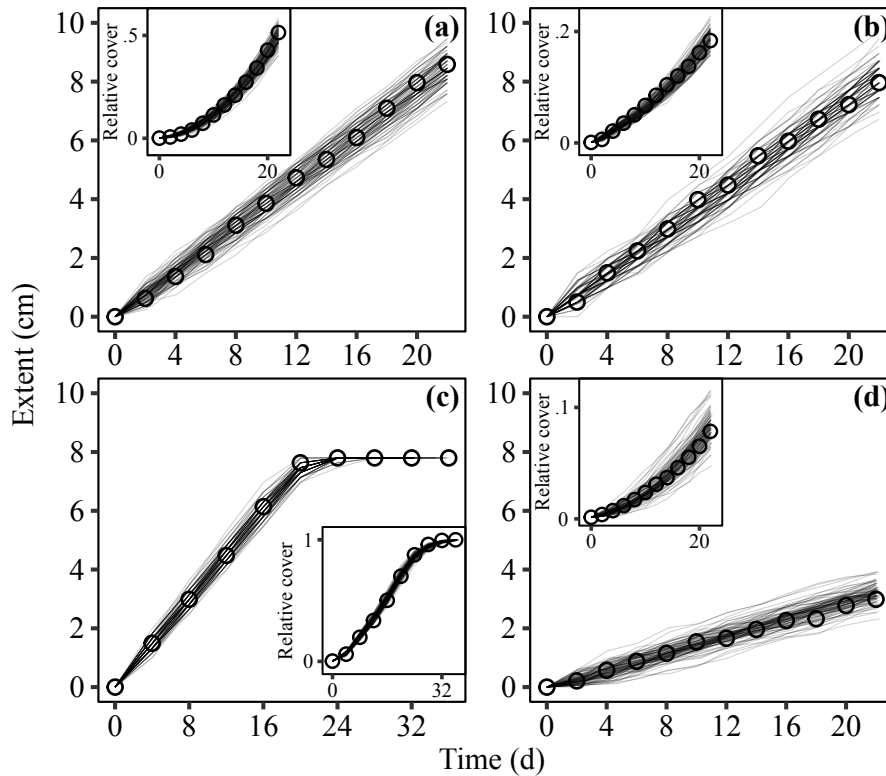


Figure 5.7: Empirical and model dynamics of mycelial extent and relative cover. Circles represent empirical values, and solid lines represent model trajectories ( $n = 100$ ). (a) Example of a Tv mycelium developing from an inoculated site, extending and covering the dish unconstrained (i.e. before reaching the dish boundaries). (b) Example of a Tv mycelium developing from a dish corner. (c) Example of three Tv mycelia closely inoculated at the dish centre, fusing to form one mycelium that extended and covered the dish. (d) Example of an Hf mycelium developing from the dish centre, extending and covering the dish at a slower rate than Tv. Extent is the mean from 2–4 directions of unconstrained empirical and model mycelial extension, except in (c) where the mycelium reached the dish boundaries after around 20 days. Model local extension rates were approximately equal to  $0.35 \text{ d}^{-1}$  for Tv, and  $0.13 \text{ d}^{-1}$  for Hf.

estimated by the backwards method (dashed vertical line segments in Fig. 5.6). Note that the Kinetic Monte Carlo algorithm's exponentially distributed inter-event times cannot fall exactly on the time points that empirical measurements were made. I was taking the last model time point before, and the first model time point after the empirical measurement time point, and I was linearly interpolating the model relative cover and extent at the exact time points corresponding to the empirical times of measurement.

## 5.2 Results

The extent and relative cover over time in model mycelia (Fig. 5.7a–d) were in agreement with the empirical dynamics (Fig. 4.4a–d), after estimating with the backwards approach the model parameters of local extension rate ( $\text{d}^{-1}$ ) from the empirical rates of boundary

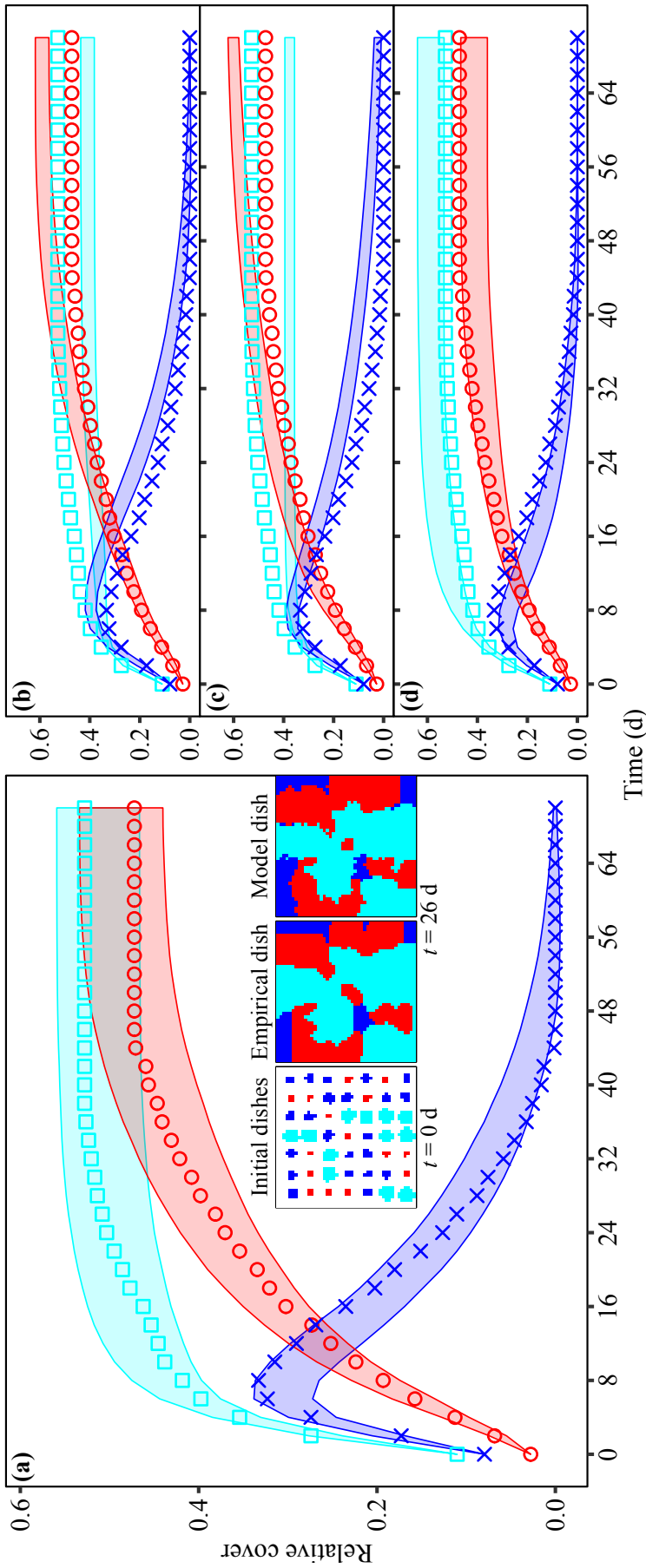


Figure 5.8: Lattice model predictions of a 3-species empirical community dynamics under four theoretical settings. The data points are for the empirical relative cover of the species in time, and the regions are 95% prediction intervals from 100 model trajectories. (a) All six experimentally characterised elements of spatial competition incorporated to the model. (b) All elements incorporated, except Element 3 for the relation of replacement with age of mycelial regions (replacement rates were fixed, as in paired mature mycelia experiments). (c) All elements incorporated, but Element 4 for the relation of replacement with mycelial cover was simplified (replacement rates were fixed, as in 1/1 cover ratio experiments). (d) All elements incorporated, but Element 5 for replacement against multiple adjacent competitors was simplified (replacement rate was as in mycelia facing undivided each adjacent competitor). In (a), the insets show the initial lattice state in the empirical and model Petri dish on the left ( $t = 0$  d), the empirical dish at a later time in the middle, and one realisation of the model at that same later time on the right (setting as in Fig. 4.1f). Colour-point (of each species): red-circle (Hf), cyan-square (Tv), and blue-cross (Vc).

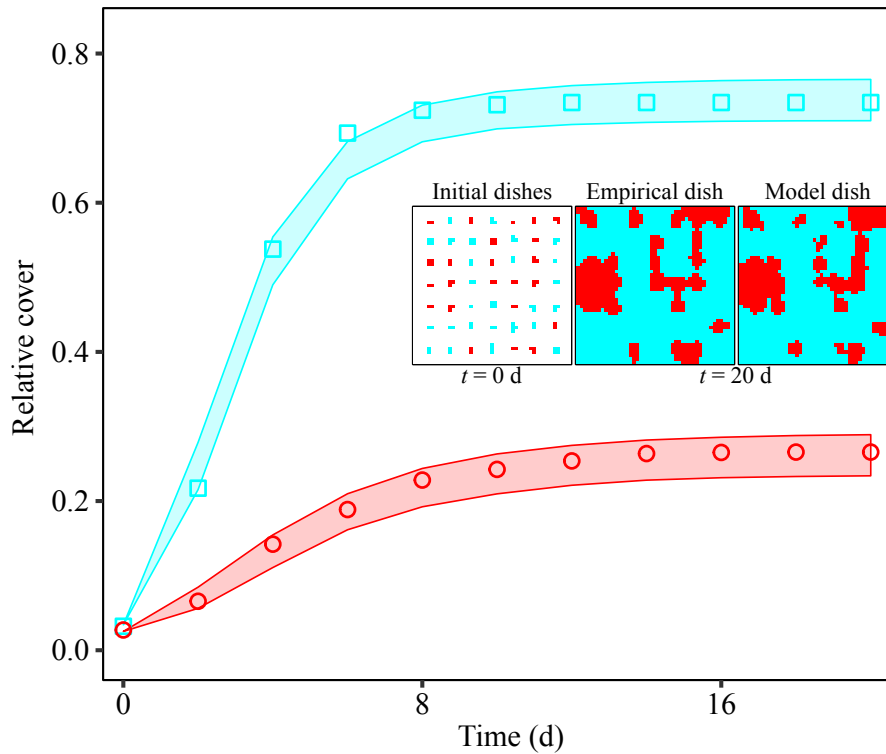


Figure 5.9: The lattice model predictions of a 2-species, Hf versus Tv, empirical community dynamics. The data points are for the empirical relative cover of the species in time, and the regions are 95% prediction intervals from 100 model trajectories. The two species deadlocked upon contact. The insets show the initial lattice state in the empirical and model Petri dishes ( $t = 0$  d), and in the empirical dish with one realisation of the model at the final time of complete deadlock. Since the two species deadlock, Elements 3–5 regarding replacement rates are not involved in the interactions, and hence could not be simplified. Colour–point (of each species): red–circle (Hf), and cyan–square (Tv).

extension ( $\text{cm d}^{-1}$ ).

With all six characterised elements incorporated, the lattice model could predict the dynamics of the 3-species and 2-species empirical community dynamics. For the 3-species community dynamics, almost all the relative cover measurements from the empirical dish fell inside the lattice model’s 95% prediction intervals (Fig. 5.8a). Additionally, model dishes closely resembled the empirical dish in the spatial configurations and shapes of the mycelia (e.g. insets in Fig. 5.8a). The lattice model could not predict well the empirical dynamics when even one of the elements of spatial competition was omitted or simplified (Fig. 5.8b–d).

Hf deadlocked with Tv in any cover ratio tested experimentally, and the model could predict this empirical community’s dynamics (Fig. 5.9). Because of deadlock, I could not exclude or simplify Elements 3–5 regarding replacement rates in the Hf–Tv community dynamics. For Hf–Vc and Tv–Vc, almost all relative cover measurements from the empirical dish fell inside the lattice model’s 95% prediction intervals (Fig. 5.10a and 5.11a). The shapes and spatial configurations of the empirical mycelia were similar

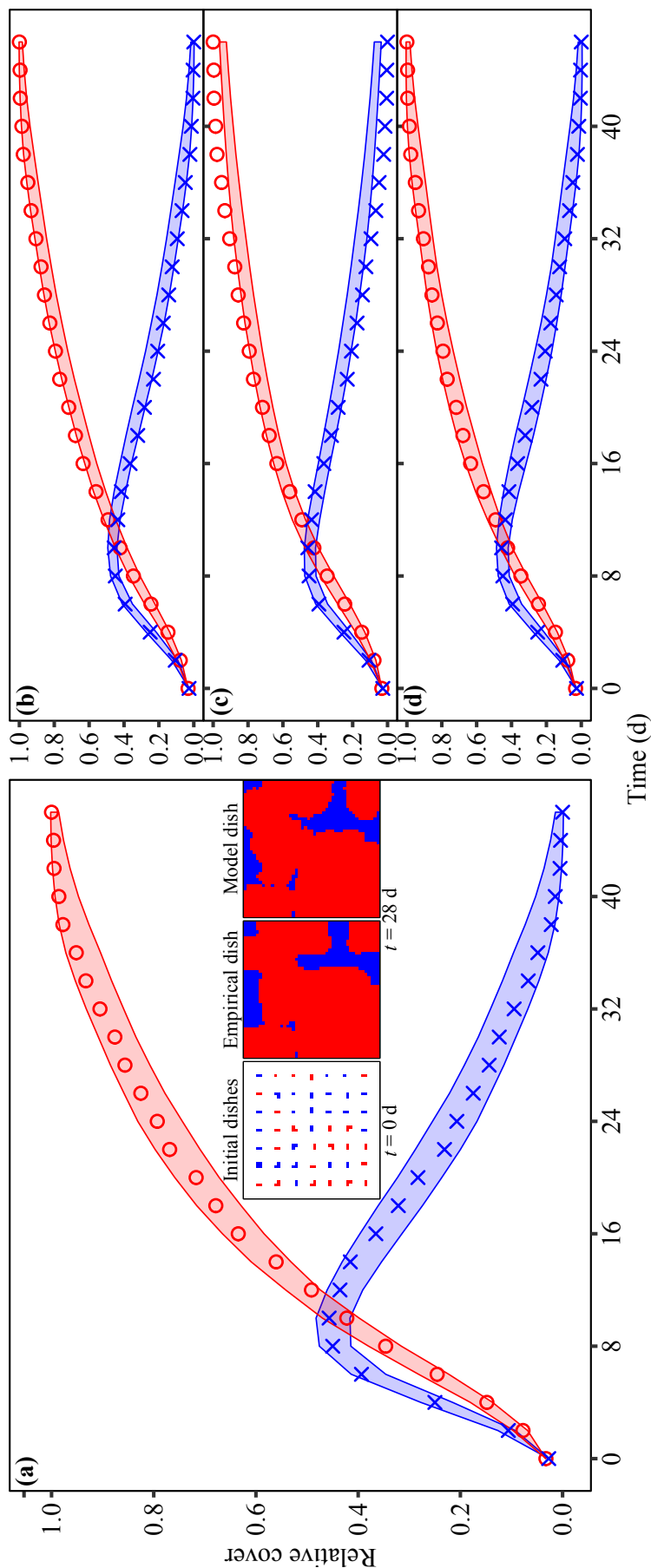


Figure 5.10: The lattice model predictions of a 2-species, Hf versus Vc, empirical community dynamics. The data points are for the empirical relative cover of the species in time, and the regions are 95% prediction intervals from 100 model trajectories. (a) All six experimentally characterised elements of spatial competition incorporated to the model. (b) All elements incorporated, except Element 3 for the relation of replacement with mycelium age. (c) All elements incorporated, but Element 4 for the relation of replacement with mycelium cover was simplified (replacement rates were fixed, as in 1/1 cover ratio experiments). (d) All elements incorporated, but Element 5 for the relation of replacement with length of boundary with heterospecifics was simplified (replacement rate was as if mycelia face undivided each one of their multiple adjacent competitors). For (a), the insets show the initial lattice state in the empirical and model Petri dishes ( $t=0$  d), and in the empirical dish with one realisation of the model at a later time. Colour-point (of each species): red-circle (Hf), and blue-cross (Vc).

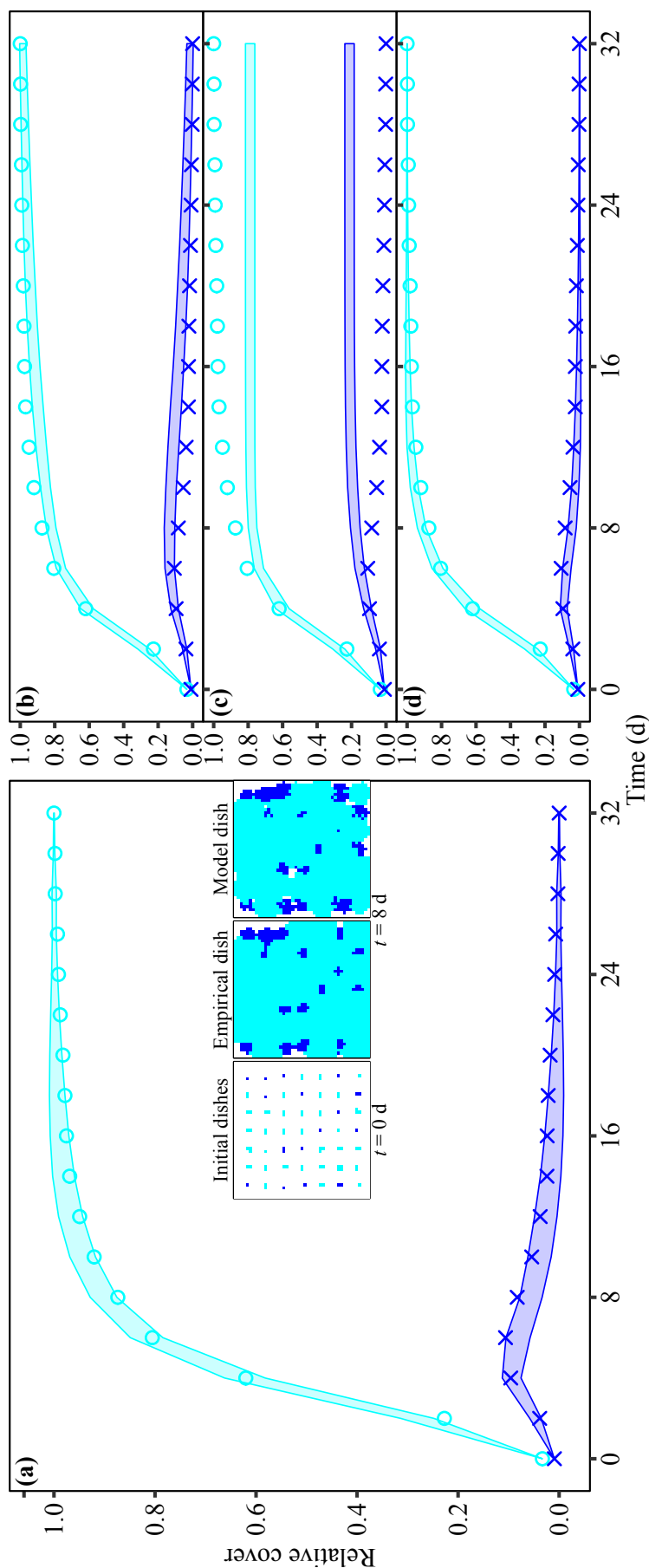


Figure 5.11: The lattice model predictions of a 2-species, Tv versus Vc, empirical community dynamics. The data points are for the empirical relative cover of the species in time, and the regions are 95% prediction intervals from 100 model trajectories. (a) All six experimentally characterised elements of spatial competition incorporated to the model. (b) All elements incorporated, except Element 3 for the relation of replacement with mycelium age (replacement rates were fixed, as in paired mature mycelium experiments). (c) All elements incorporated, but Element 4 for the relation of replacement with mycelium cover was simplified (replacement rates were fixed, as in 1/1 cover ratio experiments). (d) All elements incorporated, but Element 5 for the relation of replacement with length of boundary with heterospecifics was simplified (replacement rate was as in mycelia facing undivided each adjacent competitor). For (a), the insets show the initial lattice state in the empirical and model Petri dishes ( $t = 0$  d), and in the empirical dish with one realisation of the model at a later time. Colour-point (of each species): cyan-square (Tv), and blue- $\times$  (Vc).

to the empirical (see insets in Fig. 5.10a and 5.11a). As in the 3-species community dynamics, the lattice model could not predict well the empirical dynamics when even one of the Elements 3–5 was excluded or simplified (Fig. 5.10b–d and 5.11b–d).

### **5.3 Summary**

The theoretical prediction of fungal community dynamics requires the understanding of basic spatial competition elements (Chapter 4): (1) different rates of mycelial extension to unoccupied space; (2) inhibition or stimulation of extension by other mycelia; (3) mycelial replacement in relation to mycelial age; (4) replacement in relation to mycelial size; (5) distribution of competitive ability against multiple adjacent heterospecifics; and (6) competitive additivity of multi-species interactions. Previous theoretical models have not incorporated all these six elements, to predict empirical community dynamics. I aimed to test if all elements are required for the prediction of 3-species and 2-species laboratory community dynamics on agar with a lattice model. I show that all elements were necessary for the model to predict community dynamics. Thus, I propose that studies in natural substrata should consider these six elements, for accurate predictions of community dynamics, and hence of processes in which filamentous fungi are key players, such as biogeochemical cycling, primary production, biocontrol, and bioremediation.

# Chapter 6

## Two models of ordinary and partial differential equations for fungal community dynamics

In this Chapter, simple ODE and PDE models are developed, for predicting fungal community dynamics (validated against the empirical data from the experiments in Chapter 4). The models are based on the basic processes of extension and replacement incorporated in the lattice model of Chapter 5, according to empirical findings on filamentous fungi (Chapter 4).

### 6.1 Results

#### 6.1.1 1-species master equation

First, I will derive an ODE model of fungal interactions from the lattice model of Chapter 5. The lattice model described substrate sites occupied or unoccupied by fungal species. Similarly, the ODE model will describe number or relative abundance of resource sites occupied by the different species. In contrast to the lattice model, the ODE model will be non-spatial, assuming each site is neighbour to any other site, such as in a flask with well-mixed, liquid culture of dispersed mycelia (Prosser, 1995). We will assume there is a finite number of available sites,  $n$ , for occupancy in the agitated flask. The number of resource sites occupied by species X is symbolised with  $n_X$ , with unoccupied sites considered an extra species  $\emptyset$ .

For a single species A, the total number  $n$  of resource sites in the finite domain of a flask is the sum of the number of sites occupied by species A,  $n_A$ , plus the number of unoccupied sites,  $n_\emptyset$ :

$$n = n_A + n_\emptyset. \tag{6.1}$$

The only basic process at play will be extension of a fungus from occupied to unoccupied resource sites in the well mixed culture. We will exclude some kind of death or degeneration–recycling process because of the indeterminate growth mode of filamentous fungi, and due to our experimental setting of rich and homogeneously distributed substrate (Chapter 4). Species A occupying a site  $s_A$  can extend to a site occupied by (non)species  $\emptyset$   $s_\emptyset$ , resulting to two sites occupied by A:  $s_A + s_\emptyset \rightarrow 2s_A$ . The rate of extension will increase with the relative abundance of unoccupied sites,  $n_\emptyset/n$ , which can be alternatively expressed with Equation 6.1 as a decrease in the extension rate with the relative abundance of A,  $n_\emptyset/n = (n - n_A)/n = 1 - n_A/n$ :

$$g_A(n_A) = e_A \left(1 - \frac{n_A}{n}\right). \quad 6.2$$

The extension rates  $g_A$  and  $e_A$  are probabilities of having an extension event per unit of time, i.e. per day in our experimental and modelling settings (unit of measurement:  $\text{d}^{-1}$ ).

I will follow an ‘occupation numbers point of view’ for deriving a master equation (Torral & Colet, 2014). The master equation is a system of ODE. Each differential equation concerns the rate of change of the probability of having  $n_A$  sites occupied by species A at time  $t$ :  $\text{Pr}(n_A; t)$ . The master equation will determine the dynamics of the discrete probability distribution for the number of sites occupied by species A. In this 1-species setting, we will have  $n$  differential equations, since  $n_A$  can take the integer values  $n_A = \{1, 2, \dots, n\}$ :  $\{\text{Pr}(1; t), \text{Pr}(2; t), \dots, \text{Pr}(n; t)\}$ .  $n_A = 0$  is omitted because there can be no dynamics without any fungus present initially.

To have  $n_A$  sites occupied by A at time  $t + dt$ , either we had  $n_A - 1$  at time  $t$  and minimally one of them extended to an unoccupied site during the time interval  $dt$ , or we had  $n_A$  sites at time  $t$  and none extended to an unoccupied site. Thus, the probability of having  $n_A$  at time  $t + dt$  is:

$$\begin{aligned} \text{Pr}(n_A; t + dt) = & \text{Pr}(n_A - 1; t) \text{Pr}(\text{one of the } n_A - 1 \text{ extended}) \\ & + \text{Pr}(n_A; t) \text{Pr}(\text{none of the } n_A \text{ extended}). \end{aligned} \quad 6.3$$

From Equation 6.2, the probability that one of the  $n_A - 1$  sites extends in the time interval  $dt$  is  $g_A(n_A - 1)dt$ . Hence, the probability in Equation 6.3 for all  $n_A - 1$  sites is

$$\text{Pr}(\text{one of the } n_A - 1 \text{ extended}) = (n_A - 1)g_A(n_A - 1)dt. \quad 6.4$$

Similarly, the probability that a site occupied by A extends to an unoccupied site in the time interval  $dt$  is  $g_A(n_A)dt$ . Hence, the probability of not extending is  $1 - g_A(n_A)dt$ ,



and the respective term in Equation 6.3 for all  $n_A$  sites is

$$\begin{aligned} \Pr(\text{none of the } n_A \text{ extended}) &= (1 - g_A(n_A)dt)^{n_A} \\ &= 1 - n_A g_A(n_A)dt + O(dt^2), \end{aligned} \quad 6.5$$

by Maclaurin series expansion.

Inserting Equations 6.4 and 6.5 into Equation 6.3, gives

$$\begin{aligned} \Pr(n_A; t + dt) &= \Pr(n_A - 1; t)(n_A - 1)g_A(n_A - 1)dt \\ &\quad + \Pr(n_A; t)(1 - n_A g_A(n_A)dt) \\ &\quad + O(dt^2). \end{aligned} \quad 6.6$$

Taking  $\Pr(n_A; t)$  to the left hand side of Equation 6.6, dividing by  $dt$ , omitting the higher order terms  $O(dt^2)$ , and taking the limit as  $dt \rightarrow 0$  gives the master equation

$$\begin{aligned} \frac{d\Pr(n_A; t)}{dt} &= \Pr(n_A - 1; t)(n_A - 1)g_A(n_A - 1) \\ &\quad - \Pr(n_A; t)n_A g_A(n_A), \end{aligned} \quad 6.7$$

which can be rewritten after inserting Equation 6.2 as

$$\begin{aligned} \frac{d\Pr(n_A; t)}{dt} &= \Pr(n_A - 1; t)(n_A - 1)e_A \left(1 - \frac{n_A - 1}{n}\right) \\ &\quad - \Pr(n_A; t)n_A e_A \left(1 - \frac{n_A}{n}\right). \end{aligned} \quad 6.8$$

### 6.1.2 1-species ODE model

Since the master equation dictates the dynamics of the discrete probability distribution for  $n_A$ , I will derive the differential equation for the first moment, i.e. the mean of this distribution. The mean  $\langle n_A(t) \rangle$  of  $n_A(t)$  in the discrete probability distribution of the master equation is

$$\langle n_A(t) \rangle = \sum_{n_A=1}^n n_A \Pr(n_A; t). \quad 6.9$$

Note that because Equation 6.9 is a finite sum,

$$\begin{aligned} \frac{d\langle n_A(t) \rangle}{dt} &= \frac{d\sum_{n_A=1}^n n_A \Pr(n_A; t)}{dt} \\ &= \sum_{n_A=1}^n n_A \frac{d\Pr(n_A; t)}{dt}. \end{aligned} \quad 6.10$$

Thus, multiplying the master Equation 6.8 by  $n_A$ , and taking the sum for all possible  $n_A$ , leads to a differential equation for the mean of the discrete probability distribution described by the master equation:

$$\begin{aligned} \frac{d\langle n_A(t) \rangle}{dt} &= \sum_{n_A=1}^n \left\{ n_A \Pr(n_A - 1; t) (n_A - 1) e_A \left( 1 - \frac{n_A - 1}{n} \right) \right\} \\ &\quad - \sum_{n_A=1}^n \left\{ \Pr(n_A; t) n_A^2 e_A \left( 1 - \frac{n_A}{n} \right) \right\}. \end{aligned} \quad 6.11$$

The  $\Pr(n_A - 1; t)$  in the first sum of the right hand side of Equation 6.11 can be rewritten as  $\Pr(n_A; t)$  by changing the limits of the sum from  $n_A = \{1, \dots, n\}$  to  $n_A = \{0, \dots, n-1\}$ , and by omitting the  $n_A = 0$  term since it is zero. Additionally, the limits of the sum can become  $n_A = \{1, \dots, n\}$ , if we add and subtract a term for  $n_A = n$ . Note that this term is zero because of the  $n/n$  division:

$$\begin{aligned} &\sum_{n_A=1}^n \left\{ n_A \Pr(n_A - 1; t) (n_A - 1) e_A \left( 1 - \frac{n_A - 1}{n} \right) \right\} = \\ &= \sum_{n_A=1}^{n-1} \left\{ (n_A + 1) \Pr(n_A; t) n_A e_A \left( 1 - \frac{n_A}{n} \right) \right\} = \\ &= \sum_{n_A=1}^n \left\{ (n_A + 1) \Pr(n_A; t) n_A e_A \left( 1 - \frac{n_A}{n} \right) \right\} - (n + 1) \Pr(n; t) n e_A \left( 1 - \frac{n}{n} \right). \end{aligned} \quad 6.12$$

Doing some calculations in the final sum of Equation 6.12, gives:

$$\begin{aligned} &\sum_{n_A=1}^n \left\{ (n_A + 1) \Pr(n_A; t) n_A e_A \left( 1 - \frac{n_A}{n} \right) \right\} = \\ &= \sum_{n_A=1}^n \left\{ n_A^2 \Pr(n_A; t) e_A \left( 1 - \frac{n_A}{n} \right) \right\} + \sum_{n_A=1}^n \left\{ n_A \Pr(n_A; t) e_A \left( 1 - \frac{n_A}{n} \right) \right\}. \end{aligned} \quad 6.13$$

The final two sums in Equation 6.13 can replace the first sum of the right hand side of Equation 6.11:

$$\begin{aligned} \frac{d\langle n_A(t) \rangle}{dt} &= \sum_{n_A=1}^n \left\{ n_A^2 \Pr(n_A; t) e_A \left( 1 - \frac{n_A}{n} \right) \right\} \\ &\quad + \sum_{n_A=1}^n \left\{ n_A \Pr(n_A; t) e_A \left( 1 - \frac{n_A}{n} \right) \right\} \\ &\quad - \sum_{n_A=1}^n \left\{ \Pr(n_A; t) n_A^2 e_A \left( 1 - \frac{n_A}{n} \right) \right\}. \end{aligned} \quad 6.14$$

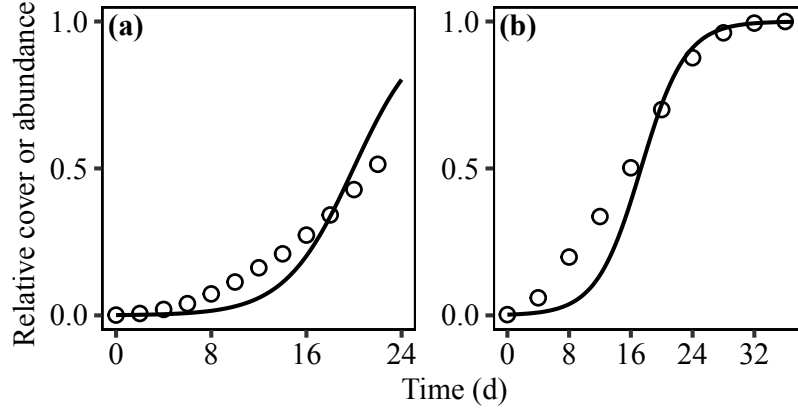


Figure 6.1: 1-species experimental dynamics compared to the model dynamics from the ODE 6.17. Circles are for the Tv experimental relative cover of the Petri dish, and curves are for the relative abundance of Tv in a well-mixed culture with the ODE model. (a) A single Tv mycelium inoculated at the centre of a dish in the experiment, extending before reaching the edges of the dish (same as in Fig. 4.4a and 5.7a). (b) Three Tv mycelia closely inoculated at the dish centre, fusing to form one mycelium which extended and covered the dish (same as in Fig. 4.4c and 5.7c). The ODE model had initial condition  $A(0)$  equal to the experimental setting, and extension rate parameter  $e_A$  equal to the local extension parameter of the lattice model in Fig. 5.7,  $e_A \approx 0.35 \text{ d}^{-1}$ .

Two of the sums in Equation 6.14 cancel out, leading to

$$\begin{aligned} \frac{d\langle n_A(t) \rangle}{dt} &= e_A \sum_{n_A=1}^n \{n_A \Pr(n_A; t)\} - \frac{e_A}{n} \sum_{n_A=1}^n \{n_A^2 \Pr(n_A; t)\} \\ &= e_A \langle n_A(t) \rangle - \frac{e_A}{n} \langle n_A^2(t) \rangle. \end{aligned} \quad 6.15$$

Thus, the dynamics of the first moment depend on the second. In long enough time, a fungus will occupy all unoccupied sites in any stochastic realisation, and hence the variance of the stochastic trajectories will tend to zero,  $\text{Var}[n_A(t)] = 0$ . Since the second moment is  $\langle n_A^2(t) \rangle = \text{Var}[n_A(t)] + \langle n_A(t) \rangle^2$ , approximately we have  $\langle n_A^2(t) \rangle = \langle n_A(t) \rangle^2$ . This leads to the final equation for the first moment dynamics:

$$\frac{d\langle n_A(t) \rangle}{dt} = e_A \langle n_A(t) \rangle - \frac{e_A}{n} \langle n_A(t) \rangle^2. \quad 6.16$$

Equation 6.16 is in terms of mean number of sites in time,  $\langle n_A(t) \rangle$ , and we can cast it in terms of mean relative abundance of species A in time,  $A(t) = \langle n_A(t) \rangle / n$ , leading to the deterministic ODE model of logistic increase in the species mean occupancy (see Fig. 6.1 for the resulting well-mixed dynamics compared to the spatial dynamics of 1-species mycelia extending on an experimental Petri dish):

$$\frac{dA(t)}{dt} = e_A A(t) (1 - A(t)). \quad 6.17$$

### 6.1.3 2-species master equation

In this subsection, we assume the following basic processes for the 2-species system: extension of species A, extension of species B, and replacement of species B by species A.

As in the 1-species case of Equation 6.2, the extension rates of the two species are function of the number of sites occupied by A and B,  $n_A$  and  $n_B$ :

$$g_A(n_A, n_B) = e_A \left(1 - \frac{n_A + n_B}{n}\right), \quad 6.18$$

$$g_B(n_A, n_B) = e_B \left(1 - \frac{n_A + n_B}{n}\right). \quad 6.19$$

The rate with which one site occupied by species A replaces a site occupied by B will be a linear function of the relative abundance of B:

$$k_A(n_B) = r_A \frac{n_B}{n}. \quad 6.20$$

Again, the extension rates  $g_A$ ,  $g_B$ ,  $e_A$  and  $e_B$ , and the replacement rates  $k_A$  and  $r_A$ , are probabilities of having an event per unit of time, i.e. per day in our experimental and modelling settings (unit of measurement:  $\text{d}^{-1}$ ).

For the master equation, the probability of having  $n_A$  and  $n_B$  at time  $t + dt$  will be

$$\begin{aligned} \Pr(n_A, n_B; t + dt) = & \Pr(n_A - 1, n_B; t) \Pr(\text{one of } n_A - 1 \text{ extended}) \\ & + \Pr(n_A, n_B - 1; t) \Pr(\text{one of } n_B - 1 \text{ extended}) \\ & + \Pr(n_A - 1, n_B + 1; t) \Pr(\text{one of } n_A - 1 \text{ replaced one of } n_B + 1) \\ & + \Pr(n_A, n_B; t) \Pr(\text{none of } n_A \text{ extended}) \Pr(\text{none of } n_B \text{ extended}) \\ & \cdot \Pr(\text{none of } n_A \text{ replaced one of } n_B). \end{aligned} \quad 6.21$$

By treating Equations 6.18–6.21 as in the steps with Equations 6.4–6.7 for the 1-species master equation, we can derive the master equation for the two species:

$$\begin{aligned} \frac{d\Pr(n_A, n_B; t)}{dt} = & \Pr(n_A - 1, n_B; t) (n_A - 1) e_A \left(1 - \frac{n_A - 1 + n_B}{n}\right) \\ & + \Pr(n_A, n_B - 1; t) (n_B - 1) e_B \left(1 - \frac{n_A + n_B - 1}{n}\right) \\ & + \Pr(n_A - 1, n_B + 1; t) (n_A - 1) r_A \frac{n_B + 1}{n} \\ & - \Pr(n_A, n_B; t) \left[ n_A e_A \left(1 - \frac{n_A + n_B}{n}\right) + n_B e_B \left(1 - \frac{n_A + n_B}{n}\right) + n_A r_A \frac{n_B}{n} \right]. \end{aligned} \quad 6.22$$

### 6.1.4 2- and 3-species ODE models

The first moments for the occupancy of the two species are:

$$\langle n_A(t) \rangle = \sum_{n_A=1}^n \sum_{n_B=1}^n n_A \Pr(n_A, n_B; t), \quad 6.23$$

$$\langle n_B(t) \rangle = \sum_{n_A=1}^n \sum_{n_B=1}^n n_B \Pr(n_A, n_B; t). \quad 6.24$$

Following the same way as in Equations 6.10–6.15 for the quantities in Equations 6.23 and 6.24, we can derive the differential equations for the first moment dynamics from the master Equation 6.22:

$$\frac{d\langle n_A(t) \rangle}{dt} = e_A \langle n_A(t) \rangle - \frac{e_A}{n} \langle n_A^2(t) \rangle + (r_A - e_A) \langle n_A n_B \rangle, \quad 6.25$$

$$\frac{d\langle n_B(t) \rangle}{dt} = e_B \langle n_B(t) \rangle - \frac{e_B}{n} \langle n_B^2(t) \rangle - (r_A + e_B) \langle n_A n_B \rangle. \quad 6.26$$

Since species A will eventually replace B in long enough time of any stochastic realisation, the variance of each species, and the covariance of A–B will tend to zero. By adopting the mean-field approximations  $\langle n_A^2(t) \rangle = \langle n_A(t) \rangle^2$ ,  $\langle n_B^2(t) \rangle = \langle n_B(t) \rangle^2$ , and  $\langle n_A(t) n_B(t) \rangle = \langle n_A(t) \rangle \langle n_B(t) \rangle$ , Equations 6.25 and 6.26 can be written as

$$\frac{d\langle n_A(t) \rangle}{dt} = e_A \langle n_A(t) \rangle - \frac{e_A}{n} \langle n_A(t) \rangle^2 + (r_A - e_A) \langle n_A(t) \rangle \langle n_B(t) \rangle, \quad 6.27$$

$$\frac{d\langle n_B(t) \rangle}{dt} = e_B \langle n_B(t) \rangle - \frac{e_B}{n} \langle n_B(t) \rangle^2 - (r_A + e_B) \langle n_A(t) \rangle \langle n_B(t) \rangle. \quad 6.28$$

Equations 6.27 and 6.28 are in terms of mean number of sites in time,  $\langle n_A(t) \rangle$  and  $\langle n_B(t) \rangle$ , and we can cast them in terms of mean relative abundance in time,  $A(t) = \langle n_A(t) \rangle / n$  and  $B(t) = \langle n_B(t) \rangle / n$ :

$$\frac{dA(t)}{dt} = e_A A(t) (1 - A(t) - B(t)) + r_A A(t) B(t), \quad 6.29$$

$$\frac{dB(t)}{dt} = e_B B(t) (1 - A(t) - B(t)) - r_A A(t) B(t). \quad 6.30$$

For species A, per capita extension is reduced with increasing relative abundance of A or B, and per capita replacement is increased with increased relative abundance of B. For species B, per capita extension is reduced with increasing relative abundance of A or B as well, and its per capita replacement is increased with increased relative abundance of A.

From the 2-species ODE model of Equations 6.29 and 6.30, we can write a 3-species ODE model in which species A and B can replace species C, as Hf and Tv did against

Vc in the experiments of Chapter 4:

$$\frac{dA(t)}{dt} = e_A A(t)(1 - A(t) - B(t) - C(t)) + r_A A(t)C(t), \quad 6.31$$

$$\frac{dB(t)}{dt} = e_B B(t)(1 - A(t) - B(t) - C(t)) + r_B B(t)C(t), \quad 6.32$$

$$\frac{dC(t)}{dt} = e_C C(t)(1 - A(t) - B(t) - C(t)) - (r_A A(t) + r_B B(t))C(t). \quad 6.33$$

Species A and B cannot replace each other.

### 6.1.5 1-species PDE model

We can use the 1-species ODE model of Equation 6.17 for a spatial, 1-species PDE model in two spatial dimensions,  $x$  and  $y$ , since the experiments and the lattice model were studied in 2-D as well. The ODE model of Equation 6.17 determines the logistic increase in the occupancy of resource sites of a species A. Equivalently in the PDE model, I will assume that the density  $A(x, y, t)$  of a mycelium at the  $x, y$  point in 2-D space grows logistically in time  $t$  (density of species A will be shortly symbolised as  $A$  hereafter), to attain the maximum density  $A = 1$ , with growth parameter  $\varepsilon_A$  ( $d^{-1}$ ). Additionally, the mycelium diffuses (i.e. extends) with diffusion coefficient  $\delta_A$  ( $cm^2 d^{-1}$ ). The resulting PDE model is the Kolmogorov, Petrovskii, Piskunov and Fisher equation (KPP–Fisher equation in Volpert & Petrovskii, 2009):

$$\frac{\partial A}{\partial t} = \varepsilon_A A(1 - A) + \delta_A \left( \frac{\partial^2 A}{\partial x^2} + \frac{\partial^2 A}{\partial y^2} \right). \quad 6.34$$

Since the simulated Petri dish has closed boundaries, I assumed that  $\partial A / \partial x = 0$  and  $\partial A / \partial y = 0$  orthogonally to the boundaries (Neumann boundary conditions). The simulated Petri dish was a square with sides of 22.4 cm.

Starting from an initial density of species A decaying exponentially in the plane, the extending mycelium's boundary attains a constant speed of front  $c_A = 2\sqrt{\varepsilon_A \delta_A}$  (Volpert & Petrovskii, 2009). We will throughout fix the ratio  $\varepsilon_A / \delta_A = 125 \text{ cm}^{-2}$ , to have sufficiently steep initial densities at the inocula and at the propagating fronts (Volpert & Petrovskii, 2009). Since the boundary extension rates of species are known from the experiments, i.e.  $c_A$  is known, and assuming  $\varepsilon_A / \delta_A = 125 \text{ cm}^{-2}$ , I can calculate the parameters  $\varepsilon_A$  and  $\delta_A$  for a species A. Such parameter estimation appeared satisfactory for 1-species dynamics of relative cover with the PDE model, both for the single Tv mycelium (Fig. 6.2a), and for the three mycelia extending to cover the whole dish (Fig. 6.2b). Note that to estimate the relative mycelial cover I had to set arbitrarily a density threshold above which a mycelium was considered present locally. A mycelium was assumed present when its density  $A > 0.01$ . The relative cover in the PDE solution was

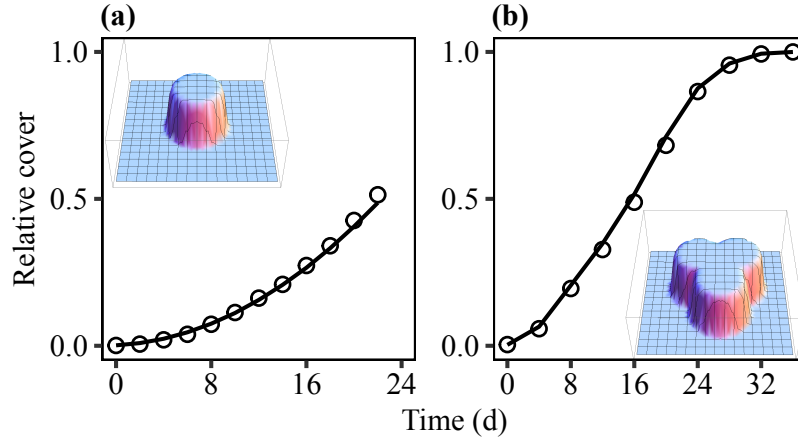


Figure 6.2: 1-species experimental dynamics compared to the model dynamics with the 1-species PDE 6.34. Circles are for the Tv experimental relative cover of the Petri dish, and curves are for Tv from the PDE model. (a) A single Tv mycelium inoculated at the centre of a dish in the experiment (inset is the PDE model's solution at  $t = 12$  d), extending before reaching the edges of the dish (same as in Fig. 4.4a, 5.7a and 6.1a). (b) Three Tv mycelia closely inoculated at the dish centre (inset is the PDE model's solution at  $t = 12$  d), fusing to form one mycelium which extended and covered the dish (same as in Fig. 4.4c, 5.7c and 6.1b). The PDE model for Tv had initial condition similar to the experimental setting, with growth rate  $\varepsilon_A = 2.16 \text{ d}^{-1}$ , and diffusion coefficient  $\delta_A = 0.017 \text{ cm}^2 \text{ d}^{-1}$ . It was assumed that a mycelium is present when its density  $A > 0.01$ . The relative cover in the PDE solution was estimated by Monte Carlo integration of the mycelium present (the curves are 95% confidence regions of the mean relative cover in the PDE solution from 100 Monte Carlo integrations).

estimated by Monte Carlo integration of mycelial presence in space. Thus, a PDE model of fungal growth and interactions might unavoidably suffer from the arbitrary choice of a threshold density which determines mycelial presence.

### 6.1.6 3-species PDE model

The PDE model for three species will follow from the 3-species ODE 6.31–6.33. Species A and B can replace C with local replacement rates  $\rho_A$  and  $\rho_B$  ( $\text{d}^{-1}$ ). The rest of the parameters for a species X have been introduced in the 1-species PDE model: growth rate of X,  $\varepsilon_X$  ( $\text{d}^{-1}$ ), and diffusion coefficient of X,  $\delta_X$  ( $\text{cm}^2 \text{ d}^{-1}$ ). The resulting model equations are (see the PDE model dynamics compared to empirical community dynamics in Fig. 6.3, with Hf represented by species A, Tv by B, and Vc by C):

$$\frac{\partial A}{\partial t} = \varepsilon_A A (1 - A - B - C) + \rho_A A C + \delta_A \left( \frac{\partial^2 A}{\partial x^2} + \frac{\partial^2 A}{\partial y^2} \right), \quad 6.35$$

$$\frac{\partial B}{\partial t} = \varepsilon_B B (1 - A - B - C) + \rho_B B C + \delta_B \left( \frac{\partial^2 B}{\partial x^2} + \frac{\partial^2 B}{\partial y^2} \right), \quad 6.36$$

$$\frac{\partial C}{\partial t} = \varepsilon_C C (1 - A - B - C) - (\rho_A A + \rho_B B) C + \delta_C \left( \frac{\partial^2 C}{\partial x^2} + \frac{\partial^2 C}{\partial y^2} \right). \quad 6.37$$

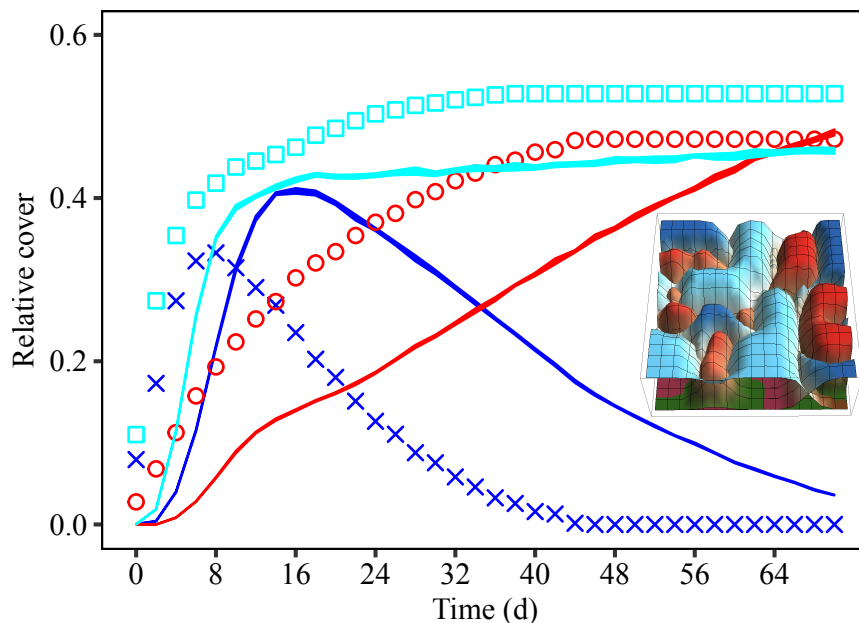


Figure 6.3: Prediction of the 3-species empirical community dynamics with the PDE 6.35–6.37. The data points are for the empirical relative cover of the species in time, and the curves are the PDE model trajectories. The inset shows the PDE numerical solution at time  $t = 40$  d. Colour–point (of each species): red–circle (Hf), cyan–square (Tv), and blue– $\times$  (Vc). The PDE model had initial conditions similar to the experimental setting, with the following parameter values (species A was Hf, B was Tv, and C was Vc):  $\epsilon_A = 0.78 \text{ d}^{-1}$ ,  $\epsilon_B = 2.16 \text{ d}^{-1}$ ,  $\epsilon_C = 1.14 \text{ d}^{-1}$ ,  $\delta_A = 0.0062 \text{ cm}^2 \text{ d}^{-1}$ ,  $\delta_B = 0.017 \text{ cm}^2 \text{ d}^{-1}$ ,  $\delta_C = 0.0091 \text{ cm}^2 \text{ d}^{-1}$ ,  $\rho_A = 0.22 \text{ d}^{-1}$ , and  $\rho_B = 0 \text{ d}^{-1}$ . The boundary replacement rates were assumed constant, as if adjacent mycelia had 1:1 cover ratio (rates taken from Fig. 4.5b,d and related experiments for spatial competition Element 4). Local replacement rates were calculated from boundary replacement rates as for extension in the 1-species PDE. The relative cover in the PDE solution was estimated by Monte Carlo integration of the mycelium present (the curves are 95% confidence regions of the mean relative cover in the PDE solution from 100 Monte Carlo integrations; density threshold for mycelial presence was arbitrarily set to 0.5).

Again, since the simulated  $22.4 \times 22.4$  cm Petri dish has closed boundaries, I assumed for any species X that  $\partial X/\partial x = 0$  and  $\partial X/\partial y = 0$  orthogonally to the boundaries (Neumann boundary conditions).

## 6.2 Summary

In this Chapter, I attempted to develop and evaluate models of ordinary and partial differential equations for fungal interactions based on the lattice model of Chapter 5. I derived master equations from the basic processes of extension and replacement in the lattice model. Since the variance and covariance of species relative abundances tend to zero in the long-term, I took mean-field approximations for the master equations' first moment. Consequently, I obtained 1-, 2- and 3-species deterministic models of ordinary



differential equations for the mean relative abundance of species in well-mixed culture of dispersed mycelia. These non-spatial models failed to capture even the 1-species dynamics in the Petri dish experiments of Chapter 4. Based on the ordinary differential equations models, I moved to reaction–diffusion partial differential equations models for 1- and 3-species. The spatial PDE models were in good agreement with the experiments for 1-species dynamics, but by their nature are unable to incorporate elements of spatial competition, such as the dependence of replacement rates on the cover ratio of the adjacent mycelia. In conclusion, the particular models tested were not able to incorporate basic elements of fungal competition for space, which appeared to be important for the prediction of empirical community dynamics (Chapters 4 and 5).



# Chapter 7

## Discussion

This thesis modelled direct biotic interactions in general, and fungal competition for space in particular, under a generalising and comprehensive perspective. The findings showed that direct biotic interactions in any type of system can be described under a common, standardised framework (Chapter 2), and that omission of framework concepts can lead to underestimation of the number of functional traits involved mechanistically in the interactions (Chapter 3). Additionally, by quantitatively considering six basic elements of fungal competition for space even phenomenologically (Chapter 4), accurate predictions of fungal community dynamics can be achieved with a spatial model (Chapter 5), but differential equation models might be less plausible in their descriptions and predictions (Chapter 6).

### 7.1 Functional traits in interaction networks

#### 7.1.1 Describing direct biotic interactions with functional traits

In Chapter 2, I introduced a novel framework describing how interaction modes and traits of individuals contribute to success or failure in direct biotic interactions, organised in three stages: (1) determination of focal tasks that appear to direct the interactions; (2) hierarchical decomposition of the focal tasks in strategies (modes) of subtasks for success; and (3) explanation of the subtask outcomes by the pairwise comparison of traits. Each stage has a main corresponding consequence: (1) a focal task failure is an outcome of interaction; (2) there can be alternative modes for focal task success; and (3) the inequality rule can handle different types of traits. I thereafter discuss the plausibility of the stages and of their conceptual consequences.

The foundational concept of the framework is the ‘task’. I adopted an intentional language of ‘tasks’ for the sake of communicating the framework more directly. To avoid teleological implications, I stress that interactions ‘appear’ to be directed by tasks (West & Gardner, 2013), recognising that the apparent task-directedness arises from the

programmed operation of biological ‘teleonomic processes’ and ‘purposive behavior’ *sensu* Mayr (1992, 1998). Note that tasks have been implicitly used in the literature, revealed by the names of ecological systems, for example, consumption in ‘food’ webs, pollination in plant–‘pollinator’ networks, and parasitism in host–‘parasite’ systems. Moreover, I have explicitly incorporated failure to obtain tasks as an integral part of this perspective (Fig. 2.1). The ‘successful interaction outcomes’ in this perspective are the ‘interactions’ typically described in the literature (Vázquez *et al.*, 2009a; Poisot *et al.*, 2015; Bartomeus *et al.*, 2016); and the ‘unsuccessful interaction outcomes’ are synonymous to the ‘forbidden links’ or ‘forbidden interactions’ of some authors (Jordano *et al.*, 2003; Morales-Castilla *et al.*, 2015). Under the task perspective, players interact given their mere inclusion in the study system, even if they never actually meet.

A potential issue in the second framework stage (mapping the interactions to a standardised form) is the seemingly arbitrary creation of the task hierarchy. The task hierarchy concept comes from the concept of the ‘hierarchical nature of performance’ (Wainwright, 2007). Higher performance breaks down to lower level performance subtraits, breaking down further to morphological, physiological, behavioural, and phenological performance subtraits. For example, a phage’s higher performance in exploiting a bacterium depends on its ability to attach on a bacterium, which depends on the phage’s possession of tail proteins able to bind to specific bacterial receptors (Dy *et al.*, 2014). In each level, performance corresponds to a function, or task in the framework’s terms (e.g. ‘performance in exploiting a bacterium’). Consequently, there must be a correspondence between the traits and subtraits of a performance trait hierarchy, and the tasks and subtasks of a task hierarchy. Studied traits are chosen based on the question, the biological level of interest, and the methods and resources at hand (Wagner, 2001). The corresponding tasks and subtasks can be chosen similarly, for the creation of the underlying task hierarchy.

With the conversion of the task hierarchy to the interaction form, I was able to incorporate explicitly the feature of alternative interaction modes observed empirically (Fig. 1.1b). In previous theoretical trait-based works, an exploiter has to overcome all the barriers or defences of a potential resource to consume or parasitise (Santamaría & Rodríguez-Gironés, 2007; Gilman *et al.*, 2012; Débarre *et al.*, 2014; Speed *et al.*, 2015). Other theoretical works adopt one of the four principal versions of the ‘ecological niche’ concept (Schoener, 1989), i.e. its ‘resource-utilisation’ approach (MacArthur & Levins, 1967). In the niche approach, the niche dimensions act in conjunction to determine the characteristics of the exploited resources (Stouffer *et al.*, 2006; Allesina *et al.*, 2008; Eklöf *et al.*, 2013). The ‘mode’ in my framework is equivalent to these two approaches, since a pursuer’s performance must be sufficiently high in all the subtasks of a mode. The framework naturally generalises to alternative interaction modes, by logically associating interaction modes via disjunction. The equivalence of this framework’s interaction mode

with the approach of previous theoretical works, and the framework generalisation to alternative interaction modes, enable comparisons between approaches, as demonstrated in Chapter 3.

For the third framework stage (of explaining the subtask outcomes), I adopted a phenotype space instead of a niche space approach. One problem with the niche approach is the loss of mechanistic information when dimensions originate phenomenologically, or abstractly from multiple trait-axes ordination (Eklöf *et al.*, 2013). For example, body size is a trait with high explanatory power in food webs (Stouffer *et al.*, 2011). However, more traits allometrically scaling with body size are mechanistically involved in trophic interactions (Woodward *et al.*, 2005). Even mechanistically, realised niches commonly span a range of the resource gradient (MacArthur & Levins, 1967; Levins, 1968), hiding two traits per niche dimension (one for each extreme of the niche range). For example, with the maximum of the prey size range limited by the predator's mouth gape, the niche range minimum must be limited by a second predator trait, like the predator's inability to capture or handle smaller prey. Another problem is that exploiters might have no place in the niche space because it is created by trait dimensions of the resources (MacArthur & Levins, 1967; Schoener, 1989), and resource traits can be irrelevant for exploiters (e.g. plant traits for herbivores). The present framework takes into account the traits of both interacting players simultaneously, and a dimension is simply a challenged trait-axis in the phenotype space of pursuers or attracters.

The inequality rule at the third framework stage is applicable to various types of traits. Continuous-valued quantitative traits can be modelled directly (e.g. the animal reaching nectar in Fig. 2.3). Comparison of traits with ordered levels (binary, semiquantitative, and quantitative but discontinuous, Legendre & Legendre, 1998) can be modelled with appropriate scaling (e.g. degree of egg similarity versus degree of discrimination ability for the bird brood parasitism example in Fig. 2.3). Categorical qualitative traits can be redefined to binary traits (e.g. the prey qualitative trait with categories 'diurnal' or 'nocturnal' was redefined to a binary trait for presence-absence of activity during the day in Fig. 2.3). Moreover, the inequality rule can model both cases of competing traits (Abrams, 2000; Santamaría & Rodríguez-Gironés, 2007; Nuismer *et al.*, 2013): difference traits (also called barrier traits, or unidirectional axes of vulnerability), and matching traits (complementarity traits, or bidirectional axes of vulnerability). The natural case in the framework is the difference traits, since larger power-toughness difference contributes to success. However, if we state the subtasks appropriately, matching traits can be reformulated as difference traits. In the brood parasitism example of Fig. 2.3, I could have compared the eggs of parasite and host as matching traits, because parasite eggs more similar to the host eggs contribute to parasitism success. Instead, I compared as difference traits the similarity of parasite eggs to the ability of the host to recognise them. Another example is the difference traits formulation for the

temporal match of predator and prey during the day (Fig. 2.3).

Hence, the three framework stages and their main conceptual consequences exhibit generality and plausibility: from the focal tasks and the trait-mediated failures, to the task hierarchy and the alternative interaction modes, to the pursuer–attractor phenotype spaces and the modelling of different types of competing traits.

### 7.1.2 Finding the minimum mechanistic dimensionality of networks

In Chapter 3, I introduced a method for calculating the minimum number of traits required for the mechanistic explanation of all interaction outcomes of a network. The method was based on a novel mechanistic framework applicable to different interaction types, modes, tasks, and types of traits (Chapter 2). By applying the method to 658 empirical systems, I showed that the minimum number of traits involved in the interactions can be underestimated when ignoring any of the three framework features combined for the first time: (1) the alternative interaction modes; (2) the trait-mediated failure outcomes; and (3) the mechanistic perspective on interactions.

With the generalised mechanistic framework, minimum mechanistic dimensionality can explicitly incorporate the alternative interaction modes observed empirically. For example, alternative feeding modes such as filter-feeding and predation can be modelled to incorporate their different tasks and traits involved (Kjørboe, 2011). Similarly, different tasks and traits can be modelled in the alternative floral signals which plants use to attract animal pollinators (Schiestl & Johnson, 2013), in the different ways via which phages infect bacteria (Meyer *et al.*, 2012), and in the variety of mechanisms involved in fungal competition for space (Boddy, 2000). The incorporation of alternative interaction modes in the minimum mechanistic dimensionality method showed that different assumptions about the interaction form can lead to alternative minimal explanations of the outcomes, as in rock–paper–scissors systems (Fig. 3.1). At least in the case of rock–paper–scissors and similar intransitive networks, these alternative explanations can enhance our understanding of the emergence and maintenance of intransitive community structures (Szolnoki *et al.*, 2014; Levine *et al.*, 2017). Additionally, with the incorporation of alternative interaction modes in the minimum mechanistic dimensionality method, it was shown that the number of traits theoretically estimated to be involved in the interactions of a system can be frequently larger under the assumption of alternative interaction modes than in a single mode (Fig. 3.3a). Thus, concluding that real community structure can be explained by a few traits must be made with caution, especially if the methods of estimation assume a single interaction mode, which is commonly not the case in many real communities tested (Eklöf *et al.*, 2013; Dalla Riva & Stouffer, 2016).

According to the mechanistic framework of Chapter 2, I adopted a phenotype space instead of a niche space approach. Equivalently to the case of multiple versus single

modes, I found that the minimum mechanistic dimensionality assuming a single interaction mode was frequently higher than the comparable phenomenological dimensionality in the niche-based approach of Eklöf *et al.* (2013) (Fig. 3.3c). Similarly and in this case, an underestimation of the minimum dimensionality of ecological networks is expected to be common, this time under a phenomenological approach, compared to a mechanistic one.

I have explicitly incorporated failure to obtain tasks as an integral part of the mechanistic framework and method. Previous theoretical works do consider failures as trait-mediated outcomes of interaction (for example, Eklöf *et al.*, 2013; Poisot *et al.*, 2015; Bartomeus *et al.*, 2016; Dalla Riva & Stouffer, 2016). One remaining case of omitting failure outcomes is in behavioural studies which commonly employ a few predictor traits for the explanation of only the observed successful interaction outcomes, e.g. of the dominance events in a social group (Chase & Seitz, 2011). In contrast, I found that three to six pairs of competing traits must be involved in several dominance systems (Fig. 3.2a). The method here regarded failures as trait-mediated outcomes of interaction, hence requiring more traits to be involved in the interactions (Fig. 3.3b). For example, in the elephant family named ‘AA’ in Archie *et al.* (2006), almost all observed dominance events are towards younger elephants, and the authors conclude the system is an age-ordered dominance hierarchy based only on the successes, agreeing with my result of one required trait pair when failures are excluded (Fig. 3.3b). The minimum mechanistic dimensionality, explicitly incorporating failures, suggests three trait pairs for this system under both minimal explanations, because there are several older–younger pairs where no dominance or aggression was observed, i.e. failures unexplained by Archie *et al.* (2006). In other words, the framework predicts mechanisms preventing the occurrence of dominance between these older–younger pairs. Most elephants dominated only younger members of their matriline, and of two specific matrilines (Archie *et al.*, 2006). These two preferences are candidates for the two extra trait pairs that I expect under the framework, which are lost when ignoring failure outcomes.

In conclusion, the method I have outlined here provides a more accurate measure of the minimum dimensionality of networks, and it is relatively straightforward to adopt and calculate. By estimating more accurately the minimum number of traits involved in the interactions of a system, we reduce the risk of missing important traits that are involved mechanistically, in alternative interaction modes, or only in failure outcomes. By parameterising network models with more accurate numbers of traits involved, we can better reproduce community structure at the interaction outcome level (Petchey *et al.*, 2008; Vázquez *et al.*, 2009a; Olito & Fox, 2015). Additionally, an accurate estimation of the minimum dimensionality of a system can concentrate our studies on traits which are necessary and contribute more to community structure (Eklöf *et al.*, 2013). Hence, this method could contribute to a better understanding, explanation, and prediction of

community structure and structure-dependent processes, such as population dynamics (Berlow *et al.*, 2009; Valdovinos *et al.*, 2010), evolution (Becerra, 2003; Sanders *et al.*, 2014), ecosystem functioning (Woodward *et al.*, 2008; Rudolf & Rasmussen, 2013), and management (Ribeiro Mello *et al.*, 2015; Pires *et al.*, 2017).

## 7.2 Fungal community dynamics of spatial competition

### 7.2.1 Quantifying six basic elements of spatial competition

Chapter 4 investigated six basic elements of spatial competition between mycelia in three wood decay fungi which—in accordance to ecological theory and empirical findings in fungi—contribute to interaction outcomes and community dynamics. Three elements had simple form: constant extension rates; no inhibition or stimulation of extension; and no higher-order interactions between the three species. For the other three elements, I found the following forms: faster replacement of immature mycelial regions; slower replacement of larger mycelia; and replacement rates as if mycelia distribute their competitive ability proportionally to the length of boundary with each adjacent competitor.

Experiments for Element 1 showed constant extension rates of mycelial boundaries for the three species (Fig. 4.4a–d). This result is in agreement with previous works reporting constant mycelial boundary extent to unoccupied space (Brown, 1923; Fawcett, 1925; Ryan *et al.*, 1943; Plomley, 1959). The specific strains used were ordered, from fastest to slowest extending as *Trametes versicolor* (Tv), *Vuilemenia comedens* (Vc), and lastly *Hypholoma fasciculare* (Hf). Although the mycelia of some fungi can replace other mycelia, larger preemption of space from faster extending mycelia is a significant element of spatial competition, especially between mycelia which deadlock. For example in this study, the faster boundary extension rate of Tv contributed to larger territory captured by Tv, before encounter and deadlock with Hf (Fig. 5.9). Space preemption is hence an important element, which has not been investigated in fungal community dynamics, but it is acknowledged and well studied for other taxa, e.g. for plants (Craine, 2005).

Previous works have found that the ability to capture unoccupied space might be inhibited or enhanced by the presence of adjacent or distant conspecific or heterospecific mycelia (Griffith & Boddy, 1991; Heilmann-Clausen & Boddy, 2005; Evans *et al.*, 2008; Sonnenbichler *et al.*, 2009). The three strains for this work's Element 2 did not show any long- or short-range inhibitory or stimulatory effects on extension rates under the conditions tested (Fig. 4.4d). This result is not unexpected though, since inhibition and stimulation of extension is relatively infrequent in wood decay fungi (Evans *et al.*, 2008). For example, the Tv and Hf strains in Evans *et al.* (2008) exhibited altered extension



rates in less than half of the cases with other mycelia present.

For replacement in relation to age of mycelial regions (Element 3), I found that both Hf and Tv showed the same pattern of decreasing replacement rate until 4–8 days old Vc mycelium region (Fig. 4.5a, c). This is an indication of replacement rates depending on the age of the replaced mycelium as I initially hypothesised, and not of the replacing mycelium which has the same age across its invading boundary (Fig. 4.2). The results for Element 3 are thus in agreement with previous works about mycelia becoming locally denser with time (Plomley, 1959; Trinci, 1969), attaining their full density and competitive potential as they mature (Stahl & Christensen, 1992).

This work presented for the first time quantitative relations of replacement rate with the relative difference in mycelial cover for Element 4. Until now, the only quantitative study on the relation between replacement and space held by mycelia had been that of Holmer & Stenlid (1993), but replacement rates are not measurable with their setting. I found lin–log relations for both Hf and Tv against Vc (Fig. 4.5b,d), i.e. increase in replacement rate was slower for relatively larger Hf or Tv mycelia. For example, the same increase in replacement rate was achieved by increasing the mycelial cover from 1 to 2 cm<sup>2</sup>, and from 32 to 64 cm<sup>2</sup>. This lin–log relation indicates the existence of constraints in the enhancement of mycelial competitive ability. It would be interesting to test if a lin–log relation is found in natural substrata, and investigate the mechanisms of its emergence. Nevertheless, the relation can be used to compare the overall competitive ability between species, in absence of physiological and other mechanistic measurements. For example from Fig. 4.5b,d, Hf appeared to be an intrinsically stronger competitor than Tv in the experiments (larger intercept in the lin–log relation), but Tv appeared more efficient in taking advantage of its larger size than Hf (steeper slope).

To my knowledge, this study is the first to address experimentally the way fungal mycelia face multiple adjacent competitors (Element 5), a situation expected to be common in natural communities. It has been considered systematically in animal territoriality (Adams, 1998), but not in empirical studies of fungi (Boddy, 2000; Kennedy, 2010; Hiscox & Boddy, 2017), or in fungal community models (Halley *et al.*, 1994, 1996; Davidson *et al.*, 1996a,b; Bown *et al.*, 1999; Falconer *et al.*, 2008; Boswell, 2012). Chapter 4 demonstrated that flanking competitors at larger boundaries realise a proportionally larger, and hence competitively stronger central mycelium (Fig. 4.6a). This suggests that mycelia distribute their translocated resources uniformly across the whole boundary with heterospecifics, an interesting hypothesis for testing in natural communities and substrata.

For Element 6, this work did not find any changes in replacement rates when all three species interact (Fig. 4.6b). Studies on the non-additive effects of competition between fungi have recently appeared in the literature (Hiscox *et al.*, 2017), but their conclusions must be taken with caution. This is because other elements of spatial competition can be

involved, leading to underestimation or overestimation of the additivity in multi-species interactions. For example, Hiscox *et al.* (2017) report that the addition of a third species destabilises the outcomes from pairwise interactions in their experimental setting of three wood blocks adjacent in a row. However, they do not disentangle the effect of mycelial size (Element 4 here), and the heterospecific boundary size (Element 5) from the effect of higher-order interactions. The comprehensive approach followed in the present work, enabled to quantify the effect of higher-order interactions after quantifying the relation of replacement rates with the size of adjacent mycelia for Element 4, and the effect of heterospecific boundary length on the replacement rates for Element 5.

A trade-off of the present work is that a larger sample size for each hypothesis was exchanged with a larger number of hypotheses, towards a more comprehensive approach to the spatial competition elements. Given the small standard error in the extension and replacement rates, our confidence could be increased regarding the results of the present study, which highlighted six elements of fungal competition as crucial for the prediction of community dynamics (to be tested with the theoretical models in Chapters 5 and 6). Some elements have been addressed for the first time quantitatively with the experiments, and encourage further investigations on natural communities or substrata.

### 7.2.2 Modelling and predicting fungal community dynamics

Chapter 5 showed that all six experimentally quantified elements were necessary for the prediction of community dynamics in artificial medium with a lattice model. Simplification of any of the latter three elements lead to inaccuracies in the prediction of community dynamics.

Each of the three elements of replacement with mycelial age, cover, and contact with multiple heterospecific mycelia appeared to influence the dynamics of the 3-species community significantly. I ran the lattice model with the full settings and same initial conditions from the empirical 3-species community, but simplified each one of these three elements. First, when replacement rates were not faster for younger mycelial regions, Tv in the model captured less space than in the empirical dish, because Tv was more slowly replacing the younger peripheral regions of Vc mycelia when making contact, enabling Hf to capture more space than in real (Fig. 5.8b). Second, when I assumed constant replacement rates as obtained from 1/1 mycelium cover ratios, Tv could not replace Vc, and thus Hf was capturing again more space than in real (Fig. 5.8c). Third, when I assumed that mycelia face in full competitive ability all adjacent heterospecifics, Tv which occupied the middle of the dish (i.e. had long boundary, with multiple heterospecific mycelia), could capture more space than in real, because it was stronger against the Vc mycelia, hence Hf was left with less space to capture (Fig. 5.8d).

The lattice model of the present study is characterised by simplicity, yet it is able to

reproduce all types of outcomes observed between interacting mycelia, and to predict empirical community dynamics. It can reproduce the replacement, deadlock, partial replacement, and even mutual replacement observed in fungi (Boddy, 2000). Previous models of fungal interactions report some types of outcomes, for example, replacement and deadlock in the cellular automata models of Halley *et al.* (1994) and Bown *et al.* (1999), deadlock in the PDE model of Davidson *et al.* (1996a), and replacement and deadlock in the PDE models of Falconer *et al.* (2008) and Boswell (2012). The same type of outcome is reproduced with different approaches in these models: phenomenologically in the cellular automata models of Halley *et al.* (1994) and Bown *et al.* (1999), and in the present lattice model; and mechanistically in the more detailed PDE models (Davidson *et al.*, 1996a; Falconer *et al.*, 2008; Boswell, 2012).

Moreover, the present lattice model was the first to predict the dynamics of a 3-species fungal community. The only previous model predicting fungal community dynamics is the cellular automaton model of Bown *et al.* (1999), for a 2-species community. Although with their interesting experimental setting of agar tiles separated by a 2 mm gap they cancel some of the spatial competition elements, their local neighbourhood model omits two important elements which have been highlighted in the literature: the size of adjacent mycelia and its effect on replacement rates (Holmer & Stenlid, 1993), and the way mycelia distribute their competitive ability among multiple adjacent heterospecifics (Hiscox *et al.*, 2017). Note though that one of their model parameters can be estimated such that it acts as surrogate for mycelial cover. Thus, even if this parameter incorporates the effect of mycelial cover phenomenologically, the Bown *et al.* (1999) model does not compute heterospecific boundary length for the effect of multiple opponents, an element which was shown to be important for the prediction of community dynamics with the present model (Chapter 5).

The use of a theoretical model was necessary for the study of community dynamics. With a theoretical, simulation model on-lattice I could compute rapidly all the experimentally obtained transitions and their rates of occurrence in large enough spatial and temporal scales, and in the complex community structures resembling natural communities (e.g. see insets of Fig. 5.8a, and Coates & Rayner, 1985; Chapela *et al.*, 1988). Additionally, building a theoretical model was an exercise of testing and keeping only the basic elements involved in the dynamics. I did not model any physiological or other mechanisms, because I did not measure any in the laboratory, although I included variables which are connected mechanistically to extension and replacement rates according to the empirical literature, e.g. the size of space occupied by a mycelium (Holmer & Stenlid, 1993). Additionally, I adopted a coarse-grained, lattice representation, omitting the finer details of mycelial hyphae at the  $\mu\text{m}$  spatial scale, because it was observationally, mathematically and computationally easier, yet adequate for the prediction of single- and multi-species dynamics at the mm–cm scale. Lastly, I implemented the model in

two spatial dimensions because I recorded relations of extension and replacement rates with mycelium cover ( $\text{cm}^2$ ) and boundary length (cm).

Regarding the models of differential equations (Chapter 6), their predictive ability appeared poor. It is apparent from the form of the ODE 6.17 that the resulting well-mixed dynamics are different from the spatial dynamics even of a single mycelium extending on an experimental Petri dish (Fig. 6.1a). The spatial dynamics of relative cover in the example of the experimental *Tv* extension is of quadratic form, since we essentially have a disk-like mycelium extending its radius linearly in time. On contrary, the dynamics in the well-mixed culture of the ODE model are initially exponential, as long as the relative abundance  $A(t)$  is relatively small. The same difference in dynamics is apparent and in another example of three *Tv* mycelia which fuse and cover the whole experimental dish (Fig. 6.1b). Nevertheless, I developed a 2- and 3-species ODE model, which helped in the development of the corresponding PDE model.

Regarding the initial conditions for the 1-species PDE model, all simulated inocula had exponentially decaying density. Since in the 3-species PDE model we had additionally the replacement rate parameters, I first estimated the extension parameters as in the 1-species PDE model. I assumed that the propagating front of a species  $X$  replacing another attains a constant speed  $c = 2\sqrt{\rho_X \delta_X}$  (Volpert & Petrovskii, 2009). The diffusion coefficient  $\delta_X$  was estimated with the extension rates, and I could estimate the replacement rate because the rate of boundary replacement was known from the experiments. In this way though, the ratio  $\rho_X/\delta_X < 125 \text{ cm}^{-2}$ , which leads to less steep fronts during replacement. The less steep replacement fronts result in difficulties to estimate the relative cover of species, since the arbitrary threshold for mycelial presence must be increased.

The PDE approach revealed some additional issues. I had to set arbitrarily the threshold above which a model mycelium is considered locally present to estimate the model relative cover as in the experiments. Additionally, setting exactly the same initial conditions as in the experiment is impossible because the exponentially decaying densities of model mycelia cannot be tweaked easily to match the initial experimental relative cover of the species in each inoculum. Moreover, due to the reaction-diffusion nature of the PDE, it is challenging to measure in experiments the two PDE processes of reaction (mycelial local growth and replacement) and diffusion (extension due to growth and replacement). Last but not least, there is no way to identify model mycelia of a species with one PDE, and hence it is impossible to estimate mycelial cover and boundary length, to have replacement rates dependent on the relative cover ratio of adjacent mycelia, and on the length of boundary with heterospecifics, which were both crucial for the prediction of empirical community dynamics with the lattice model which incorporated them (Chapter 5). An alternative approach would be to model each mycelium of each species with a separate PDE, but this would lead to very heavy

models. Given these limitations, and that the lattice model had to incorporate all six experimentally quantified elements of spatial competition to reproduce empirical dynamics, it was expected that the PDE model will be unable to predict the 3-species empirical community dynamics (Fig. 6.3).

Taking together the results from both the lattice model and the differential equations (Chapters 5 and 6), it appears that a spatial model able to incorporate all six experimentally quantified elements would be a preferred starting point for accurate prediction of fungal community dynamics. Despite their lack of stochasticity and their liability to mathematical analysis, differential equation models display some inherent properties which do not allow them to model and parameterise fungal interactions in space in a plausible way. A workaround would be to add more details and levels in an ODE or PDE model, and perhaps this is the reason that previous differential equation models for fungi are more detailed (Davidson *et al.*, 1996a; Falconer *et al.*, 2008), or with reduced number of spatial dimensions to 1-D (Boswell, 2012). As a consequence of the details implemented though, such models become computationally heavy to solve for larger spatial and temporal scales which are characteristic in the level of communities. The advantages of a computational model such as the present lattice model are the easier development through programming (especially for fungal ecologists lacking mathematical background to develop differential equation models), the easier model parameterisation given the lattice model's limited number of necessary rate parameters, the easiness for further development (e.g. by adding spatial competition elements, or a third spatial dimension), and the faster simulation of community dynamics at large spatial and temporal scales (since PDE models have to become very detailed to capture empirical community dynamics at these scales).

### 7.3 Limitations and future directions

It is important to acknowledge the limitations of the mechanistic and phenomenological approaches in the two main contributions of this thesis, and to identify future directions of addressing these limitations, or expanding on identified merits of the approaches.

As one example of general limitation in the mechanistic approach, the framework offers a detailed description of how direct biotic interactions occur, but this leads to cumbersome mathematical and computational constructs. The minimum mechanistic dimensionality method, which was based on the mechanistic framework, can create large systems of linear inequalities, making the feasibility search a computationally demanding task. As one example of general limitation in the phenomenological approach on quantifying experimentally basic elements of spatial competition for the lattice model, we have to experimentally quantify again all the relations for extension and replacement in different abiotic and biotic environmental conditions. Acknowledging such limitations

can help us benefit from the contributions of this thesis according to their intended scope of development and use.

In general, given the scope and despite the limitations, different future directions for the contributions of this thesis can be identified. The mechanistic framework of Chapter 2 can provide the common mechanistic basis for describing and comparing empirical systems in a standardised way, and for trait-based modelling of ecological, evolutionary and coevolutionary processes in different systems. It would be interesting to extend and apply the minimum mechanistic dimensionality method of Chapter 3 to weighted or multilayer ecological networks, and to compare and explain the calculated theoretical minimum dimensionalities to the empirical dimensionalities of the same systems. The synthesised view of the different spatial competition elements of Chapter 4 would be interesting to be tested in natural substrata and communities, not only for fungi, but for other taxa involved in direct competition for space. Such findings could lead to the development of general models of spatial competition, based on the lattice model of Chapter 5.

In particular, by incorporating all four features of the empirical description of interactions explicitly (Fig. 1.1), the mechanistic framework of Chapter 2 can support more comprehensive and mechanistic trait-based approaches to proximate and evolutionary questions. For proximate questions, it encourages the systematic description of empirical systems as networks, in a standardised and hence comparable form. Theoretical investigations could benefit from the novel conceptual consequences, e.g. including alternative interaction modes in trait-based models of animal social network dynamics (Pinter-Wollman *et al.*, 2014). For evolutionary questions, it can inspire new hypotheses, e.g. about the reasons for redundancy in interaction modes, tasks, or performance in empirical systems, compared to minimal systems constructed theoretically (Chapter 3). Apart from its simplicity, the established phenotype space approach (Dietrich & Skipper Jr., 2012; Pigliucci, 2013), adopted by the mechanistic framework, can be proved useful, for instance, in studying trade-offs in traits used in different subtasks, interaction modes, or focal tasks (Arnold, 1983; Ghalambor *et al.*, 2003; Fontaine *et al.*, 2011; Shoval *et al.*, 2012; Pilosof *et al.*, 2017). In general, the mechanistic framework can be used to dictate how players interact mechanistically, for example: in game theoretical models with interaction payoffs (Archetti *et al.*, 2011); in coevolutionary models with phylogenetic history (Manceau *et al.*, 2017); and in spatial models with interacting dispersers or foragers, for the effect of neutrality on community assembly or invasion (Morales & Vázquez, 2008).

The proposed method of Chapter 3 for calculating the minimum dimensionality is mechanistic, based on biologically plausible features of interactions; yet, it is simple with its phenotype space representation, and easy to adjust and extend. In this first account, I assumed two simple and extreme minimal interaction forms (minimal explanations I

and II), but the user can input any minimum number of traits and trait values, in any interaction form. Additionally, I presented a deterministic version, but future versions could be probabilistic (Dalla Riva & Stouffer, 2016; Poisot *et al.*, 2016), e.g. with more probable outcomes explained by larger power–toughness differences. The traits in the current method were continuous, but they could be integer, or binary. Assuming adequate sampling effort, the mechanistic description has not considered the effects of phylogenetic relationship (Rohr & Bascompte, 2014; Eklöf & Stouffer, 2016), and abundance (Vázquez & Aizen, 2003), which could be incorporated in future extensions.

The experimental findings of Chapter 4 open new questions. Do mycelia in natural substrata and communities distribute their competitive ability uniformly across the boundary with adjacent heterospecifics as was found for the specific wood decay fungal strains on artificial substrate? This new hypothesis could be tested similarly to the settings of Hiscox *et al.* (2017), stimulating further enquiries about the selective advantage of mycelia allocating their resources against competitors in a simple, ‘uninformative’ way despite the complex, multi-enemy structure of natural communities (Coates & Rayner, 1985; Chapela *et al.*, 1988). Another example of opening question concerns the form of relation between replacement rate and cover or volume ratio between paired heterospecific mycelia in natural substrata or communities. Does mycelial replacement increase with mycelial size in a lin–log fashion in natural settings as well? And which are the proximate and evolutionary reasons behind the displayed relation?

The lattice model of Chapter 5 was implemented in two spatial dimensions because I recorded relations of extension and replacement rates with mycelium cover ( $\text{cm}^2$ ) and boundary length (cm). In future, the model can be extended to three dimensions by introducing the extra neighbours in a 3-D lattice, for testing the predictability of fungal community dynamics ultimately in natural substrata, e.g. in wood. Moreover, other elements of spatial competition can be added to the lattice model, simulating realistic conditions of natural variability in temperature, substratum quality, and other abiotic and biotic elements.

The multiple research pathways which appear as future directions offer an encouraging sign about the plausibility of the contributions of this thesis for proximate and evolutionary questions on direct biotic interactions in different ecological systems. I hope further development and testing of the contributions of this thesis will open new research paths, and give fresh insight into previous work dealing with ecological systems under mechanistic and phenomenological trait-based approaches.





# References

- Abrams, P. A. (1987). On classifying interactions between populations. *Oecologia*, 73, 272–281. 1, 11
- Abrams, P. A. (2000). The evolution of predator–prey interactions: theory and evidence. *Annual Review of Ecology and Systematics*, 31, 79–105. 4, 77
- Adams, E. S. (1998). Territory size and shape in fire ants: a model based on neighborhood interactions. *Ecology*, 79, 1125–1134. 81
- Allesina, S., Alonso, D. & Pascual, M. (2008). A general model for food web structure. *Science*, 320, 658–661. 4, 6, 76
- Archetti, M., Scheuring, I., Hoffman, M., Frederickson, M. E., Pierce, N. E. & Yu, D. W. (2011). Economic game theory for mutualism and cooperation. *Ecology Letters*, 14, 1300–1312. 86
- Archie, E. A., Morrison, T. A., Foley, C. A. H., Moss, C. J. & Alberts, S. C. (2006). Dominance rank relationships among wild female African elephants, *Loxodonta africana*. *Animal Behaviour*, 71, 117–127. 79, 79, 79
- Arnold, S. J. (1983). Morphology, performance and fitness. *American Zoologist*, 23, 347–361. 2, 4, 86
- Bartomeus, I., Gravel, D., Tylianakis, J. M., Aizen, M. A., Dickie, I. A. & Bernard-Verdier, M. (2016). A common framework for identifying linkage rules across different types of interactions. *Functional Ecology*, 30, 1894–1903. 2, 4, 5, 76, 79
- Bastazini, V. A. G., Ferreira, P. M. A., Azambuja, B. O., Casas, G., Debastiani, V. J., Guimarães Jr., P. R. & Pillar, V. D. (2017). Untangling the tangled bank: a novel method for partitioning the effects of phylogenies and traits on ecological networks. *Evolutionary Biology*, 44, 312–324. 4
- Becerra, J. X. (2003). Synchronous coadaptation in an ancient case of herbivory. *Proceedings of the National Academy of Sciences*, 100, 12804–12807. 1, 2, 5, 80

- Berlow, E. L., Dunne, J. A., Martinez, N. D., Stark, P. B., Williams, R. J. & Brose, U. (2009). Simple prediction of interaction strengths in complex food webs. *Proceedings of the National Academy of Sciences of the United States of America*, 106, 187–191. 5, 80
- Boddy, L. (2000). Interspecific combative interactions between wood-decaying basidiomycetes. *FEMS Microbiology Ecology*, 31, 185–194. 4, 7, 7, 78, 81, 83
- Bortz, A. B., Kalos, M. H. & Lebowitz, J. L. (1975). A new algorithm for Monte Carlo simulation of Ising spin systems. *Journal of Computational Physics*, 17, 10–18. 50
- Boswell, G. P. (2012). Modelling combat strategies in fungal mycelia. *Journal of Theoretical Biology*, 304, 226–234. 2, 8, 9, 81, 83, 83, 85
- Bown, J. L., Sturrock, C. J., Samson, W. B., Staines, H. J., Palfreyman, J. W., White, N. A., Ritz, K. & Crawford, J. W. (1999). Evidence for emergent behaviour in the community-scale dynamics of a fungal microcosm. *Proceedings of the Royal Society of London B: Biological Sciences*, 266, 1947–1952. 2, 7, 8, 8, 9, 81, 83, 83, 83, 83
- Brown, W. (1923). Experiments on the growth of fungi on culture media. *Annals of Botany*, 37, 105–129. 7, 80
- Buchkowski, R. W., Bradford, M. A., Grandy, A. S., Schmitz, O. J. & Wieder, W. R. (2017). Applying population and community ecology theory to advance understanding of belowground biogeochemistry. *Ecology Letters*, 20, 231–245. 8
- Burkholder, P. R. (1952). Cooperation and conflict among primitive organisms. *American Scientist*, 40, 600–631. 1
- Campbell, C., Yang, S., Albert, R. & Shea, K. (2011). A network model for plant–pollinator community assembly. *Proceedings of the National Academy of Sciences*, 108, 197–202. 4
- Cattin, M.-F., Bersier, L.-F., Banašek-Richter, C., Baltensperger, R. & Gabriel, J.-P. (2004). Phylogenetic constraints and adaptation explain food-web structure. *Nature*, 427, 835–839. 4
- Chapela, I. H., Boddy, L. & Rayner, A. D. M. (1988). Structure and development of fungal communities in beech logs four and a half years after felling. *FEMS Microbiology Letters*, 53, 59–70. 83, 87
- Chase, I. D. & Seitz, K. (2011). Self-structuring properties of dominance hierarchies: a new perspective. *Advances in Genetics*, 75, 51–81. 79

- Coates, D. & Rayner, A. D. M. (1985). Fungal population and community development in cut beech logs. III. Spatial dynamics, interactions and strategies. *New Phytologist*, 101, 183–198. 83, 87
- Cohen, J. E. (1977). Food webs and the dimensionality of trophic niche space. *Proceedings of the National Academy of Sciences*, 74, 4533–4536. 6
- Cohen, J. E. & Newman, C. M. (1985). A stochastic theory of community food webs I. Models and aggregated data. *Proceedings of the Royal Society B: Biological Sciences*, 224, 421–448. 4
- Cohn, P. M. (2003). Lattices and categories. In: *Basic algebra: groups, rings and fields*. Springer-Verlag, London, UK, pp. 51–78. 15
- Craine, J. M. (2005). Reconciling plant strategy theories of Grime and Tilman. *Journal of Ecology*, 93, 1041–1052. 80
- Dalla Riva, G. V. & Stouffer, D. B. (2016). Exploring the evolutionary signature of food webs' backbones using functional traits. *Oikos*, 125, 446–456. 4, 6, 6, 78, 79, 87
- Davidson, F. A., Sleeman, B. D., Rayner, A. D. M., Crawford, J. W. & Ritz, K. (1996a). Context-dependent macroscopic patterns in growing and interacting mycelial networks. *Proceedings of the Royal Society B: Biological Sciences*, 263, 873–880. 2, 8, 8, 81, 83, 83, 85
- Davidson, F. A., Sleeman, B. D., Rayner, A. D. M., Crawford, J. W. & Ritz, K. (1996b). Large-scale behavior of fungal mycelia. *Mathematical and Computer Modelling*, 24, 81–87. 8, 81
- Davies, N. B., Krebs, J. R. & West, S. A. (2012). *An introduction to behavioural ecology*. 4th edn. Wiley-Blackwell, Oxford, UK. 1, 3
- Débarre, F., Nuismer, S. L. & Doebeli, M. (2014). Multidimensional (co)evolutionary stability. *The American Naturalist*, 184, 158–171. 76
- Dehling, D. M., Jordano, P., Schaefer, H. M., Böhning-Gaese, K. & Schleuning, M. (2016). Morphology predicts species' functional roles and their degree of specialization in plant–frugivore interactions. *Proceedings of the Royal Society B: Biological Sciences*, 283, 20152444. 1
- Dewsbury, D. A. (1999). The proximate and the ultimate: past, present, and future. *Behavioural Processes*, 46, 189–199. 1

- Dietrich, M. R. & Skipper Jr., R. A. (2012). A shifting terrain: a brief history of the adaptive landscape. In: *The adaptive landscape in evolutionary biology* (eds. Svensson, E. I. & Calsbeek, R.). Oxford University Press, Oxford, UK, pp. 3–15. 86
- Dy, R. L., Richter, C., Salmond, G. P. C. & Fineran, P. C. (2014). Remarkable mechanisms in microbes to resist phage infections. *Annual Review of Virology*, 1, 307–331. 1, 2, 4, 14, 76
- Eklöf, A., Jacob, U., Kopp, J., Bosch, J., Castro-Urgal, R., Chacoff, N. P., Dalsgaard, B., de Sassi, C., Galetti, M., Guimarães, P. R., Lomáscolo, S. B., Martín González, A. M., Pizo, M. A., Rader, R., Rodrigo, A., Tylianakis, J. M., Vázquez, D. P. & Allesina, S. (2013). The dimensionality of ecological networks. *Ecology Letters*, 16, 577–583. 1, 4, 6, 6, 6, 7, 29, 29, 29, 29, 32, 33, 33, 76, 77, 78, 79, 79, 79
- Eklöf, A. & Stouffer, D. B. (2016). The phylogenetic component of food web structure and intervality. *Theoretical Ecology*, 9, 107–115. 87
- Elton, C. (1927). *Animal Ecology*. Macmillan, London, UK. 1
- Endler, J. A. (1991). Interactions between predators and prey. In: *Behavioural ecology: an evolutionary approach* (eds. Krebs, J. R. & Davies, N. B.), 3rd edn. Blackwell Scientific Publications, Oxford, UK, pp. 169–196. 4
- Evans, J. A., Eyre, C. A., Rogers, H. J., Boddy, L. & Müller, C. T. (2008). Changes in volatile production during interspecific interactions between four wood rotting fungi growing in artificial media. *Fungal Ecology*, 1, 57–68. 7, 80, 80, 80
- Falconer, R. E., Bown, J. L., White, N. A. & Crawford, J. W. (2008). Modelling interactions in fungi. *Journal of the Royal Society Interface*, 5, 603–615. 2, 8, 9, 81, 83, 83, 85
- Fawcett, H. S. (1925). Maintained growth rates in fungus cultures of long duration. *Annals of Applied Biology*, 12, 191–198. 7, 80
- Fontaine, C., Guimarães Jr., P. R., Kéfi, S., Loeuille, N., Memmott, J., van der Putten, W. H., van Veen, F. J. F. & Thébault, E. (2011). The ecological and evolutionary implications of merging different types of networks. *Ecology Letters*, 14, 1170–1181. 12, 86
- Fricker, M. D., Heaton, L. L. M., Jones, N. S. & Boddy, L. (2017). The mycelium as a network. *Microbiology Spectrum*, 5, 1–32. 7
- Garfield, R. (2017). *Magic: The Gathering® comprehensive rules*. Wizards of the Coast LLC, Renton, WA, USA. 15, 16, 16

- Ghalambor, C. K., Walker, J. A. & Reznick, D. N. (2003). Multi-trait selection, adaptation, and constraints on the evolution of burst swimming performance. *Integrative and Comparative Biology*, 43, 431–438. 86
- Gillespie, D. T. (1976). A general method for numerically simulating the stochastic time evolution of coupled chemical reactions. *Journal of computational physics*, 22, 403–434. 50
- Gilman, R. T., Nuismer, S. L. & Jhvueng, D.-C. (2012). Coevolution in multidimensional trait space favours escape from parasites and pathogens. *Nature*, 483, 328–330. 4, 76
- Gravel, D., Poisot, T., Albouy, C., Velez, L. & Mouillot, D. (2013). Inferring food web structure from predator–prey body size relationships. *Methods in Ecology and Evolution*, 4, 1083–1090. 4
- Griffith, G. S. & Boddy, L. (1991). Fungal decomposition of attached angiosperm twigs. IV. Effect of water potential on interactions between fungi on agar and in wood. *The New Phytologist*, 117, 633–641. 7, 80
- Guimarães Jr, P. R., Jordano, P. & Thompson, J. N. (2011). Evolution and coevolution in mutualistic networks. *Ecology Letters*, 14, 877–885. 4
- Gurobi Optimization and Inc. (2017). Gurobi optimizer, version 7.5. <http://www.gurobi.com>. 29
- Haeckel, A. H. P. A. (1866). *Generelle Morphologie Der Organismen*. Georg Reimer, Berlin, Germany. 1
- Halley, J. M., Comins, H. N., Lawton, J. H. & Hassell, M. P. (1994). Competition, succession and pattern in fungal communities: towards a cellular automation model. *Oikos*, 70, 435–442. 2, 8, 8, 81, 83, 83
- Halley, J. M., Robinson, C. H., Comins, H. N. & Dighton, J. (1996). Predicting straw decomposition by a four-species fungal community: a cellular automaton model. *Journal of Applied Ecology*, 33, 493–507. 81
- Hamilton, W. D. (1964). The genetical evolution of social behaviour. I. *Journal of Theoretical Biology*, 7, 1–16. 1, 15
- Hartig, F., Calabrese, J. M., Reineking, B., Wiegand, T. & Huth, A. (2011). Statistical inference for stochastic simulation models – theory and application. *Ecology Letters*, 14, 816–827. 56

- Heilmann-Clausen, J. & Boddy, L. (2005). Inhibition and stimulation effects in communities of wood decay fungi: exudates from colonized wood influence growth by other species. *Microbial Ecology*, 49, 399–406. 7, 80
- Hiscox, J. & Boddy, L. (2017). Armed and dangerous – Chemical warfare in wood decay communities. *Fungal Biology Reviews*, 31, 169–184. 7, 81
- Hiscox, J., Savoury, M., Toledo, S., Kingscott-Edmunds, J., Bettridge, A., Al Waili, N. & Boddy, L. (2017). Threesomes destabilise certain relationships: multispecies interactions between wood decay fungi in natural resources. *FEMS Microbiology Ecology*, 93, fix014. 7, 8, 8, 81, 82, 83, 87
- Hiscox, J., Savoury, M., Vaughan, I. P., Müller, C. T. & Boddy, L. (2015). Antagonistic fungal interactions influence carbon dioxide evolution from decomposing wood. *Fungal Ecology*, 14, 24–32. 8
- Holmer, L. & Stenlid, J. (1993). The importance of inoculum size for the competitive ability of wood decomposing fungi. *FEMS Microbiology Ecology*, 12, 169–176. 7, 81, 83, 83
- Ibanez, S., Gallet, C. & Després, L. (2012). Plant insecticidal toxins in ecological networks. *Toxins*, 4, 228–243. 1
- Ings, T. C., Montoya, J. M., Bascompte, J., Blüthgen, N., Brown, L., Dormann, C. F., Edwards, F., Figueroa, D., Jacob, U., Jones, J. I., Lauridsen, R. B., Ledger, M. E., Lewis, H. M., Olesen, J. M., van Veen, F. J. F., Warren, P. H. & Woodward, G. (2009). Ecological networks – beyond food webs. *Journal of Animal Ecology*, 78, 253–269. 1, 11, 12
- Jackson, J. B. C. & Buss, L. (1975). Allelopathy and spatial competition among coral reef invertebrates. *Proceedings of the National Academy of Sciences*, 72, 5160–5163. 24, 24, 25, 25
- Jennings, D. H. (1987). Translocation of solutes in fungi. *Biological Reviews*, 62, 215–243. 7
- Jordano, P., Bascompte, J. & Olesen, J. M. (2003). Invariant properties in coevolutionary networks of plant–animal interactions. *Ecology Letters*, 6, 69–81. 76
- Kennedy, H. (1978). Systematics and pollination of the “closed-flowered” species of *Calathea* (Marantaceae). *University of California Publications in Botany*, 71, 1–90. 17, 18, 19, 25

- Kennedy, P. (2010). Ectomycorrhizal fungi and interspecific competition: species interactions, community structure, coexistence mechanisms, and future research directions. *New Phytologist*, 187, 895–910. 7, 81
- Kertesz, J. & Vicsek, T. (1986). Diffusion-limited aggregation and regular patterns: fluctuations versus anisotropy. *Journal of Physics A: Mathematical and General*, 19, L257. 52
- Kjørboe, T. (2011). How zooplankton feed: mechanisms, traits and trade-offs. *Biological Reviews*, 86, 311–339. 3, 78
- Kivelä, M., Arenas, A., Barthelemy, M., Gleeson, J. P., Moreno, Y. & Porter, M. A. (2014). Multilayer networks. *Journal of Complex Networks*, 2, 203–271. 12
- Kiziridis, D., Boddy, L., Eastwood, D. C., Yuan, C. & Fowler, M. S. (2017). A mechanistic perspective of ecological networks highlights the contribution of alternative interaction strategies. *bioRxiv*, 192260. 30
- Kopp, M. & Gavrillets, S. (2006). Multilocus genetics and the coevolution of quantitative traits. *Evolution*, 60, 1321–1336. 4
- Legendre, P. & Legendre, L. (1998). *Numerical ecology*. 2nd edn. Elsevier Science, Amsterdam. 77
- Levine, J. M., Bascompte, J., Adler, P. B. & Allesina, S. (2017). Beyond pairwise mechanisms of species coexistence in complex communities. *Nature*, 546, 56–64. 78
- Levins, R. (1968). *Evolution in changing environments: some theoretical explorations*. Princeton University Press, Princeton, NJ, USA. 77
- Lindahl, B., Stenlid, J. & Finlay, R. (2001). Effects of resource availability on mycelial interactions and <sup>32</sup>P transfer between a saprotrophic and an ectomycorrhizal fungus in soil microcosms. *FEMS Microbiology Ecology*, 38, 43–52. 7
- MacArthur, R. & Levins, R. (1967). The limiting similarity, convergence, and divergence of coexisting species. *The American Naturalist*, 101, 377–385. 76, 77, 77
- Manceau, M., Lambert, A. & Morlon, H. (2017). A unifying comparative phylogenetic framework including traits coevolving across interacting lineages. *Systematic Biology*, 66, 551–568. 86
- Martín-Herrero, J. (2004). Hybrid cluster identification. *Journal of Physics A: Mathematical and General*, 37, 9377. 42
- Mayr, E. (1992). The idea of teleology. *Journal of the History of Ideas*, 53, 117–135. 76

- Mayr, E. (1998). The multiple meanings of 'teleological'. *History and Philosophy of the Life Sciences*, 20, 35–40. 76
- McGill, B. J., Enquist, B. J., Weiher, E. & Westoby, M. (2006). Rebuilding community ecology from functional traits. *Trends in Ecology & Evolution*, 21, 178–185. 2, 4
- Meyer, J. R., Dobias, D. T., Weitz, J. S., Barrick, J. E., Quick, R. T. & Lenski, R. E. (2012). Repeatability and contingency in the evolution of a key innovation in phage lambda. *Science*, 335, 428–432. 4, 78
- Moeller, H. V. & Peay, K. G. (2016). Competition-function tradeoffs in ectomycorrhizal fungi. *Peerj*, 4, e2270. 8
- Morales, J. M. & Vázquez, D. P. (2008). The effect of space in plant–animal mutualistic networks: insights from a simulation study. *Oikos*, 117, 1362–1370. 86
- Morales-Castilla, I., Matias, M. G., Gravel, D. & Araújo, M. B. (2015). Inferring biotic interactions from proxies. *Trends in Ecology & Evolution*, 30, 347–356. 76
- Morin, P. J. (2011). *Community ecology*. 2nd edn. Wiley-Blackwell, West Sussex, UK. 1, 3
- Newman, M. E. J. (2003). The structure and function of complex networks. *SIAM Review*, 45, 167–256. 5, 11
- Nittmann, J. & Stanley, H. E. (1986). Tip splitting without interfacial tension and dendritic growth patterns arising from molecular anisotropy. *Nature*, 321, 663–668. 52
- Nuismer, S. L., Doebeli, M. & Browning, D. (2005). The coevolutionary dynamics of antagonistic interactions mediated by quantitative traits with evolving variances. *Evolution*, 59, 2073–2082. 4
- Nuismer, S. L., Jordano, P. & Bascompte, J. (2013). Coevolution and the architecture of mutualistic networks. *Evolution*, 67, 338–354. 4, 77
- Nuismer, S. L. & Thompson, J. N. (2006). Coevolutionary alternation in antagonistic interactions. *Evolution*, 60, 2207–2217. 4
- Olito, C. & Fox, J. W. (2015). Species traits and abundances predict metrics of plant–pollinator network structure, but not pairwise interactions. *Oikos*, 124, 428–436. 1, 79



- Oliva, J., Messal, M., Wendt, L. & Elfstrand, M. (2017). Quantitative interactions between the biocontrol fungus *Phlebiopsis gigantea*, the forest pathogen *Heterobasidion annosum* and the fungal community inhabiting Norway spruce stumps. *Forest Ecology and Management*, 402, 253–264. 8
- Olsson, S. (1999). Nutrient translocation and electrical signalling in mycelia. In: *The fungal colony* (eds. Gow, N. A. R., Robson, G. D. & Gadd, G. M.). Cambridge University Press, Cambridge, UK, pp. 25–48. 7
- Ortega, R., Fortuna, M. A. & Bascompte, J. (2017). Web of Life dataset. 30, 30
- Ovaskainen, O., Tikhonov, G., Norberg, A., Blanchet, F. G., Duan, L., Dunson, D., Roslin, T. & Abrego, N. (2017). How to make more out of community data? A conceptual framework and its implementation as models and software. *Ecology Letters*, 20, 561–576. 4
- Petchey, O. L., Beckerman, A. P., Riede, J. O. & Warren, P. H. (2008). Size, foraging, and food web structure. *Proceedings of the National Academy of Sciences*, 105, 4191–4196. 2, 4, 79
- Pigliucci, M. (2013). Landscapes, surfaces, and morphospaces: what are they good for? In: *The adaptive landscape in evolutionary biology* (eds. Svensson, E. I. & Calsbeek, R.). Oxford University Press, Oxford, UK, pp. 26–38. 86
- Pilosof, S., Porter, M. A., Pascual, M. & Kéfi, S. (2017). The multilayer nature of ecological networks. *Nature Ecology & Evolution*, 1, 0101. 12, 86
- Pinter-Wollman, N., Hobson, E. A., Smith, J. E., Edelman, A. J., Shizuka, D., de Silva, S., Waters, J. S., Prager, S. D., Sasaki, T., Wittemyer, G., Fewell, J. & McDonald, D. B. (2014). The dynamics of animal social networks: analytical, conceptual, and theoretical advances. *Behavioral Ecology*, 25, 242–255. 1, 86
- Pires, M. M., Marquitti, F. M. D. & Guimaraes, P. R. (2017). The friendship paradox in species-rich ecological networks: Implications for conservation and monitoring. *Biological Conservation*, 209, 245–252. 5, 80
- Plomley, N. J. B. (1959). Formation of the colony in the fungus *Chaetomium*. *Australian Journal of Biological Sciences*, 12, 53–64. 7, 7, 7, 80, 81
- Poisot, T., Cirtwill, A. R., Cazelles, K., Gravel, D., Fortin, M.-J. & Stouffer, D. B. (2016). The structure of probabilistic networks. *Methods in Ecology and Evolution*, 7, 303–312. 87

- Poisot, T., Stouffer, D. B. & Gravel, D. (2015). Beyond species: why ecological interaction networks vary through space and time. *Oikos*, 124, 243–251. 2, 4, 5, 76, 79
- Prosser, J. I. (1995). Kinetics of filamentous growth and branching. In: *The Growing Fungus* (eds. Gow, N. A. R. & Gadd, G. M.). Chapman & Hall, London, UK, pp. 301–318. 63
- Prosser, J. I. & Trinci, A. P. J. (1979). A model for hyphal growth and branching. *Journal of General Microbiology*, 111, 153–164. 7
- R Core Team (2017). R: a language and environment for statistical computing, version 3.4.0. <https://www.R-project.org/>. 36
- Rasband, W. S. (2016). ImageJ, U. S. National Institutes of Health, Bethesda, Maryland, USA. <https://imagej.nih.gov/ij/>. 41, 41
- Ribeiro Mello, M. A., Rodrigues, F. A., Costa, L. d. F., Daniel Kissling, W., Sekercioglu, C. H., Darcie Marquitti, F. M. & Viktoria Kalko, E. K. (2015). Keystone species in seed dispersal networks are mainly determined by dietary specialization. *Oikos*, 124, 1031–1039. 5, 80
- Rohr, R. P. & Bascompte, J. (2014). Components of phylogenetic signal in antagonistic and mutualistic networks. *The American Naturalist*, 184, 556–564. 87
- Rossberg, A. G., Brannstrom, A. & Dieckmann, U. (2010). Food-web structure in low- and high-dimensional trophic niche spaces. *Journal of the Royal Society Interface*, 7, 1735–1743. 6
- Rudolf, V. H. W. & Rasmussen, N. L. (2013). Population structure determines functional differences among species and ecosystem processes. *Nature Communications*, 4, 2318. 5, 80
- Ryan, F. J., Beadle, G. W. & Tatum, E. L. (1943). The tube method of measuring the growth rate of *Neurospora*. *American Journal of Botany*, 30, 784–799. 7, 80
- Ryan, M. J. & Cummings, M. E. (2013). Perceptual biases and mate choice. *Annual Review of Ecology, Evolution, and Systematics*, 44, 437–459. 1
- Sanders, J. G., Powell, S., Kronauer, D. J. C., Vasconcelos, H. L., Frederickson, M. E. & Pierce, N. E. (2014). Stability and phylogenetic correlation in gut microbiota: lessons from ants and apes. *Molecular Ecology*, 23, 1268–1283. 1, 5, 80

- Santamaría, L. & Rodríguez-Gironés, M. A. (2007). Linkage rules for plant–pollinator networks: trait complementarity or exploitation barriers? *PLOS Biology*, 5, e31. 2, 4, 76, 77
- Santamaría, L. & Rodríguez-Gironés, M. A. (2015). Are flowers red in teeth and claw? Exploitation barriers and the antagonist nature of mutualisms. *Evolutionary Ecology*, 29, 311–322. 18, 18, 25
- Schiestl, F. P. & Johnson, S. D. (2013). Pollinator-mediated evolution of floral signals. *Trends in Ecology & Evolution*, 28, 307–315. 4, 78
- Schoener, T. W. (1989). The ecological niche. In: *Ecological concepts: the contribution of ecology to an understanding of the natural world* (ed. Cherrett, J. M.). Blackwell Scientific Publications, Oxford, UK, pp. 79–114. 7, 76, 77
- Seppälä, O. (2015). Natural selection on quantitative immune defence traits: a comparison between theory and data. *Journal of Evolutionary Biology*, 28, 1–9. 1
- Shoval, O., Sheftel, H., Shinar, G., Hart, Y., Ramote, O., Mayo, A., Dekel, E., Kavanagh, K. & Alon, U. (2012). Evolutionary trade-offs, Pareto optimality, and the geometry of phenotype space. *Science*, 336, 1157–1160. 86
- Sih, A., Cote, J., Evans, M., Fogarty, S. & Pruitt, J. (2012). Ecological implications of behavioural syndromes. *Ecology Letters*, 15, 278–289. 1
- Song, Z., Vail, A., Sadowsky, M. J. & Schilling, J. S. (2015). Influence of hyphal inoculum potential on the competitive success of fungi colonizing wood. *Microbial Ecology*, 69, 758–767. 7
- Sonnenbichler, J., Dietrich, J. & Peipp, H. (2009). Secondary fungal metabolites and their biological activities, V. Investigations concerning the induction of the biosynthesis of toxic secondary metabolites in basidiomycetes. *Biological Chemistry*, 375, 71–79. 7, 80
- Speed, M. P., Fenton, A., Jones, M. G., Ruxton, G. D. & Brockhurst, M. A. (2015). Coevolution can explain defensive secondary metabolite diversity in plants. *New Phytologist*, 208, 1251–1263. 76
- Stahl, P. D. & Christensen, M. (1992). *In vitro* mycelial interactions among members of a soil microfungal community. *Soil Biology and Biochemistry*, 24, 309–316. 7, 36, 81
- Stella, T., Covino, S., Čvančarová, M., Filipová, A., Petruccioli, M., D’Annibale, A. & Cajthaml, T. (2017). Bioremediation of long-term PCB-contaminated soil by white-rot fungi. *Journal of Hazardous Materials*, 324, 701–710. 8

- Stouffer, D. B., Camacho, J. & Amaral, L. A. N. (2006). A robust measure of food web intervality. *Proceedings of the National Academy of Sciences*, 103, 19015–19020. 4, 6, 76
- Stouffer, D. B., Rezende, E. L. & Amaral, L. A. N. (2011). The role of body mass in diet contiguity and food-web structure. *Journal of Animal Ecology*, 80, 632–639. 77
- Strauss, S. Y. (2014). Ecological and evolutionary responses in complex communities: implications for invasions and eco-evolutionary feedbacks. *Oikos*, 123, 257–266. 1
- Sturrock, C. J., Ritz, K., Samson, W. B., Bown, J. L., Staines, H. J., Palfreyman, J. W., Crawford, J. W. & White, N. A. (2002). The effects of fungal inoculum arrangement (scale and context) on emergent community development in an agar model system. *FEMS Microbiology Ecology*, 39, 9–16. 7, 8
- Stuurman, N. (2006). Binner plugin for ImageJ. <https://valelab4.ucsf.edu/~nstuurman/IJplugins/Binner.html>. 41
- Szolnoki, A., Mobilia, M., Jiang, L.-L., Szczesny, B., Rucklidge, A. M. & Perc, M. (2014). Cyclic dominance in evolutionary games: a review. *Journal of The Royal Society Interface*, 11, 20140735. 78
- Tang, C. (1985). Diffusion-limited aggregation and the Saffman-Taylor problem. *Physical Review A*, 31, 1977–1979. 52
- Toral, R. & Colet, P. (2014). Introduction to master equations. In: *Stochastic numerical methods: an introduction for students and scientists*. Wiley-VCH, Weinheim, Germany, pp. 235–260. 64
- Trinci, A. P. J. (1969). A kinetic study of the growth of *Aspergillus nidulans* and other fungi. *Journal of General Microbiology*, 57, 11–24. 7, 81
- Valdovinos, F. S., Ramos-Jiliberto, R., Garay-Narvaez, L., Urbani, P. & Dunne, J. A. (2010). Consequences of adaptive behaviour for the structure and dynamics of food webs. *Ecology Letters*, 13, 1546–1559. 5, 80
- Vázquez, D. P. & Aizen, M. A. (2003). Null model analyses of specialization in plant–pollinator interactions. *Ecology*, 84, 2493–2501. 87
- Vázquez, D. P., Blüthgen, N., Cagnolo, L. & Chacoff, N. P. (2009a). Uniting pattern and process in plant–animal mutualistic networks: a review. *Annals of Botany*, 103, 1445–1457. 4, 76, 79
- Vázquez, D. P., Chacoff, N. P. & Cagnolo, L. (2009b). Evaluating multiple determinants of the structure of plant–animal mutualistic networks. *Ecology*, 90, 2039–2046. 5

- Vieira, M. C. & Peixoto, P. E. C. (2013). Winners and losers: a meta-analysis of functional determinants of fighting ability in arthropod contests. *Functional Ecology*, 27, 305–313. 1
- Violle, C., Navas, M.-L., Vile, D., Kazakou, E., Fortunel, C., Hummel, I. & Garnier, E. (2007). Let the concept of trait be functional! *Oikos*, 116, 882–892. 2, 4
- Volpert, V. & Petrovskii, S. (2009). Reaction–diffusion waves in biology. *Physics of Life Reviews*, 6, 267–310. 70, 70, 70, 84
- Wagner, G. P. (2001). Characters, units and natural kinds: an introduction. In: *The character concept in evolutionary biology* (ed. Wagner, G. P.). Academic Press, San Diego, CA, USA, pp. 1–10. 1, 76
- Wainwright, P. C. (2007). Functional versus morphological diversity in macroevolution. *Annual Review of Ecology, Evolution, and Systematics*, 38, 381–401. 76
- West, S. A. & Gardner, A. (2013). Adaptation and inclusive fitness. *Current Biology*, 23, R577–R584. 15, 75
- White, N. A., Sturrock, C., Ritz, K., Samson, W. B., Bown, J., Staines, H. J., Palfreyman, J. W. & Crawford, J. (1998). Interspecific fungal interactions in spatially heterogeneous systems. *FEMS Microbiology Ecology*, 27, 21–32. 7, 8
- Williams, H. P. (2013). *Model building in mathematical programming*. 5th edn. Wiley-Blackwell, West Sussex, UK. 26, 26, 28, 29
- Williams, R. J. & Martinez, N. D. (2000). Simple rules yield complex food webs. *Nature*, 404, 180–183. 2, 4, 6
- Woodward, G., Ebenman, B., Emmerson, M., Montoya, J. M., Olesen, J. M., Valido, A. & Warren, P. H. (2005). Body size in ecological networks. *Trends in Ecology & Evolution*, 20, 402–409. 77
- Woodward, G., Papanтониου, G., Edwards, F. & Lauridsen, R. B. (2008). Trophic trickles and cascades in a complex food web: Impacts of a keystone predator on stream community structure and ecosystem processes. *Oikos*, 117, 683–692. 5, 80
- Wootton, J. T. (1994). The nature and consequences of indirect effects in ecological communities. *Annual Review of Ecology and Systematics*, 25, 443–466. 1, 11